Studies on Synthesis and Characterization of Cyclodextrin-based Glyco-clusters

Doctoral Dissertation

Bin Han

Division of Environmental Materials Science

Graduate School of Environmental Science

Hokkaido University

2018

Table of Contents

Chapter **Page**

Chapter 1

General Introduction

1.1 Research background

Carbohydrates are prominently displayed on the surface of cell membranes and on the exposed regions of macromolecules in bodily fluids. Their structural diversity and abundant presence in cell surface make them suitable for transferring biological signals in the forms that are recognizable by other biological systems. Carbohydrate-mediated molecular recognition underlies many aspects of biological processes[1-6]. These include important cellular events, such as fertilization[7], embryonic development[8], cell differentiation and cell-cell communication[9-11], and many molecular processes that are mediated or regulated by carbohydrate bio-signals. Exploration of sugar chain diversities and their roles in molecular recognition and bio-signaling is one of the current challenges to functional glycomics investigation.

Lectin is a carbohydrate-binding protein. In a variety of everyday biological phenomena, carbohydrate-lectin recognition is a very important process. Oligosaccharides are now known to mediate cell-cell recognition, the recognition could influence physiological phenomena and activities which could be happening at every moment such as the moderation of enzymes and other proteins, the various functions in the immune response, and the infection of cells by bacteria and viruses[12-14]. Cell-surface lectins plays as a vital role in the process of intercellular recognition due to its specific recognition ability to corresponsive carbohydrate groups. In addition, carbohydrate moieties which attached to membrane glycoproteins

and glycolipids constitute the potential recognition sites for carbohydrate-mediated interactions between cells and drug molecule carriers bearing targeting ligands[15]. Taken the specific recognition ability of part carbohydrate compounds to cell-surface lectins into consideration, some representative carbohydrates could be ideal targeting ligands in the construction of molecular vehicle for bioactive compounds.

Several kinds of D-galactose-β-cyclodextrin conjugates were designed and synthesized as drug-carrying clusters. These conjugates had remarkably high inclusion associations of 10^5-10^7 M^{-1} levels for the immobilized doxorubicin[16]. In addition, heptamannosylated β-CD was also applied in the research of targeting anticancer therapy recently[17].

In this research, the molecular vehicle bearing targeting ligands will be used to construct host-guest inclusion complexes with bioactive guest molecule as a model molecule. And the inclusion complexes could be analyzed by using lectin-contained column such as Griffonia simplicifolia to test the recognition abilities of lectins to carbohydrate moieties, the carbohydrate moieties which vary from pure original carbohydrates and play as the targeting ligands in the inclusion system. Therefore, it is necessary to select the appropriate host molecule and bioactive guest molecule for the inclusion system.

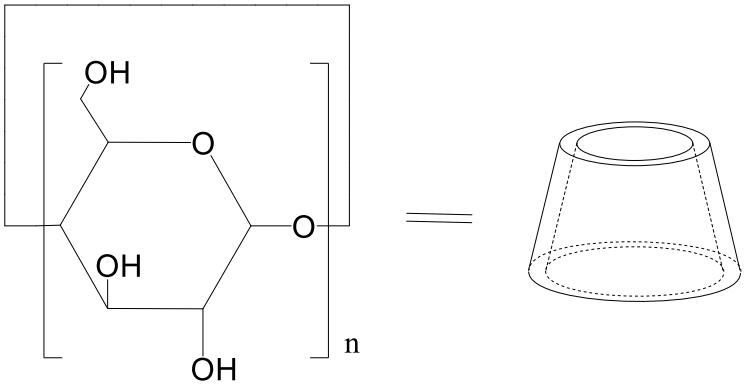

n = 6, α-CD
n = 7, β-CD
n = 8, γ-CD

Figure 1. The chemical structure of α, β, and γ-Cyclodextrins.

Cyclodextrins (CDs) are a family of macrocyclic oligosaccharides linked by α-1,4-glucosidic bonds, have a unique property to form an inclusion complex with a variety of compounds into their hydrophobic cavity, and are regarded as potential materials for the encapsulation of various bioactive molecules[18]. The α, β, and γ-CDs are widely used natural cyclodextrins, which consisting of six, seven, and eight α-D-glucopyranose residues, respectively (Figure 1). β-CD is the most extensively studied natural cyclodextrin among these three kinds of cyclodextrins, and it has 21 hydroxyl groups: 7 primary and 14 secondary hydroxyl groups. These hydroxyl groups are available for structural modifications, and various functional groups have been introduced to modify the chemical properties and inclusion ability of the parent host molecule β-CD[19]. For example, the 2-hydroxypropyl-β-CD (HP-β-CD) and sulfobutylether-β-cyclodextrin (SBE-β-CD) are β-CD derivatives with increased water solubility

properties compared to parent β-CD, and have been studied to design the drug dosage form in the previous research[20].

In addition, as the β-CD is the most accessible, the lowest priced and generally the most studied cyclodextrin, it has been extensively studied and applied in the field of pharmaceutical chemistry as well as α-CD and γ-CD[21]. For examples, HP-β-CD was used to construct the inclusion complex with myricetin (Figure 2) by Ji G et al, the myricetin which has been reported to exhibit various effects such as anti-oxidative; and the solubility, dissolution rate; the oral bioavailability of myricetin was increased after inclusion[22]. And the anticancer resveratrol/SBE-β-CD inclusion complex was prepared by Ventura CA et al, the complex which improved the water solubility of resveratrol; the experimental results also showed the improvement of resveratrol's anticancer activity on human breast cancer cell line (MCF-7)[23].

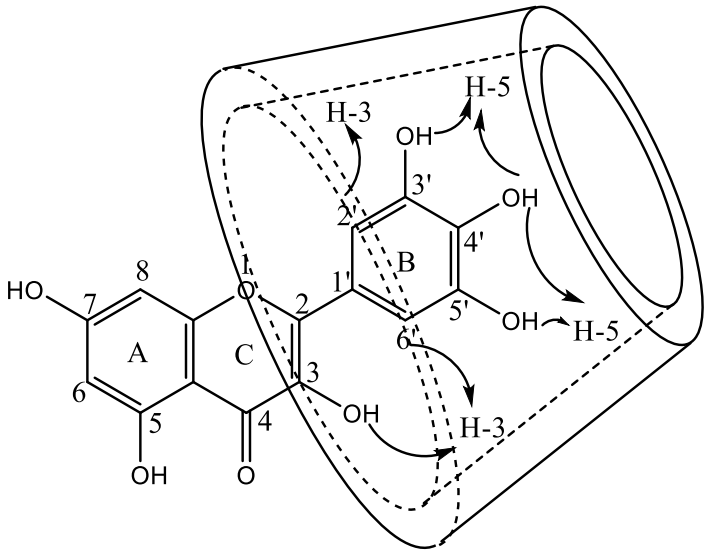

Figure 2. The possible inclusion mode of HP-β-CD/myricetin inclusion complex.

Besides the application of inclusion behavior, the β-CD could also play a role to synthesize CD conjugates for colon-specific or cecum-specific drug delivery. When targeting drugs to the colon, the drugs are protected from the hostile environments of the stomach and small intestine. The protection in the upper gastrointestinal tract is affected by conjugation with carrier moieties, forming prodrugs, then the prodrugs undergo enzymatic cleavage in the colon and regenerate the drug. For examples, Uekama K selectively conjugated biphenylyl acetic acid to one of the primary hydroxyl groups of β-CD through an ester-linkage to synthesize the ester-type conjugate, the conjugate which was expected to serve as a colon-targeting prodrug due to its stability in contents of both stomach and intestine, and its released ability in contents of colon and cecum[24]. Uekama K also prepared the 5-fluorouracil acetic acid/β-cyclodextrin conjugates (Figure 3) through ester-linkage, and the experimental results showed that the conjugate was hydrolyzed in rat cecal contents[25].

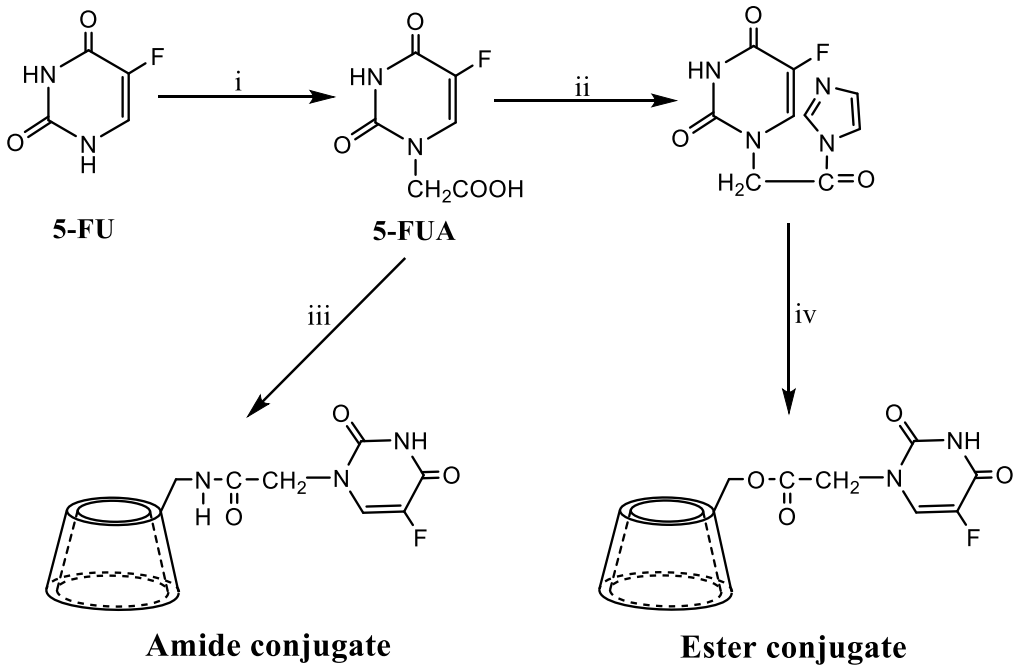

i. α-chloroacetic acid in aq. KOH at 100 °C, 2 h;
ii. CDI in DMSO at r.t., 3 h;
iii. Amino-β-CyD, DCC and HONSu in DMSO at 50 °C, 5 days;
iv. β-CyD in DMSO, TEA, at r.t., 48 h.

Figure 3. The chemical synthesis of 5-Fluorouracil acetic acid/β-cyclodextrin conjugates.

As mentioned above, one kind of CD's targeting properties is the colon or cecum-specific property, which should be credited to enzymes existed in colon such as α-amylase. Besides, another kind of CD's targeting properties is depended on connecting targeting ligands to CD moieties, the targeting ligands could be folic acid, saccharides and hyaluronic acid[26]. For example, folic acid has been used as a targeting ligand due to its selectivity for folic acid receptor overexpressed on the surface of tumor cells. In the previous study, some CD-based targeting drug carriers were constructed and showed the relevant targeting properties in the biological assessment.

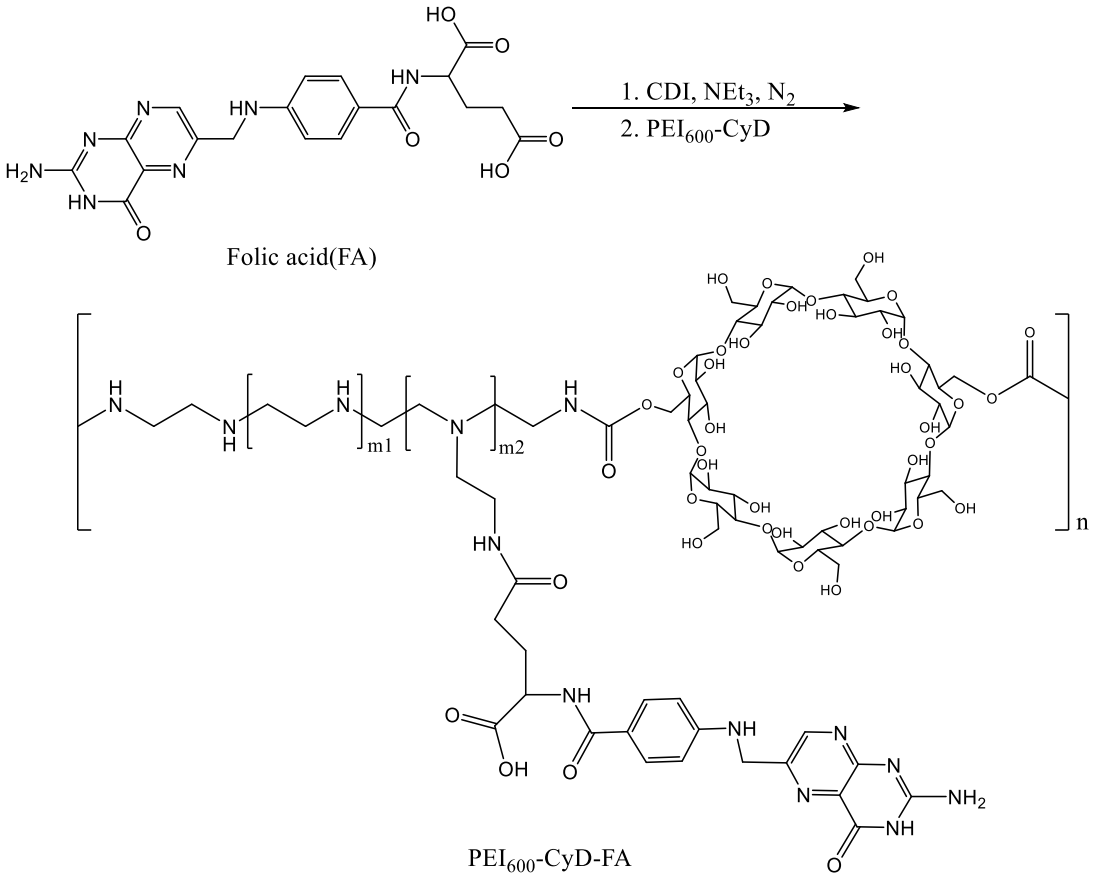

Figure 4. Synthesis and structure of folate-PEI-cyclodextrin nanopolymer.

For instance, Ying H recently prepared docetaxel/folic acid-cyclodextrin inclusion complex and the experimental results of targeting antitumor effects indicated that docetaxel/folic acid-cyclodextrin could serve as an effective delivery system for antitumor therapy[27]. The folate–PEI600–cyclodextrin nanopolymer (Figure 4) for gene transfection was constructed and characterized by Lin MC, showed the safe and efficiency both in vitro and vivo transfection of plasmid DNA[28]. Besides, the maltose-polyrotaxane conjugate (Figure 5) was synthesized from carboxyethyl ester-polyrotaxane and β-maltosylamine in the early study by

Nobuhiko Y et al, which applied α-CD in the preparation of polyrotaxane and showed the rapid binding ability to concanavalin A (Con A)[29].

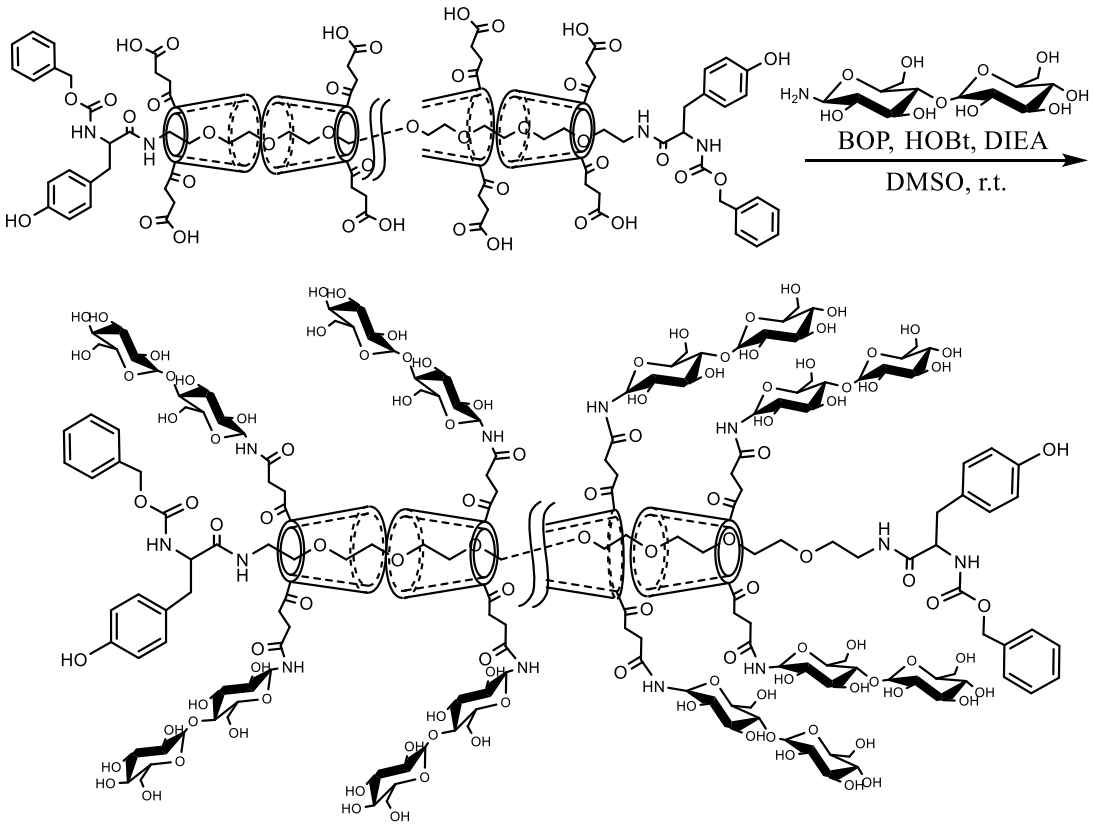

Figure 5. Synthesis of maltose-polyrotaxane conjugates.

Considerate the extensive applications of CDs in the pharmaceutical and supramolecular chemistry, with the properties such as well-defined chemical structure, low toxicity and low pharmacological activity, the β-CD and its derivatives could be used as appropriate host molecule in this study. The following step is to find an efficient chemical method to connect β-CD to carbohydrate moieties.

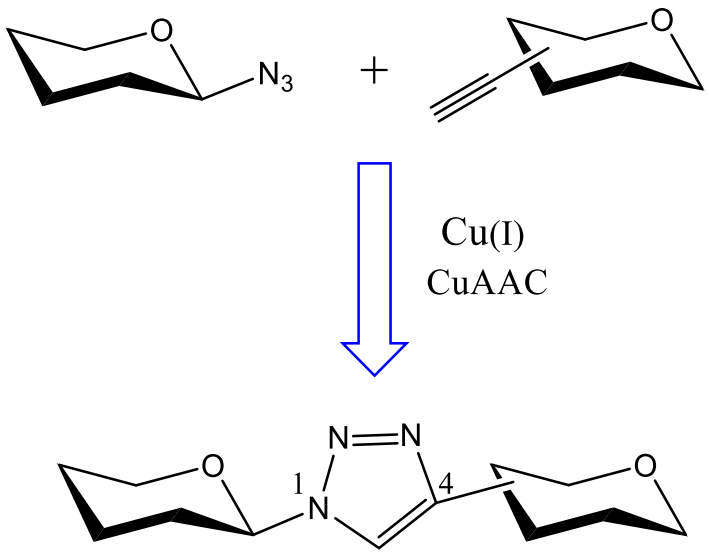

Figure 6. The schematic illustration of Cu-mediated CuAAC reaction of carbohydrate compounds.

It is well known that Cu(I)-catalyzed azide-alkyne 1,3-dipolar cycloaddition (CuAAC), which are popularly known as the “click reaction”, serves as the most potent and highly dependable tool for facile construction of complex architectures at the molecular level (Figure 6)[30]. In the year of 2001, Sharpless KB published the landmark review described a new strategy for organic chemistry, as the authors also put it “the reinvigoration of an old style of organic synthesis”[31]. The named “click chemistry” was created to describe this guiding principle, a principle born to meet the demands of modern day chemistry and in particular, the demands of drug discovery[32]. Therefore, the Cu-mediated “click reaction” was selected in the present study to construct the β-CD based clusters as the author took the advantages of “click reaction” such as simple reaction conditions, readily available starting materials, readily available reagents, easily removed solvent and simple product isolation into consideration.

1.2 The purpose of research

In this study, the author made a plan to synthesize a series of CD-based glyco-clusters by Cu-mediated “click reaction”, which could be regarded as host molecules in the construction of inclusion complexes. The inclusion complexes could be analyzed by lectin-contained column to measure the lectin recognition abilities and find the relevant affecting factors. The first important thing should be that to understand the orientation of the guest molecule in the CD cavity in detail, with the consideration of complicated structure of glyco-clusters and the possibility that the substituted glycosyl groups may enter into the cavity of CD moieties. Therefore, the detailed NMR studies on glyco-clusters and inclusion complexes are necessary. The theoretical lectin recognition abilities of α-mannosyl, α-glucosyl and α-galactosyl residues which in the status of ligands of CD carrier, are expected to be useful to the future study.

In this research, the author selected three kinds of natural saccharides D-mannose, maltose and melibiose as starting materials (Figure 7). These natural saccharides could be easily obtained from nature and containing α-mannosyl, α-glucosyl and α-galactosyl residues, respectively. In addition, these CD-based glyco-clusters are also the potential modules in the future construction of inclusion complex or polyrotaxane for drug delivery, with the consideration of potential targeting properties. Firstly, the author plan to study and compare the inclusion abilities of these CD-based glyco-clusters in this research.

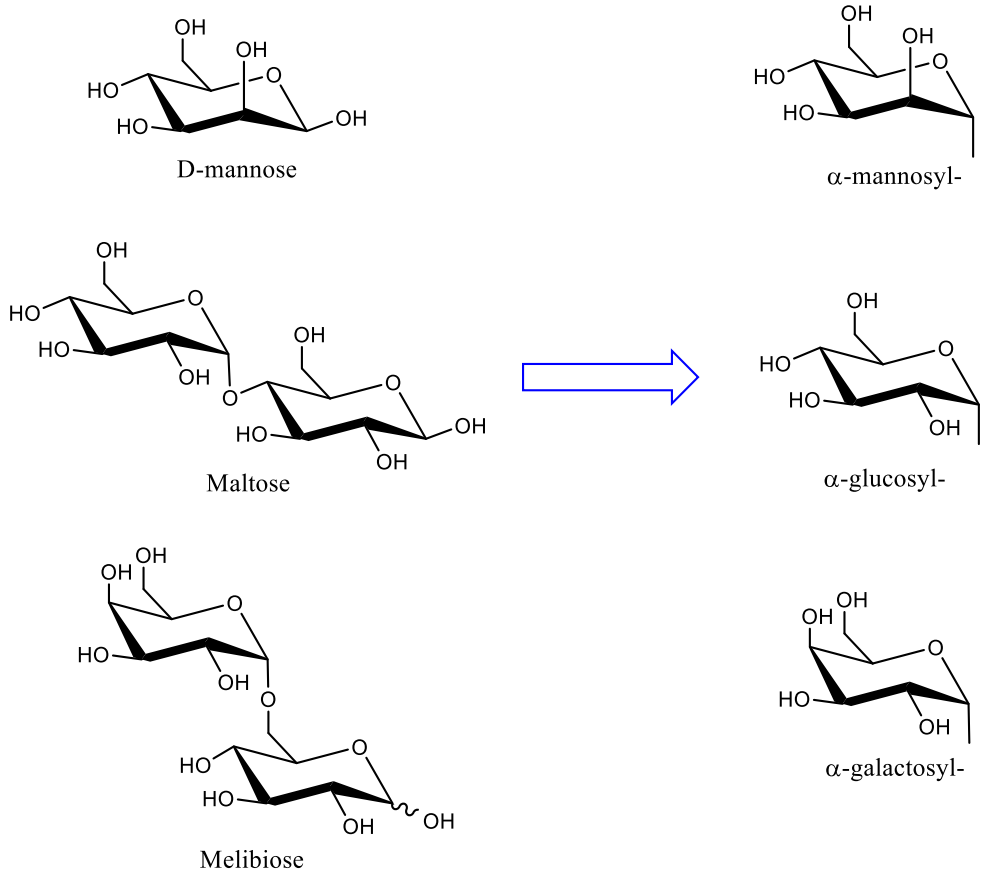

Figure 7. The chemical structure of D-mannose, maltose, melibiose and respective functional groups.

This thesis consists of five chapters. In chapter 1, the author stated the biological significance of carbohydrates and the recent applications of CD and its derivatives, as well as the chemical advantages of “click reaction”. In chapter 2, the author described the procedures of preparation and detailed characterization of CD-based glyco-clusters. In chapter 3, the author confirmed the formation of inclusion complexes between CD-based glyco-clusters and antiphlogistic ibuprofen by analyzing chemical shifts’ change in NMR spectrum. In chapter 4, the author studied the NMR characterization of CD-based glyco-clusters/IBUNa inclusion complexes

and deduced potential inclusion modes as much as possible. In chapter 5, the author summarized the conclusion and prospects according to the experimental results and observations.

Chapter 2

Preparation and characterization of cyclodextrin-based glyco-clusters

2.1 Introduction

Since Sharpless' discovery of the Cu-mediated “click reaction", it has been already extensively applied in carbohydrate chemistry including cyclodextrin modification. For example, Theresa MR synthesized a series of multivalent polycationic β-cyclodextrin clusters (Figure 1) by using copper-catalyzed “click reaction”, these macromolecules could bind and compact pDNA into nanoparticles for efficient delivery[33]. In addition, the β-cyclodextrin based chiral stationary phase used for chiral separation was also prepared by using Cu-mediated “click reaction” in the early study[34].

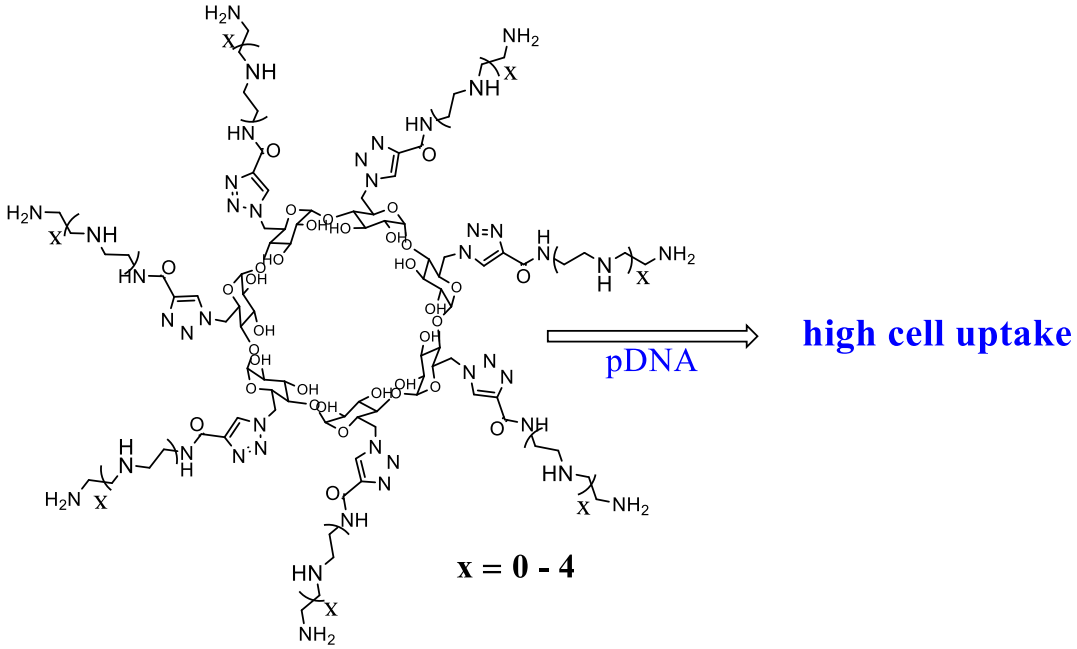

Figure 1. The polycationic β-cyclodextrin clusters prepared by “click reaction”.

Under these situations, the author had an interest in the Cu-mediated “click reaction” to construct the CD-based glyco-clusters, with the consideration that the chemical advantages of “click reaction” such as simple reaction conditions, readily available starting materials, readily available reagents, easily removed solvent and simple product isolation. This chapter describes the preparation of three CD-based glyco-clusters, which contains α-mannosyl, α-glucosyl and α-galactosyl residues, respectively.

2.2 Experiment

2.2.1 Materials and method

All reagents including β-CD were used from commercial resources without further purification. Air and water-sensitive reactions were conducted under nitrogen atmosphere in dry solvents. β-CD was dried in vaccum overnight at 80 ℃ in advance. The I-CD, N_3-CD and Man-CD were synthesized by methods as follows, which have been reported and applied in a series of research[35-37].

^{1}H NMR spectrum were recorded on Bruker Ultrafield Avance 300, JEOL Excalibur 400 and JEOL ECA 600 spectrometers at 300, 400 and 600 MHz, respectively. 2D NMR spectrum were recorded on JEOL ECA 600 spectrometer at High-resolution NMR laboratory, Graduate School of Science, Hokkaido University. Mass spectrum was recorded on Thermo Scientific Exactive at Global Facility Center, Hokkaido University.

2.2.2 Heptakis-(6-deoxy-6-iodine)-β-cyclodextrin (I-CD)

Ph_3P (13.1 g, 49.9 mmol) and iodine (10.1 g, 79.6 mmol) were slowly dissolved in dry DMF (50 ml), then the β-CD (2.9 g, 2.55 mmol) was added. Under the condition of 80 ℃ temperature, the reaction was processed for 36 hours under nitrogen atmosphere. Added the methanol solution of sodium methoxide (3 M, 15 ml) followed by the reaction mixture was slowly dropped into methanol (250 ml), then the precipitate appeared and was filtered gradually. The remaining iodine and DMF in

collected crude product was removed by Soxhlet extractor for 2 days, then the sample was dried under vaccum at 40 ℃ for overnight to obtain I-CD (2.36 g, 1.8 mmol) with a yield of 48.6%. The 300 MHz ^{1}H NMR spectrum showed that all the 6-OH groups of β-CD were disappeared, indicating that the β-CD was reacted sufficiently. ^{1}H NMR (DMSO-d_6, 300 MHz): δ = 6.03-6.05 ppm (OH-2, 7 H), 5.94 (OH-3, 7 H), 4.99 (H-1, 7 H), 3.26-3.83 (H-3, H-5, H-6, H-2, H-4, 42 H, partial peaks were overlapped with H_2O). The mass spectrum of I-CD was calculated for $(M + Na)^+$: $C_{42}H_{63}O_{28}I_7Na$, 1926.67108; found, 1926.67773.

2.2.3 Heptakis-(6-deoxy-6-azido)-β-cyclodextrin (N_3-CD)

I-CD (2.36 g, 1.8 mmol) was dissolved in dry DMF (50 ml), then the NaN_3 (0.9 g, 13.8 mmol) was added slowly by using plastic instrument. The reaction was processing at 70 ℃. After 48 hours' reaction under nitrogen atmosphere, the reaction mixture was dropped into deionized water to have a white precipitate. The precipitate was filtered and dried under vacuum to obtain N_3-CD with a yield of 36.2%. ^{1}H NMR (DMSO-d_6, 300 MHz): δ = 5.91-5.93 ppm (OH-2, 7 H), 5.77 (OH-3, 7 H), 4.92 (H-1, 7 H), 3.57-3.81 (H-3, H-5 and H-6, 28 H, peaks of H-2 and H-4 were overlapped with H_2O), The mass spectrum of N_3-CD was calculated for $(M + Na)^+$: $C_{42}H_{63}O_{28}N_{21}Na$, 1332.40436; found, 1332.40768.

2.2.4 Propargyl α-D-mannopyranoside

Fully acetylated D-mannose (4.45 g, 11.7 mmol) was dissolved in 50 ml dried CH_2Cl_2 with molecular sieve 4A (5 g), then the propargyl alcohol (0.9 ml, 15.6 mmol) and $BF_3.OEt_2$ (2.5 ml, 19.7 mmol) was added. The reaction was conducted at room temperature under nitrogen atmosphere, reacted for 24 hours, process of reaction was monitored by TLC (Toluene : EtOAc = 3:1). After reaction quenched by addition of K_2CO_3, the crude product was extracted from reaction mixture by $CHCl_3$ and then purified by silica gel column with mobile phase (Toluene : EtOAc = 7:1), followed by deprotection of O-acetyl groups under the MeOH/NaOMe conditions. Through a series of processes, the final propargyl α-D-mannopyranoside (1.1 g, 5.05 mmol) was obtained with a yield of 43.2%. The chemical structure of the product in methanol-d_4 was confirmed by 300 MHz ^{1}H NMR spectrum, some significant peaks were observed. ^{1}H NMR (methanol-d_4, 300 MHz): δ = 4.98-4.99 ppm (d, H-1, 1 H), 4.29-4.30 (d, -CH_2-, 2 H), 2.87-2.88 (t, CH ≡ C, 1 H).

2.2.5 Propargyl β-maltoside

Fully acetylated β-maltose (4.2 g, 6.2 mmol) was dissolved in 50 ml dried CH_2Cl_2 with molecular sieve 4A (5 g), then the propargyl alcohol (0.5 ml, 8.7 mmol) and $BF_3.OEt_2$ (2 ml, 15.8 mmol) was added. The reaction was conducted at 30 ℃ under nitrogen atmosphere, reacted for 36 hours, process of reaction was monitored by TLC (Toluene : EtOAc = 2:1). After reaction quenched by addition of K_2CO_3, the crude product was extracted

from reaction mixture by $CHCl_3$ and then purified by silica gel column with mobile phase (Toluene : EtOAc = 4:1), followed by deprotection of O-acetyl groups under the MeOH/NaOMe condition. Through a series of processes, the final propargyl β-maltoside (1.16 g, 3.1 mmol) was obtained with a yield of 50.0%. The chemical structure of product in methanol-d_4 was confirmed by 400 MHz ^{1}H NMR spectrum, some significant peaks were observed. ^{1}H NMR (methanol-d_4, 400 MHz): δ = 5.15-5.16 ppm (H'-1, 1 H), 4.36-4.48 (H-1 and -CH_2-, 3 H), 2.86-2.87 (CH ≡ C, 1 H).

2.2.6 Propargyl β-melibiose

Fully acetylated β-melibiose (4.2 g, 6.2 mmol) was dissolved in 50 ml dried CH_2Cl_2 with molecular sieve 4A (5 g), then the propargyl alcohol (0.5 ml, 8.67 mmol) and $BF_3.OEt_2$ (2 ml, 15.9 mmol) was added. The reaction was conducted at 30 ℃ under nitrogen atmosphere, reacted for 36 hours, process of reaction was monitored by TLC (Toluene : EtOAc = 2:1). The crude product was extracted from reaction mixture by $CHCl_3$ and then purified by silica gel column with mobile phase (Toluene : EtOAc = 4:1), followed by deprotection of O-acetyl groups under the MeOH/NaOMe conditions. Through a series of processes, the final propargyl β-melibiose (0.75 g, 1.97 mmol) was obtained with a yield of 31.8%. The chemical structure of product in methanol-d_4 was confirmed by 300 MHz ^{1}H NMR spectrum, some significant peaks were observed. ^{1}H NMR (methanol-d_4, 300 MHz): δ = 4.49-4.51 ppm (H-1, 1 H), 4.41-4.43 (-CH_2-, 2 H), 2.90-2.92 (CH ≡ C, 1 H), the signal peak of H'-1 was overlapped in H_2O.

2.2.7 Per-D-mannose-grafted-β-cyclodextrin (Man-CD)

The propargyl D-mannose (0.62 g, 2.8 mmol), N_3-CD (0.39 g, 0.3 mmol) and PMDETA (N, N, N', N'', N''-Pentamethyldiethylenetriamine) (83 mg, 0.48 mmol) were dissolved in 25 ml dry DMF. The solution was protected under nitrogen atmosphere and CuBr (70 mg, 0.49 mmol) was added. The reaction mixture was then stirred continuously at 75 ℃ for 60 h under nitrogen atmosphere. The reaction was monitored upon TLC method by using TLC mobile phase (1-propanol : EtOAc : H_2O : $NH_3{\cdot}H_2O$ = 6:1:3:1 or n-butyl alcohol : ethanol : H_2O = 5:4:3). The mixture was dropped into diethyl ether to give precipitate, then the collected precipitate was dissolved in 20 ml deionized water and dialyzed in 2000 ml deionized water for 3 days to give Man-CD (197 mg, 0.07 mmol) as a white solid after overnight freeze-drying with a yield of 23.2%. The dialysis was proceeded in deionized water by using 2kD dialysis membrane, the deionized water for dialysis was replaced for several times. The Man-CD was characterized by 600 MHz ^{1}H NMR and Mass spectrum. ^{1}H NMR (D_2O, 600 MHz): δ = 8.03 ppm (NCH = C, 7 H), 5.15-5.16 (G1,7 H), 4.84 (M1, 7 H), 4.65-4.67 (Partial -CH_2-, 7 H), 4.43-4.47 (Partial -CH_2- and Partial G6, overlapped with D_2O, 14 H), 4.26-4.33 (G5 and partial G6, 14 H), 4.03-4.06 (G3, 7 H), 3.85-3.87 (Partial M6, 7 H), 3.82 (M2, 7 H), 3.75-3.78 (Partial M6, 7 H), 3.64-3.67 (M3, M4 and G2, 21 H), 3.58 (M5, 7 H) and 3.40-3.43 (G4, 7 H). The mass spectrum of Man-CD was calculated for $(M + 2Na)^{2+}/2$: $C_{105}H_{161}O_{70}N_{21}Na_2/2$, 1440.97342; found, 1440.97656.

2.2.8 Per-D-maltose-grafted-β-cyclodextrin (Mal-CD)

The propargyl β-maltoside (1.16g, 3.1 mmol), N_3-CD (0.52g, 0.4 mmol) and PMDETA (N, N, N', N'', N''-Pentamethyldiethylenetriamine) (57mg, 0.33 mmol) were dissolved in 25 ml dry DMF under nitrogen atmosphere. The solution was protected under nitrogen atmosphere and CuBr (50mg, 0.35 mmol) was added. The reaction mixture was then stirred continuously at 80 ℃ for 60 h under nitrogen atmosphere. The reaction was monitored upon TLC method by using TLC mobile phase (1-propanol : EtOAc : H_2O : $NH_3{\cdot}H_2O$ = 6:1:3:1 or n-butyl alcohol : ethanol : H_2O = 5:4:3). The mixture was dropped into diethyl ether to give precipitate, then the collected precipitate was dissolved in 15 ml deionized water and dialyzed in 2000 ml deionized water for 3 days to give Mal-CD (174 mg, 0.044 mmol) as a white solid after overnight freeze-drying with a yield of 11.0%. The dialysis was proceeded in deionized water by using 2kD dialysis membrane, the deionized water for dialysis was replaced for several times. The Mal-CD was characterized by 600 MHz ^{1}H NMR and Mass spectrum. ^{1}H NMR (D_2O, 600 MHz): δ = 8.10 ppm (NCH = C, 7 H), 5.35-5.36 (H'1, 7 H), 5.17-5.18 (G1, 7 H), 4.68-4.82 (-CH_2-, overlapped with D_2O, 14 H), 4.49-4.50 (H1 and partial G6, 14 H), 4.30-4.35 (G5 and partial G6, 14 H), 4.03-4.07 (G3, 7 H), 3.85-3.90 (H5 and H'5, 14 H), 3.75-3.79 (H'6 and H6, 28 H), 3.67-3.74 (H3 and H'3, 14 H), 3.63-3.65 (G2, 7 H), 3.56-3.60 (H'2 and H4, 14 H), 3.39-3.44 (G4 and H'4, 14 H), 3.23-3.26 (H2, 7 H). The mass spectrum of Mal-CD was calculated for $(M + 2Na)^{2+}$: $C_{147}H_{231}O_{105}N_{21}Na_2$, 4016.31770; found, 4016.31912.

2.2.9 Per-D-melibiose-grafted-β-cyclodextrin (Meli-CD)

The propargyl β-melibiose (0.75g, 1.97 mmol), N_3-CD (0.32 g, 0.24 mmol) and PMDETA (N, N, N', N'', N''-Pentamethyldiethylenetriamine) (35 mg, 0.2 mmol) were dissolved in 25 ml dry DMF under nitrogen atmosphere. The solution was protected under nitrogen atmosphere and CuBr (29 mg, 0.2 mmol) was added. The reaction mixture was then stirred continuously at 80 ℃ for 60 h under nitrogen atmosphere. The reaction was monitored upon TLC method by using TLC mobile phase (1-propanol : EtOAc : H_2O : $NH_3{\cdot}H_2O$ = 6:1:3:1 or n-butyl alcohol : ethanol : H_2O = 5:4:3). The mixture was dropped into diethyl ether to give precipitate, then the collected precipitate was dissolved in 15 ml deionized water and dialyzed in 2000 ml deionized water for 3 days to give Meli-CD (160 mg, 0.04 mmol) as a white solid after overnight freeze-drying with a yield of 16.7%. The dialysis was proceeded in deionized water by using 2kD dialysis membrane, the deionized water for dialysis was replaced for several times. The Meli-CD was characterized by 600 MHz ^{1}H NMR and Mass spectrum. ^{1}H NMR (D_2O, 600 MHz): δ = 8.08 ppm (NCH = C, 7 H), 5.18-5.19 (G1, 7 H), 4.98-4.99 (H'1, 7 H), 4.66-4.68 (Partial -CH_2-, 7 H), 4.50-4.53 (G6 and H1, 21 H), 4.31-4.36 (G5, 7 H), 4.04-4.07 (G3, 7 H), 4.00-4.01 (H'4, 7 H), 3.82-3.91 (H'3 and H'2, 14 H), 3.62-3.64 (G2 and H5, 14 H), 3.39-3.54 (H4, H3 and G4, 21 H), 3.23-3.26 (H2, 7 H). The mass spectrum of Meli-CD was calculated for $(M + 2Na)^{2+}$: $C_{147}H_{231}O_{105}N_{21}Na_2$, 4016.31770; found, 4016.32720.

2.3 Results and discussion

2.3.1 The detailed characterization of Man-CD

As it is stated before, some β-CD-based glyco-clusters were synthesized by Cu-catalyzed “click reaction” recently, which revealed that they had a high loading capacity of anti-HIV[38] and enhanced antibiotic activity. And heptamannosylated β-CD was also applied in the research of targeting anticancer therapy recently. However, the chemical structure and detailed peaks assignment of the glyco-clusters has not been determined fully. In this research, the author plan to study NMR spectroscopic characterization of per-D-mannose-grafted-β-CD derivative (Man-CD) as a host model molecule.

Man-CD was synthesized by a slightly modified procedure reported form β-CD through heptakis-(6-deoxy-6-iodine)-β-cyclodextrin (I-CD) and heptakis-(6-deoxy-6-azido)-β-cyclodextrin (N_3-CD) as shown in Scheme 1. Propargyl α-D-mannopyranoside prepared by Lewis acid-catalyzed glycosylation[39] of fully acetylated D-mannose and propargyl alcohol (Scheme 2) was next subjected to Cu-catalyzed “click reaction” with N_3-CD.

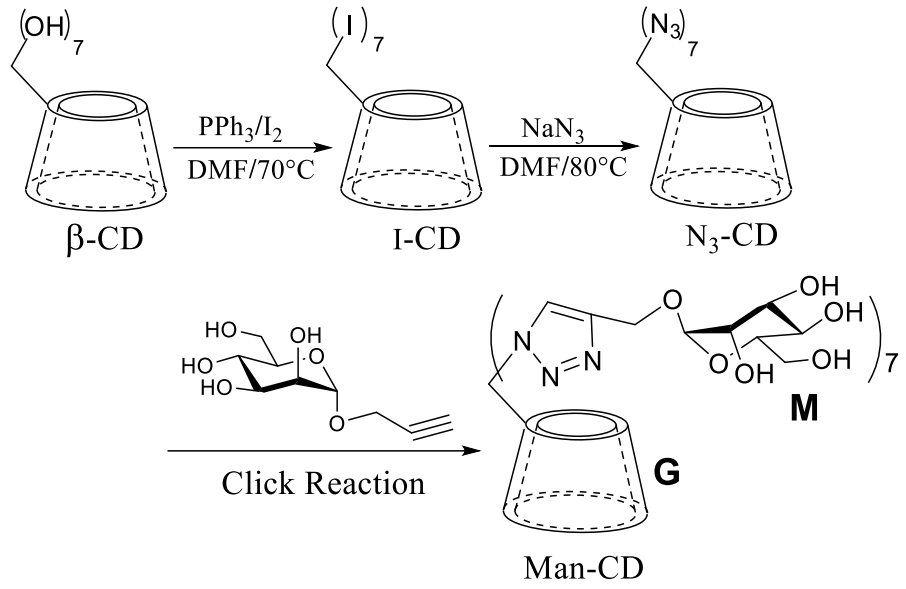

Scheme 1. The “click reaction” to synthesize Man-CD from β-CD.

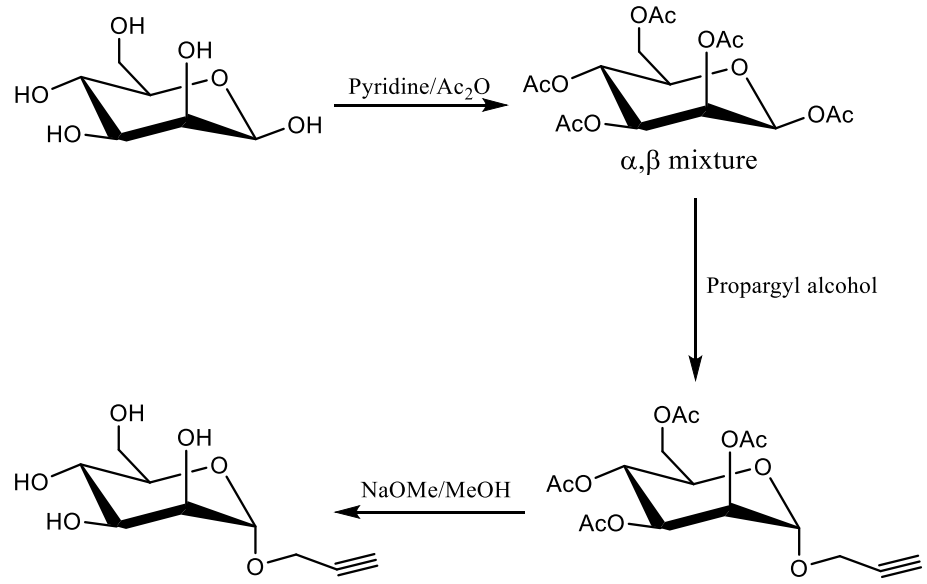

Propargyl α-D-mannopyranoside

Scheme 2. The synthetic route of propargyl α-D-mannopyranoside.

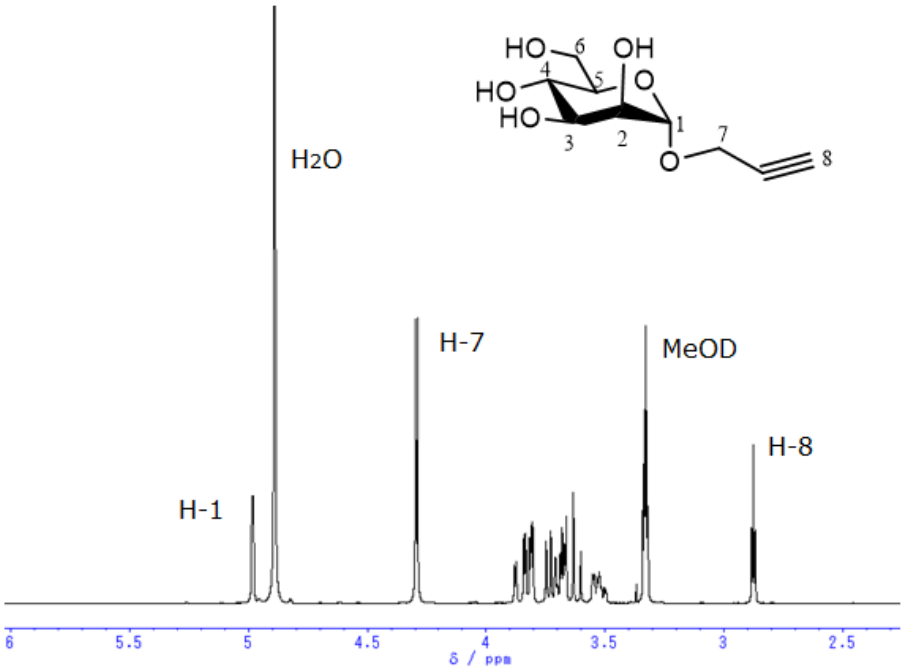

Figure 1. The 300 MHz ^{1}H NMR spectrum of Propargyl α-D-mannopyranoside in methanol-d_4.

The peak of H-8 proton was observed in 300 MHz ^{1}H NMR spectrum (Figure 1), which represent the proton of alkynyl group and indicated that the propargyl α-D-mannopyranoside was successfully prepared, with the consideration of integrate calculation in NMR spectrum. For another starting materials, it is worth mentioning that the process to synthesize I-CD is difficult to be monitored due to the dark color of iodine, so that the excessive triphenylphosphine was added and the reaction time was extended as much as possible. After the 48 hours' reaction, the reaction mixture was dropped into methanol and the precipitate appeared, then the precipitate was collected as the crude product of I-CD. The next step is to

remove the remaining iodine and DMF out from the I-CD's crude product, by using methanol in Soxhlet extractor at the temperature of 80 °C. The ^{1}H NMR results of I-CD in DMSO-d_6 showed that all the 6-OH hydroxyl groups have been substituted for iodo- groups (Figure 2). Then the I-CD was dissolved in dried DMF, with the NaN_3 was added slowly by using plastic instruments to prepare N_3-CD. The metal instruments are forbidden in the preparation of N_3-CD, with the consideration of explosiveness of NaN_3. The reaction mixture was dropped into deionized water to have a precipitate after 48 hours' reaction, the white precipitate was collected and dried under vacuum. As the azido- groups also have no signal peaks in NMR spectrum, the FT-IR spectrum of I-CD and N_3-CD was measured to confirm that all the I-CD was reacted (Figure 3 and Figure 4).

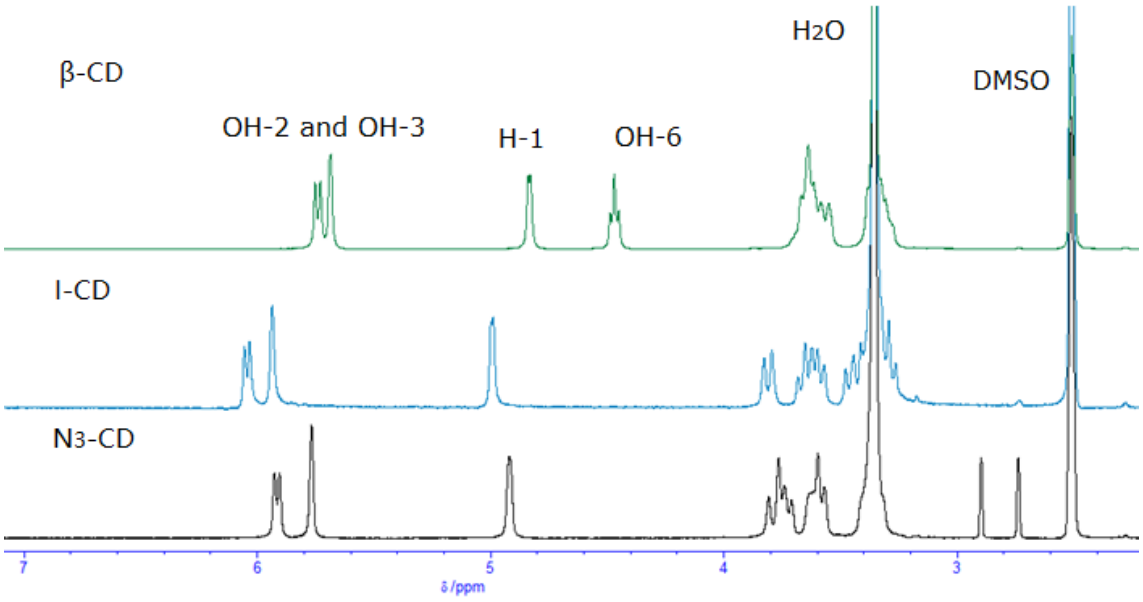

Figure 2. The 300 MHz ^{1}H NMR spectrum of β-CD, I-CD and N_3-CD in DMSO-d_6.

As it is stated, the I-CD and N_3-CD were characterized by mass spectrum. MS m/z: I-CD was calculated for $C_{42}H_{63}O_{28}I_7Na$, 1926.67108; found, 1926.67773. N_3-CD was calculated for $C_{42}H_{63}O_{28}N_{21}Na$, 1332.40436; found, 1332.40768.

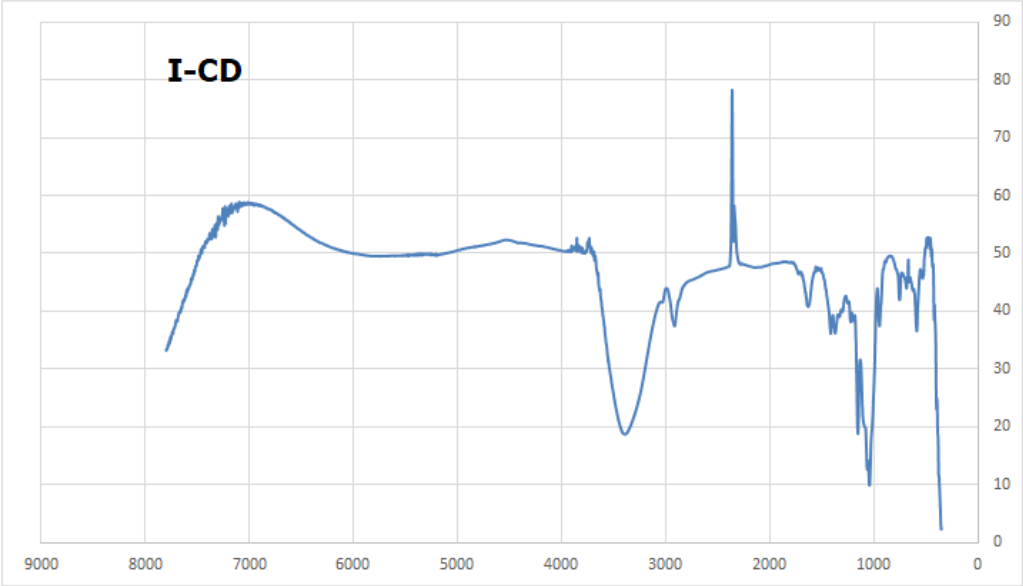

Figure 3. The FT-IR spectrum of I-CD.

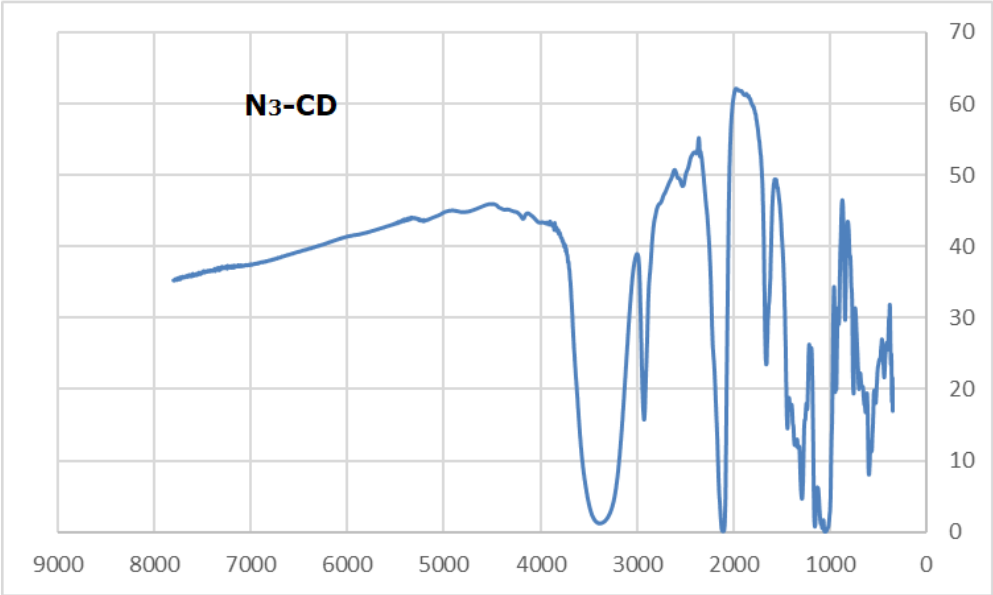

Figure 4. The FT-IR spectrum of N_3-CD.

Then the starting materials for “click reaction” as propargyl α-D-mannopyranoside, N_3-CD were used to synthesize glyco-clusters. The reaction was mediated by CuBr and PMDETA under nitrogen atmosphere. The reaction reacted for a relative long time so that the monitor method should be necessary. Through practice, it was confirmed that the reaction could be monitored upon TLC method by using TLC mobile phase (1-propanol : EtOAc : H_2O : $NH_3.H_2O$ = 6:1:3:1 or N-butyl alcohol : ethanol : H_2O = 5:4:3). Along with the process of reaction, the product points on the TLC board was coming to the bottom gradually due to the increasing polarity. The reaction mixture was then dropped into diethyl ether to give a precipitate, followed by dialysis in deionized water for 3 days to give Man-CD as a white solid after overnight freeze-drying (23.2% yield). The calculated yield is lower than the previous research, and the supposed potential reasons are the long-time dialysis. The dialysis was proceeded in deionized water by using 2KD dialysis membrane, and the deionized water was replaced on time. Based on the mass spectrum and the integrate calculation in ^{1}H NMR spectrum, it could be concluded that the high purity Man-CD was obtained successfully after long-time dialysis. The signal peak of triazole ring proton was also observed in 600 MHz ^{1}H NMR (Figure 3), indicated the successful construction of Man-CD. The mass spectrum of Man-CD was calculated for $C_{105}H_{161}O_{70}N_{21}Na_2/2$, 1440.97342; found, 1440.97656. Because of the complicated chemical structure of Man-CD, the protons of Man-CD were named as G and M, respectively. For example, the G means the protons of CD moiety; the M

means the protons of terminal mannosyl unit.

In the following preparation of Mal-CD and Meli-CD, the basic route is similar to Man-CD, but the difference of molecular size and the resulted steric effect should be taken into consideration. The relative low yields of Mal-CD (11.0%) and Meli-CD (16.7%) could also represent that supposition. With these consideration, the reaction temperature was increased slightly in the preparation of Mal-CD and Meli-CD.

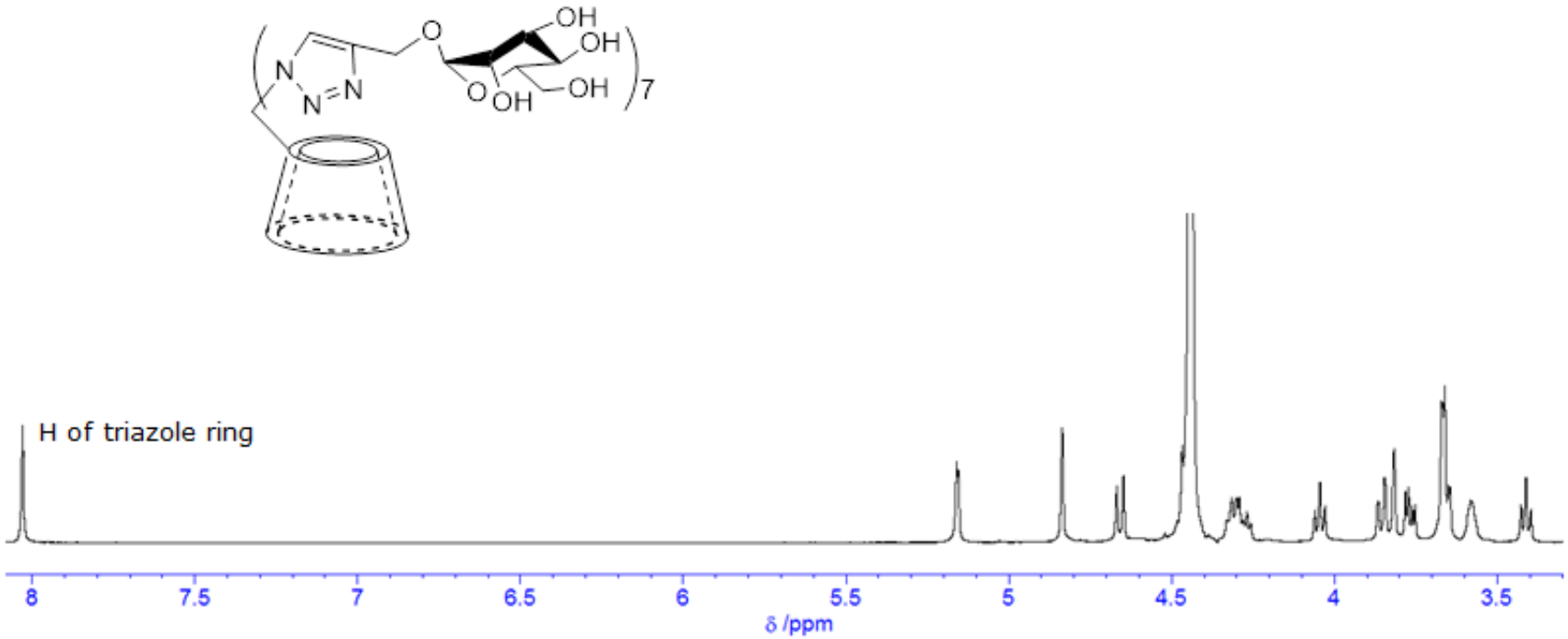

Figure 3. The 600 MHz ^{1}H NMR spectrum of Man-CD in D_2O.

Now it could be confirmed that the successful obtainment of high purity Man-CD, and it is necessary to certain the peaks assignment in the ^{1}NMR spectrum, as it is very useful and convenient to study the inclusion conformation of Man-CD with a detailed information on peaks assignment. The all proton signals of Man-CD in D_2O were consistently assigned by analysis of 2D COSY and TOCSY spectra (from next page, Figure 4 and Figure 5), providing the possibility of NMR spectroscopic analysis of host-guest complexation in the following inclusion study.

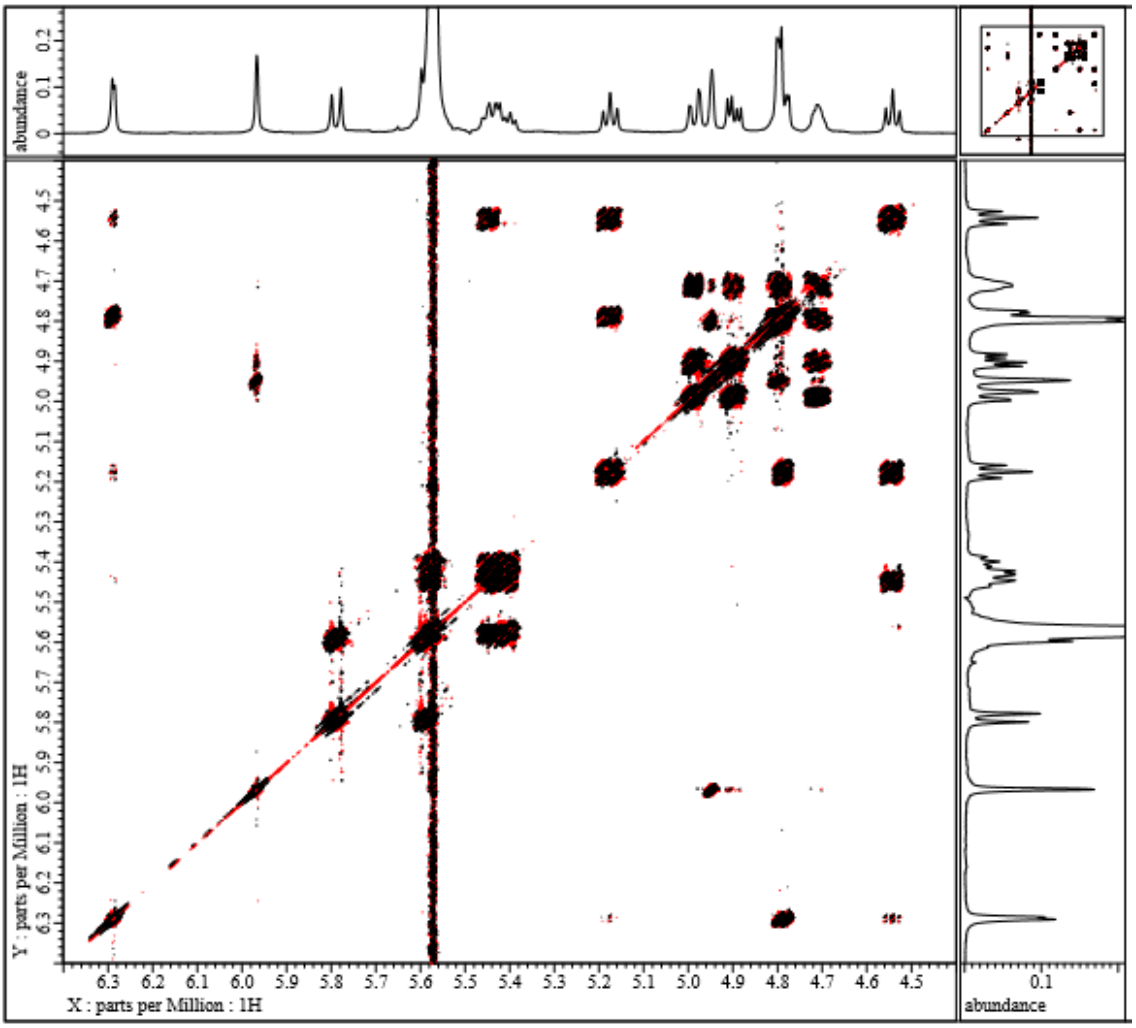

Figure 4. The 600 MHz 2D COSY spectrum of Man-CD in D_2O.

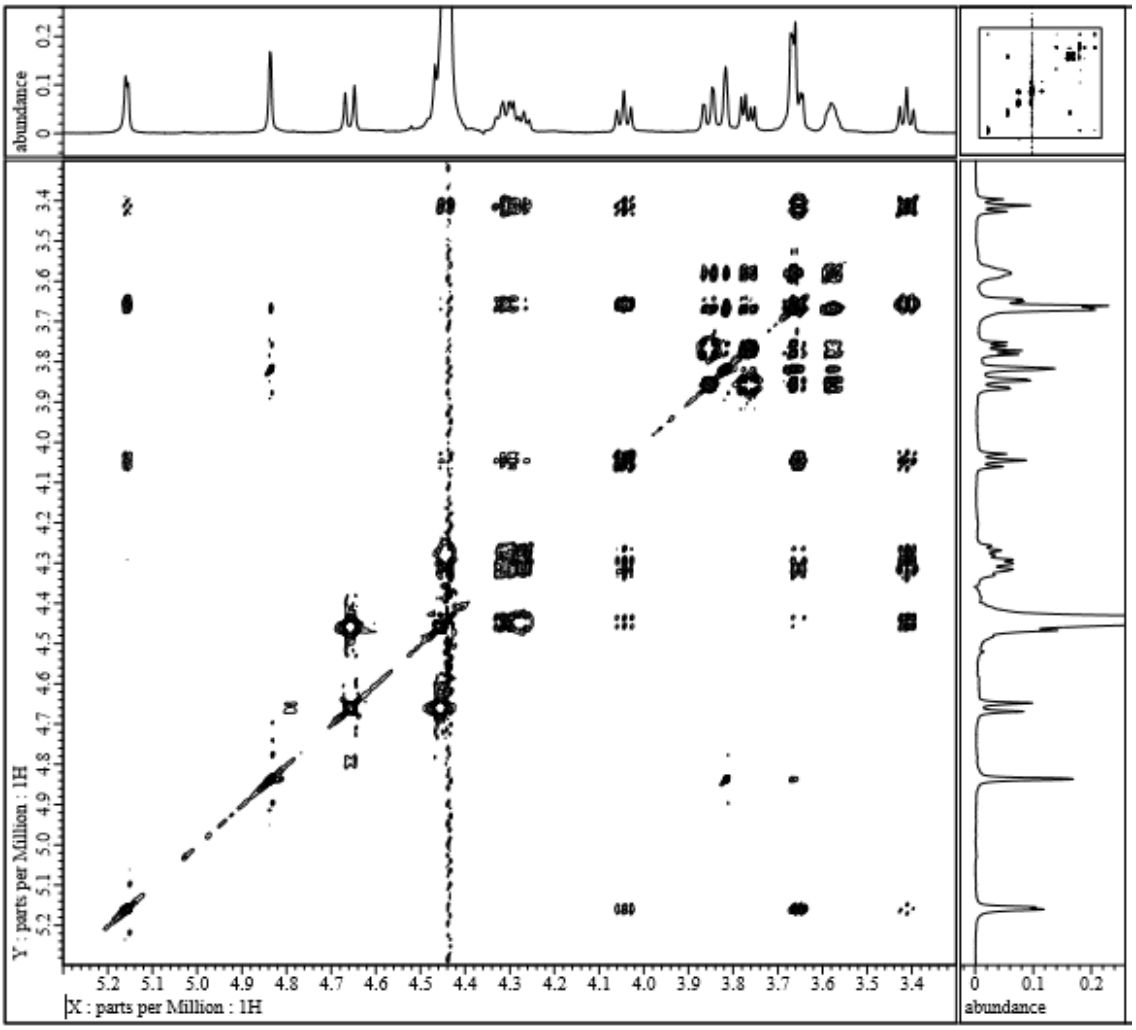

Figure 5. The 600 MHz 2D TOCSY spectrum of Man-CD in D_2O.

According to the observations from 2D COSY and TOCSY spectrum, the ^1H NMR peaks assignment of Man-CD in D_2O was confirmed.

In comparison with ^1H NMR spectra of β-CD (Figure 6), remarkable downfield shift of H-5 and H-6 protons of D-glucose residue (G5 and G6) of Man-CD revealed that 1,2,3-triazole ring was introduced after the "click reaction". The difference of temperature may lead to the shift of D_2O peak.

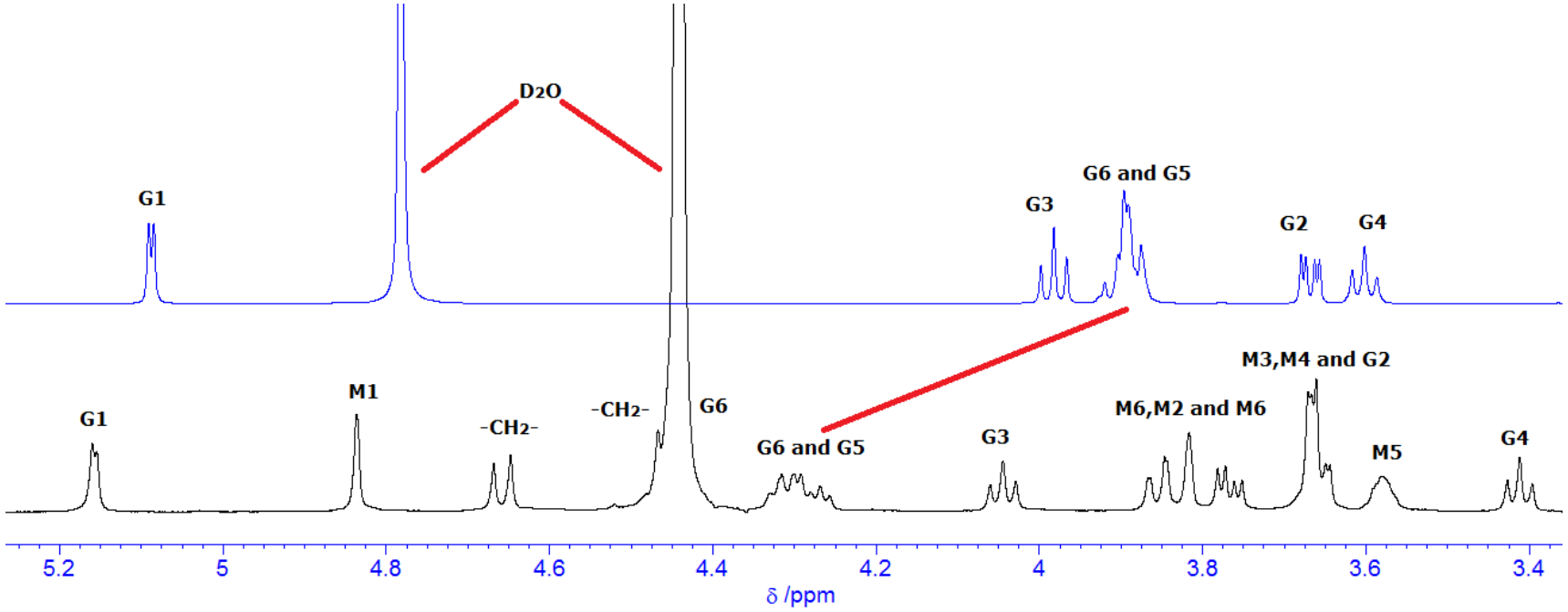

Figure 6. The comparison of 600 MHz ^{1}H NMR spectrum of β-CD and Man-CD in D_2O.

2.3.2 Synthesis of per-D-maltose-grafted-β-cyclodextrin (Mal-CD)

As the concanavalin A (Con A) has specificity for the α-pyranose forms of the monosaccharides glucose and mannose which contain similar hydroxyl group configurations at the 3-, 4-, and 6-positions[40-41], it is significant to synthesize per-β-maltose-grafted-β-cyclodextrin (Mal-CD) due to the specific binding abilities of concanavalin A to α-D-glucosides or α-D-mannosides. Considerate the chemical structures' difference of mannose and maltose, the inclusion properties and lectin binding abilities of Man-CD and Mal-CD should be studied and contrasted. But before that, it is necessary to recognize the inclusion abilities of Mal-CD. Firstly, N_3-CD was also synthesized as the starting material to Mal-CD. The NaN_3 should be used carefully due to its explosive properties.

The propargyl β-maltoside prepared by Lewis acid-catalyzed glycosylation of fully acetylated maltose and propargyl alcohol (Scheme 3) was next subjected to Cu-mediated "click reaction" with N_3-CD (Scheme 4).

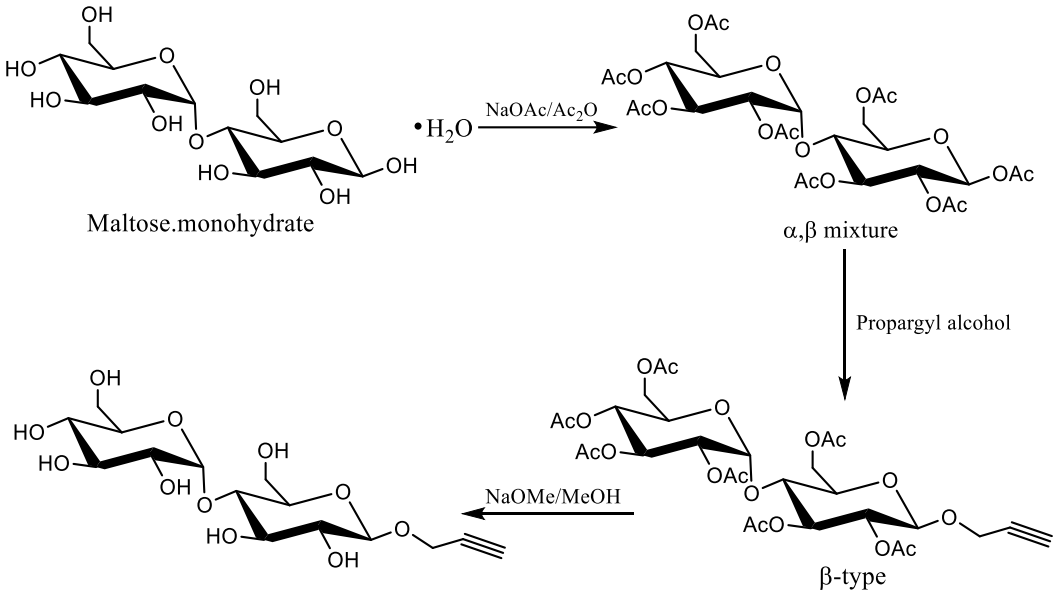

Scheme 3. The synthetic route of propargyl β-maltoside.

Some significant signal peaks of propargyl β-maltoside were observed in 400 MHz ^{1}H NMR spectrum in methanol-d_4 (Figure 7). The signal peaks of H-8 proton (2.86-2.87 ppm), H-7 proton (4.36-4.45 ppm), H-1 proton (4.46-4.48 ppm) and H'-1 proton (5.15-5.16 ppm) were pointed out, and the relative integrate calculation showed that the ratio of H-8 to H'-1 or H-1 is nearly 1:1. Based on the ^{1}H NMR spectrum and integrate calculation, the chemical structure of propargyl β-maltoside was confirmed. In the next step, the propargyl β-maltoside was reacted with N_3-CD to synthesize Mal-CD by Cu-mediated "click reaction". Because of the complicated chemical structure of Mal-CD, the protons of Mal-CD were named as G, H and H', respectively. For example, the G means the protons of CD moiety; the H' means the protons of terminal glucosyl moiety; and the H means the middle glucosyl moiety.

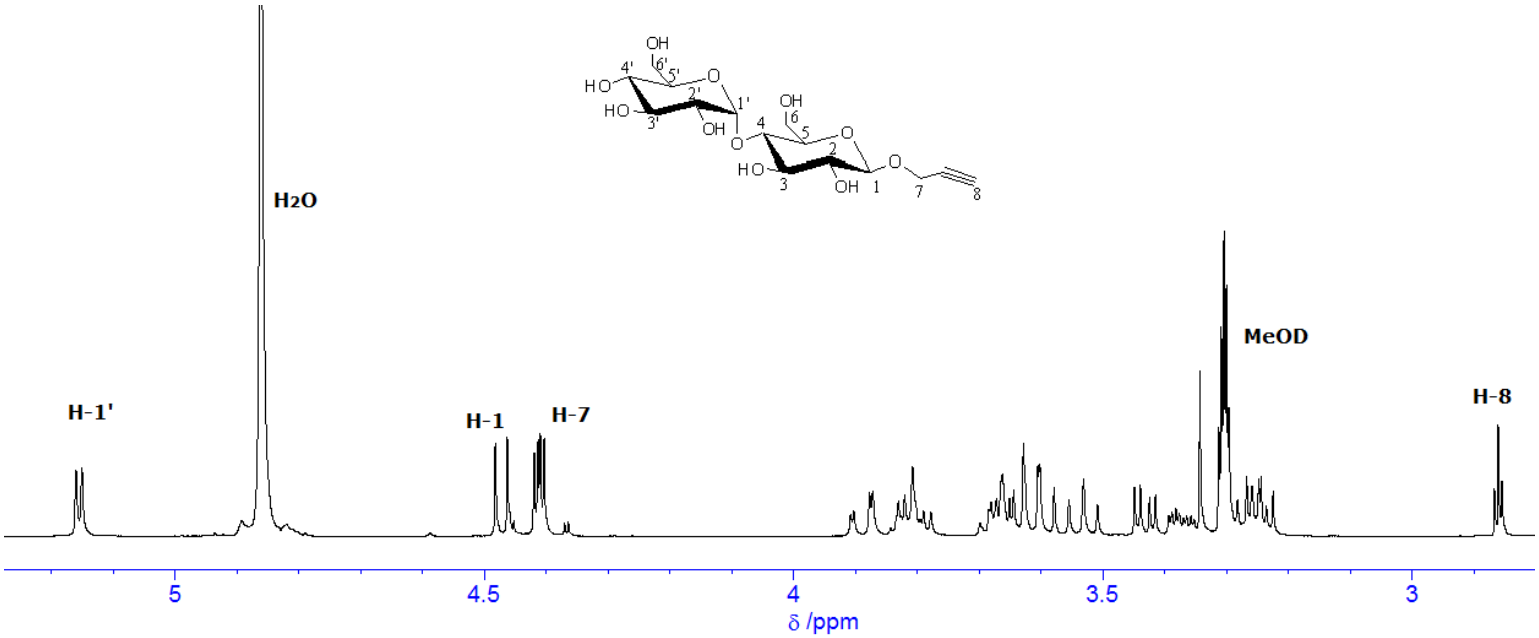

Figure 7. The 400 MHz ^{1}H NMR spectrum of propargyl β-maltoside in methanol-d_4.

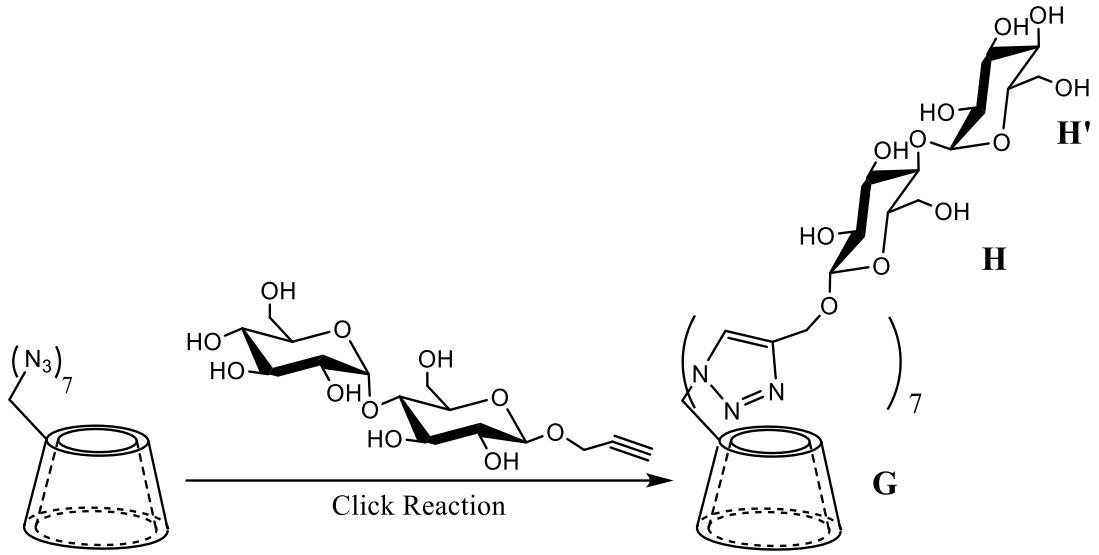

Scheme 4. The “click reaction” to synthesize Mal-CD.

The Mal-CD was synthesized from propargyl β-maltoside and N_3-CD in DMF, with CuBr and PMDETA under nitrogen atmosphere. The solution was stirred continuously at 80 ℃ for about 60 h. The reaction temperature has been increased with the consideration of possible steric effect. The reaction was monitored by using TLC mobile phase (1-propanol : EtOAc : H_2O : $NH_3{\cdot}H_2O$ = 6:1:3:1 or n-butyl alcohol : ethanol : H_2O = 5:4:3). As the TLC results showed the end of reaction, the reaction mixture was dropped into diethyl ether to give a precipitate, followed by dialysis in deionized water for 3 days to give Mal-CD as a white solid (11.0% yield) after overnight freeze-drying. The dialysis was proceeded in deionized water by using 2kD dialysis membrane, and the deionized water was replaced on time. The Mal-CD was characterized by 600 MHz ^{1}H NMR spectrum (Figure 8) firstly. The mass spectrum of Mal-CD was calculated for $(M + 2Na)^{2+}$: $C_{147}H_{231}O_{105}N_{21}Na_2$, 4016.31770; found, 4016.31912.

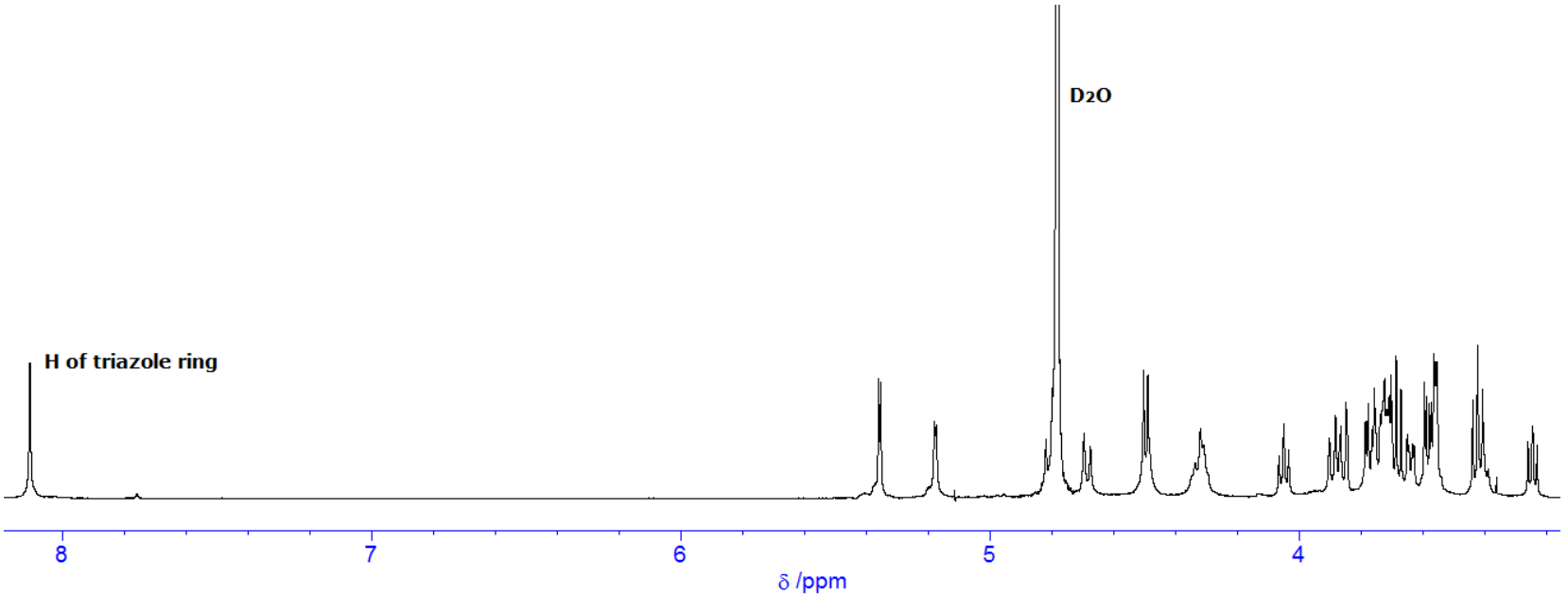

Figure 8. The 600 MHz ^{1}H NMR spectrum of Mal-CD in D_2O.

In addition, the 2D NMR COSY and TOCSY spectrum of Mal-CD were measured to have a recognition on detailed peaks assignment (Figure 9 and Figure 10). In the 600 MHz ^{1}H NMR spectrum of Mal-CD, the signal peak of triazole ring proton (8.10 ppm) was observed.

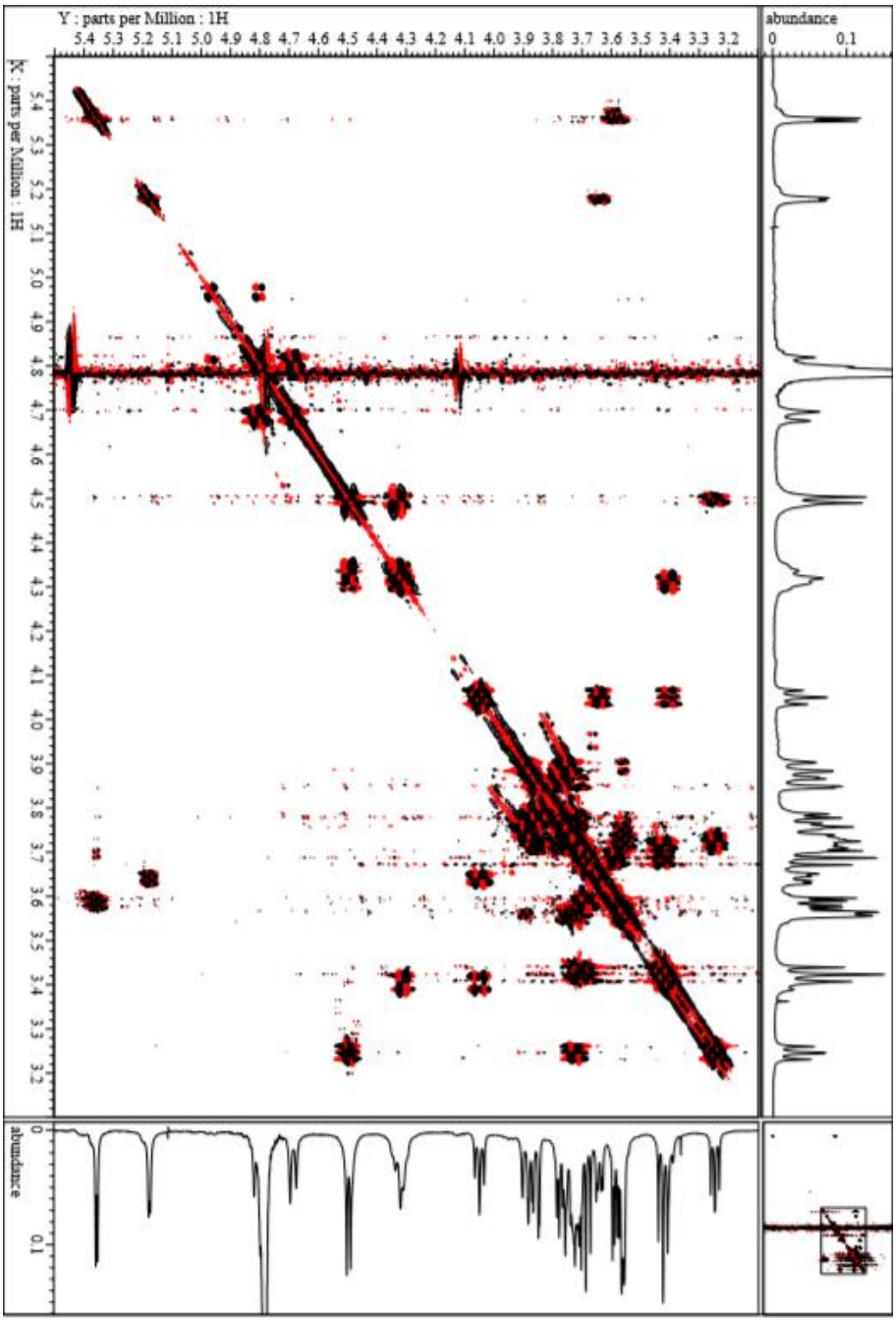

Figure 9. The 600 MHz 2D COSY spectrum of Mal-CD in D_2O.

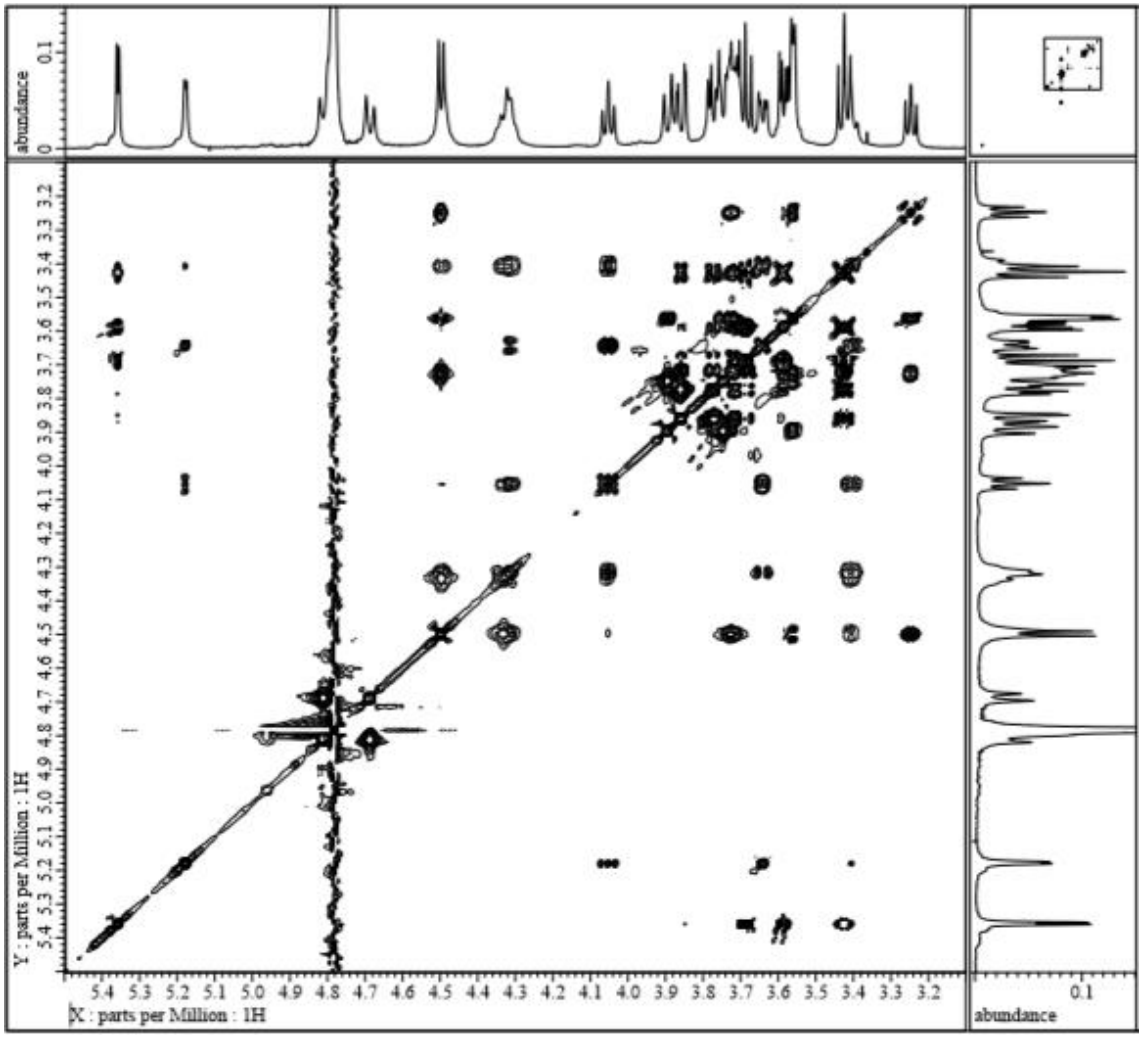

Figure 10. The 600 MHz 2D TOCSY spectrum of Mal-CD in D_2O.

Based on the observations from 2D COSY and TOCSY spectrum, the detailed peaks assignment of Mal-CD in D_2O was deduced. In comparison with β-CD (Figure 11), the protons of G1, G3, G5 and G6 showed the chemical shifts' change to the low magnetic field, and G2, G4 protons showed the contrastive chemical shift's change to high magnetic field.

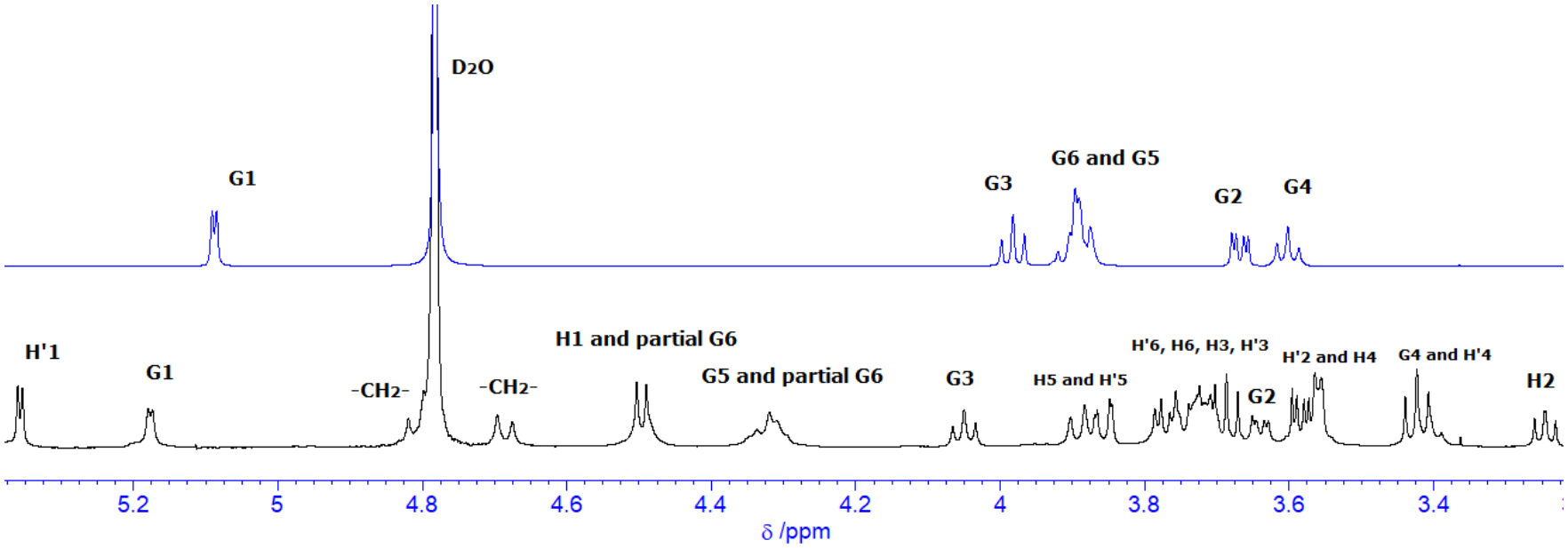

Figure 11. The comparison of 600 MHz ^{1}H NMR spectrum of β-CD and Mal-CD in D_2O.

2.3.3 Synthesis of per-D-melibiose-grafted-β-cyclodextrin (Meli-CD)

Similarly, the per-β-melibiose-grafted-β-cyclodextrin (Meli-CD) was synthesized by Cu-mediated “click reaction”. Because that the α-galactosyl residues of melibiose could bind Griffonia simpiicifolia I (GS I) lectin specifically[42-43], the Meli-CD could be regarded as potential host molecule to construct the targeting drug delivery system. And the study on inclusion abilities of Meli-CD is necessary as well as Man-CD and Mal-CD before the study on lectin recognition abilities.

Before the “click reaction”, propargyl β-melibiose was synthesized by Lewis acid-catalyzed glycosylation of fully acetylated melibiose and propargyl alcohol (Scheme 5) was next subjected to Cu-catalyzed “click reaction” with N_3-CD. The chemical structure of propargyl β-melibiose was characterized by 300 MHz ^{1}H NMR spectrum (Figure 12).

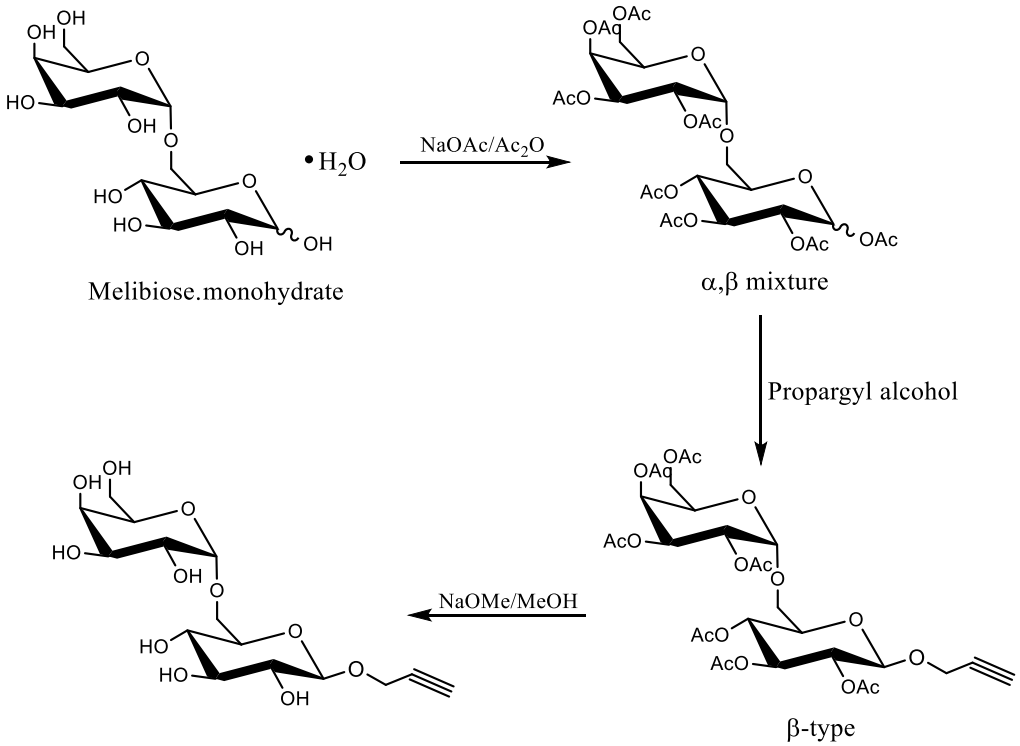

Scheme 5. The synthetic route of propargyl β-melibiose.

In Figure 12, some significant signal peaks of propargyl β-melibiose were observed in 300 MHz ^{1}H NMR spectrum in methanol-d_4. The signal peaks of H-8 proton (2.90-2.92 ppm), H-7 proton (4.41-4.43 ppm), H-1 proton (4.49-4.51 ppm) and H'-1 proton were pointed out, peak of H'-1 proton was overlapped in H_2O. The relative integrate calculation in ^{1}H NMR spectrum showed that the ratio of H-8 to H-1 is nearly 1:1, the ratio of H-8 to H-7 is nearly 1:2. Based on the ^{1}H NMR spectrum and integrate calculation, the chemical structure of propargyl β-melibiose was confirmed.

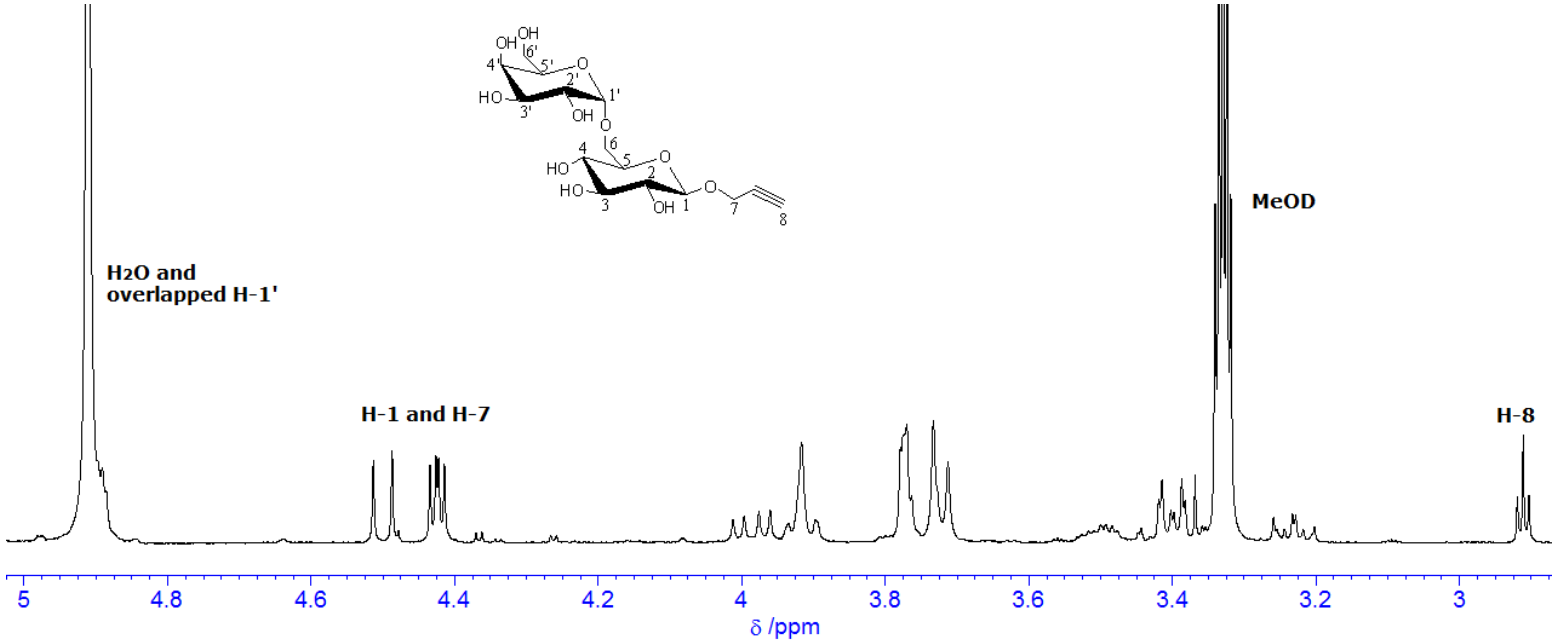

Figure 12. The 300 MHz ^{1}H NMR spectrum of propargyl β-melibiose in methanol-d_4.

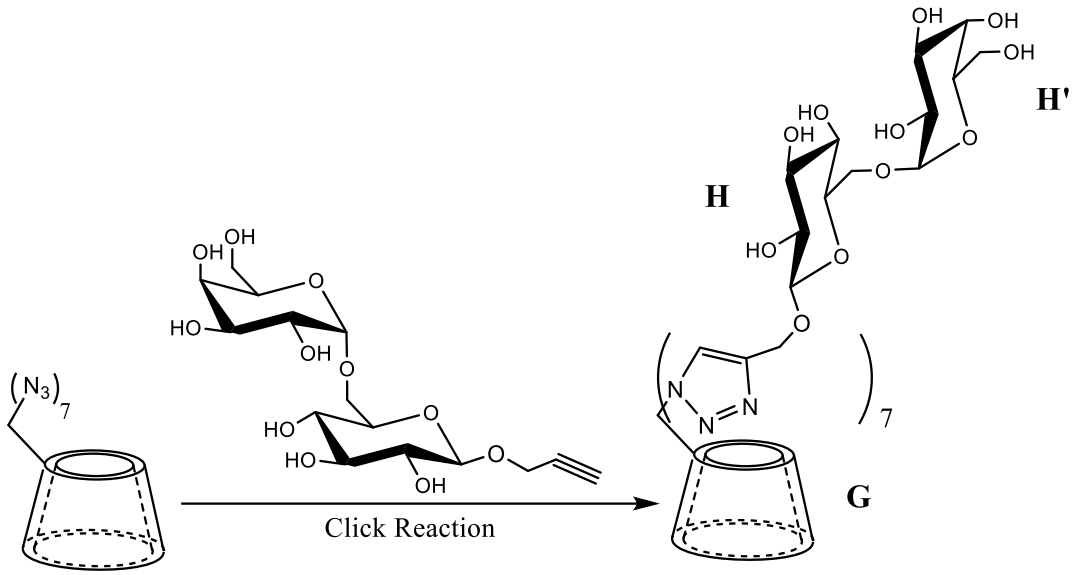

Scheme 6. The “click reaction” to synthesize Meli-CD.

Then the propargyl β-melibiose was reacted with N_3-CD to synthesize Meli-CD in DMF solvent (Scheme 6). The PMDETA and CuBr are important factors in “click reaction” system. The reaction mixture was then stirred continuously at 80 ℃ for 60 h under nitrogen atmosphere. The same as preparations of Man-CD and Mal-CD, the reaction process of Meli-CD was monitored upon TLC method by using TLC mobile phase (1-propanol : EtOAc : H_2O : $NH_3{\cdot}H_2O$ = 6:1:3:1 or n-butyl alcohol : ethanol : H_2O = 5:4:3). With the reaction processing, the product points was coming to the bottom of TLC board due to the increasing polarity. After the end of reaction, the mixture was dropped into diethyl ether to give a precipitate, followed by dialysis in deionized water for 3 days to give Meli-CD as a white solid (16.7% yield) after overnight freeze-drying. The dialysis was proceeded in deionized water by using 2kD dialysis membrane, and the deionized water for dialysis was replaced on time for several times. The chemical structure of Meli-CD was confirmed firstly by 600 MHz ^{1}H

NMR spectrum (Figure 13). The mass spectrum of Meli-CD was calculated for $(M + 2Na)^{2+}$: $C_{147}H_{231}O_{105}N_{21}Na_2$, 4016.31770; found, 4016.32720. Because of the complicated chemical structure of Meli-CD, the protons of Meli-CD were also named as G, H and H', respectively. For example, the G means the protons of CD moiety; the H' means the protons of terminal galactosyl moiety; and the H means the middle glucosyl moiety.

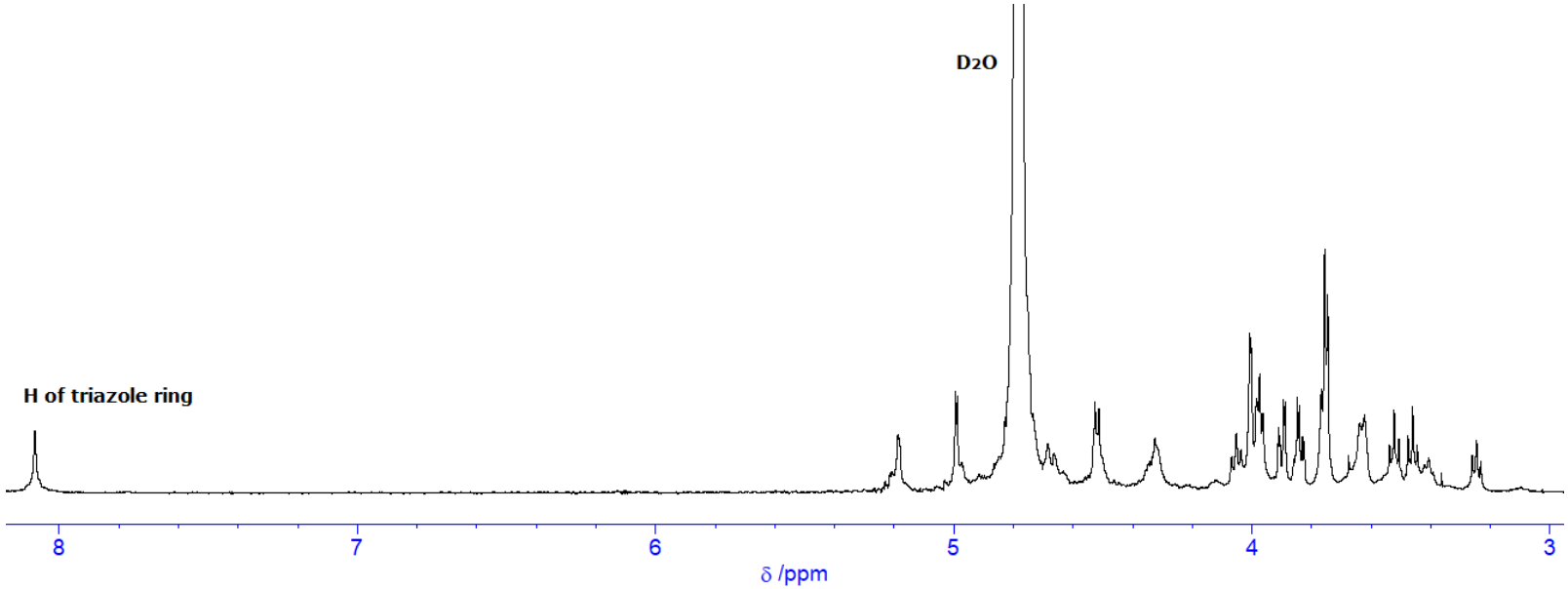

Figure 13. The 600 MHz ^{1}H NMR spectrum of Meli-CD in D_2O.

Based on the observations from the 2D COSY and TOCSY spectrum of Meli-CD (Figure 14 and Figure 15), the relative detailed peaks assignment of Meli-CD was also deduced and will be useful to the analysis on the inclusion behavior with guest molecule.

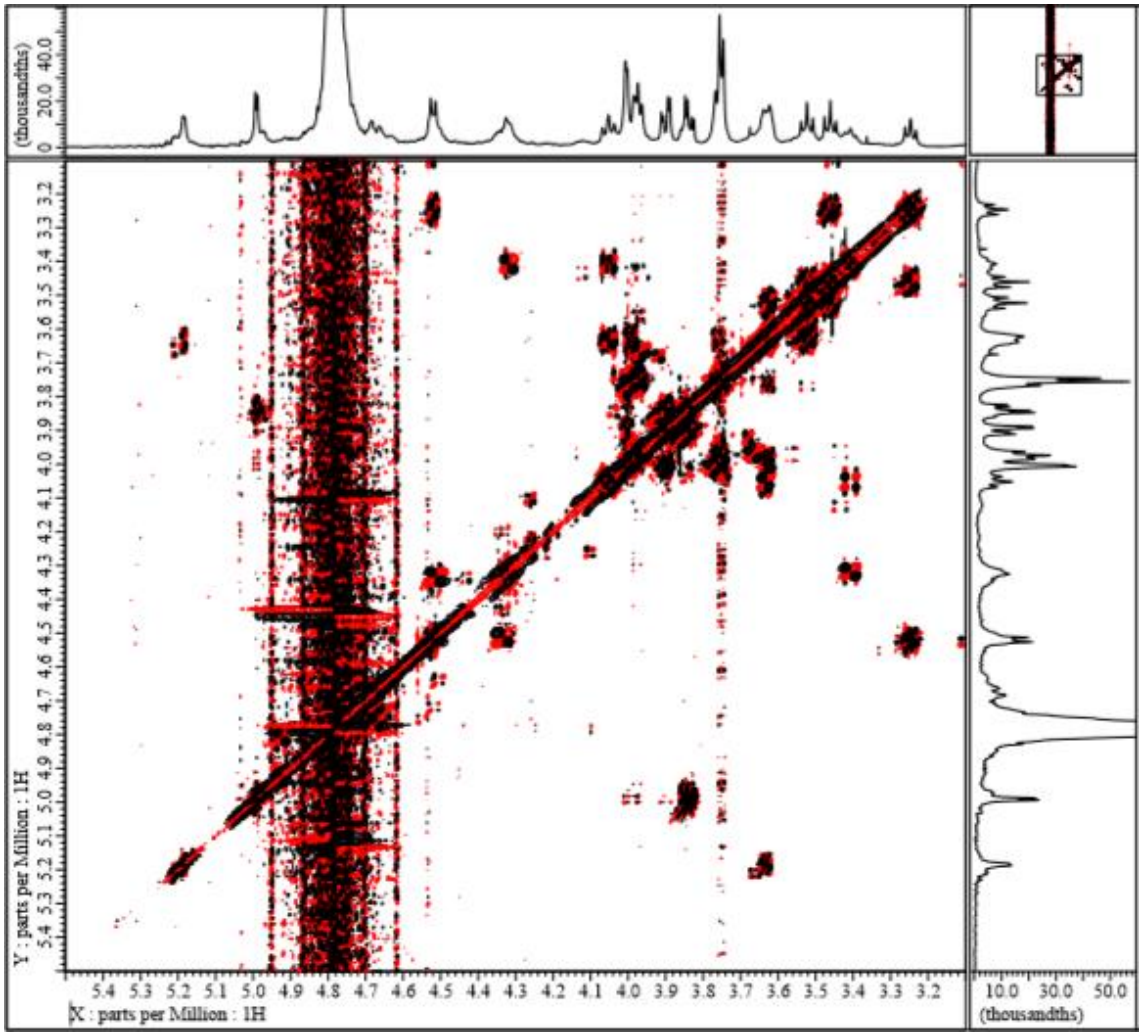

Figure 14. The 600 MHz 2D COSY spectrum of Meli-CD in D_2O.

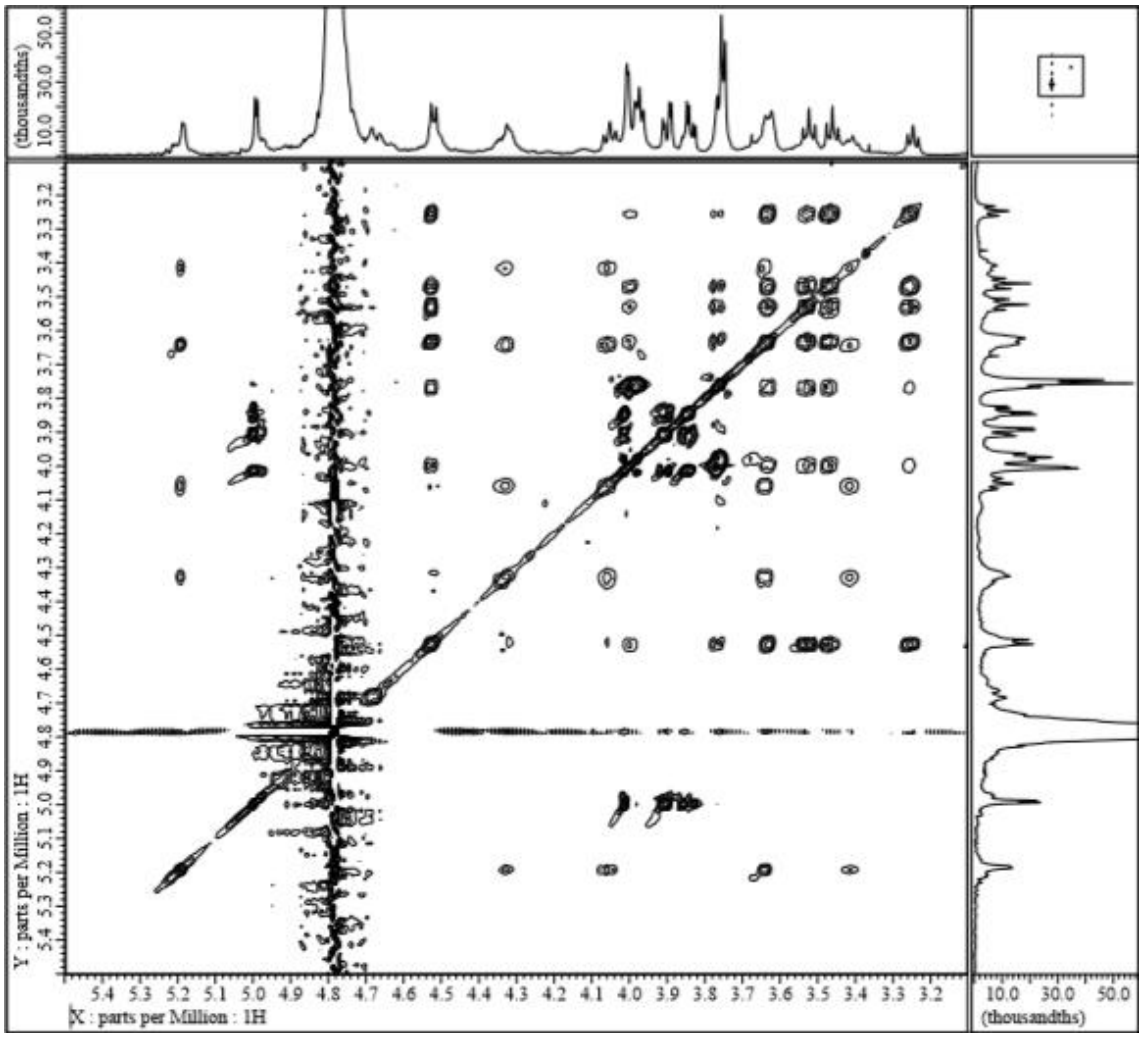

Figure 15. The 600 MHz 2D TOCSY spectrum of Meli-CD in D_2O.

The detailed peaks assignment of Meli-CD was deduced, and some shifted peaks were observed in NMR spectrum clearly. In comparison with β-CD (Figure 16), Meli-CD presented some same phenomenon as Mal-CD. The protons of G1, G3, G5 and G6 also showed the chemical shifts' change to the low magnetic field, and G2, G4 protons showed the contrastive chemical shift's change to high magnetic field, respectively.

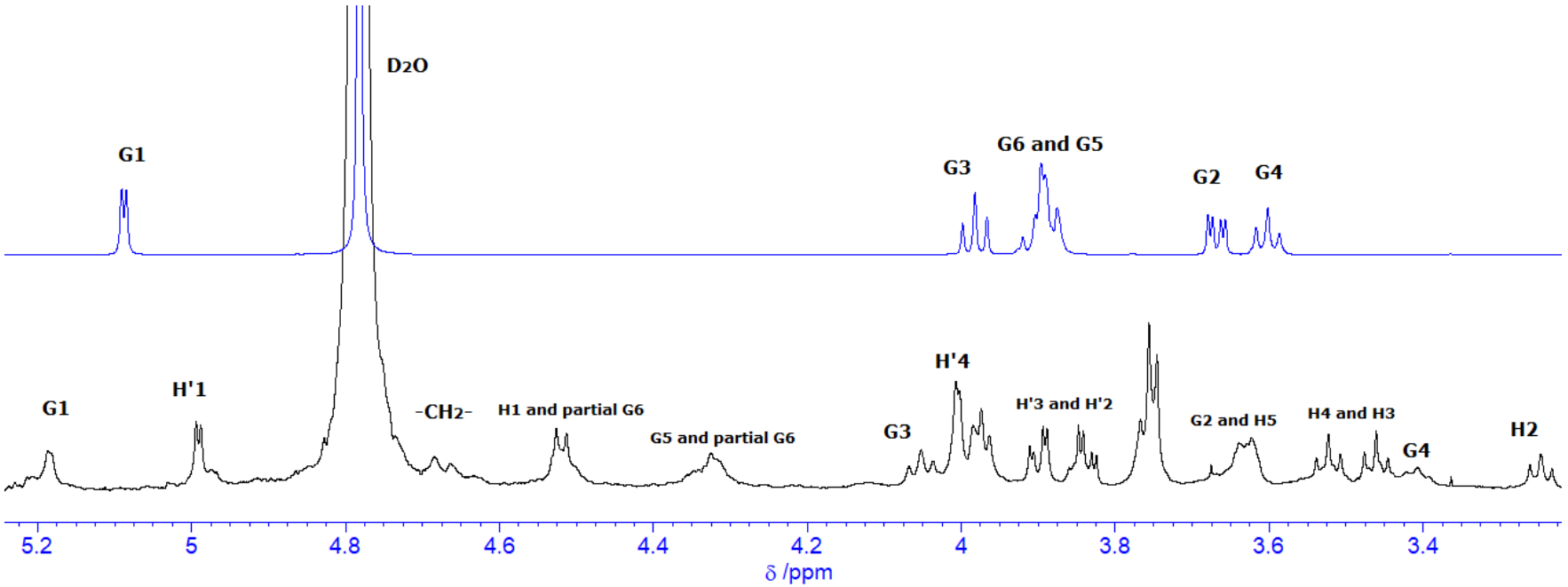

Figure 16. The comparison of 600 MHz ^{1}H NMR spectrum of β-CD and Meli-CD in D_2O.

Besides the ^{1}H and 2D NMR spectrum, the DEPT135 ^{13}C NMR spectrum (Figure 17) was used to characterize the chemical structures of Man-CD, Mal-CD and Meli-CD. Considerate the chemical structures of these three kinds of CD-based glyco-clusters, there are four types of methylene in the chemical structures of Mal-CD and Meli-CD; and three types of methylene in the chemical structure of Man-CD. In the DEPT135 ^{13}C NMR spectrum, the only downward peak of β-CD was observed; the three downward peaks of Man-CD were observed; the four downward peaks of Mal-CD and Meli-CD were observed.

The above observations from DEPT135 ^{13}C NMR spectrum were in accordance with the preconceived chemical structures of these three kinds of CD-based glyco-clusters, and provided the further confirmation for the chemical structures of Man-CD, Mal-CD and Meli-CD.

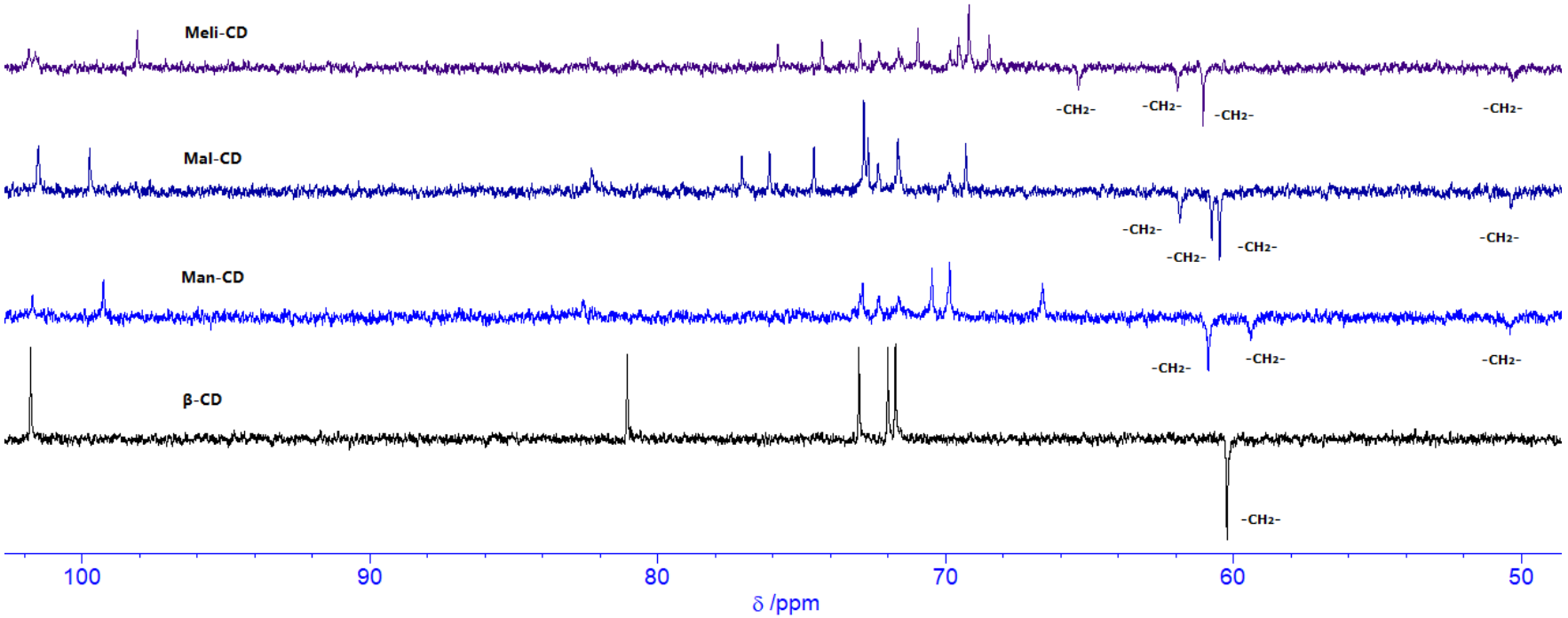

Figure 17. The 300 MHz DEPT135 ^{13}C NMR spectrum of β-CD, Man-CD, Mal-CD and Meli-CD in D_2O.

2.4 Conclusion

The Man-CD, Mal-CD and Meli-CD were successfully synthesized by slightly modified chemical method and characterized by ^{1}H NMR spectrum, 2D NMR spectrum, DEPT135 ^{13}C NMR spectrum and Mass spectrum.

The chemical structures and high purities of Man-CD, Mal-CD and Meli-CD were also confirmed through different characterizations. The potential reason for the low yields of Man-CD, Mal-CD and Meli-CD was supposed as the long-time dialysis in deionized water.

Based on the observations from 2D COSY and TOCSY spectrum, the detailed peaks assignment of Man-CD, Mal-CD and Meli-CD were illustrated. Considerate the multi-substituted sugar groups and complicated space structures of Man-CD, Mal-CD and Meli-CD, the illustration for detailed peaks assignments are significant and useful to the inclusion applications of these CD-based glyco-clusters. In next chapter, the Man-CD, Mal-CD and Meli-CD were used as host molecules in the research on inclusion abilities with selected guest molecule.

Chapter 3

Formation of inclusion complexes between cyclodextrin-based glyco-clusters and antiphlogistic ibuprofen

3.1 Introduction

As it is stated in the general introduction, the β-CD and its derivatives have been extensively applied to increase the physicochemical properties of guest molecules through host-guest inclusion behavior. Besides, CD-based glyco-clusters could be regarded as molecule vehicle due to the carbohydrate-lectin specific recognition abilities. In order to examine the applicability of the CD-based glyco-clusters described in the previous chapter, their inclusion abilities were firstly examined using a model drug molecule, ibuprofen sodium salt.

Ibuprofen (IBU), one of the nonsteroidal anti-inflammatory drugs, was developed as an antirheumatic drug in the 1960s[44], and it also has the physiological properties such as analgesic, antipyretic and antimicrobial activities[45]. As detailed information of inclusion complex between IBU and CD derivatives has been accumulated[46-47], IBU was thought to be an ideal guest molecule to investigate the inclusion abilities of Man-CD, Mal-CD and Meli-CD. It is worth mentioning that the racemic IBU is in clinical use nowadays[48]. For example, the (S)-ibuprofen is over 100-fold more potent than (R)-ibuprofen as an inhibitor of cyclooxygenase I, but the inactive (R)-enantiomer could undergo chiral inversion into the active (S)-enantiomer in the body[49].

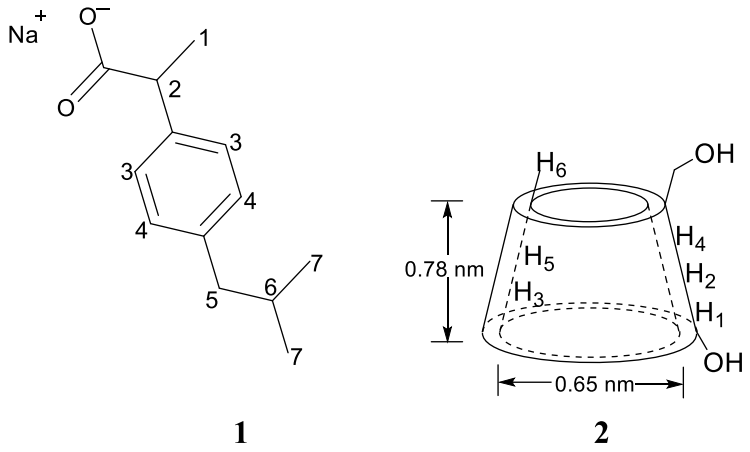

Figure 1. The chemical structure of IBUNa and β-CD.

As IBU could be very slightly dissolved in pH 7 aqueous media[50], the author used an ionic derivative of it: racemic IBU sodium salt (IBUNa) **1**. Molecular size of IBU is approximately 1.3 nm length and 0.6 nm width, which are approximately 1.7 times larger than depth of β-CD **2** cavity (0.78 nm) and slightly smaller than the cavity diameter (0.65 nm), respectively (Figure 1)[51]. In this chapter, the author would like to discuss the effect of the highly functionalized substituents of CD-based glyco-clusters including triazole moiety on inclusion modes in terms of NMR spectroscopy. The inclusion behavior between original β-CD and IBUNa was also investigated in this chapter to have a contrast to CD-based glyco-clusters. The NMR Job's plot experiments for β-CD and CD-based glyco-clusters were conducted, to have a further understanding of stoichiometry and inclusion properties of Man-CD, Mal-CD and Meli-CD.

3.2 Experiment

3.2.1 Materials and methods

All reagents including β-CD and IBUNa were used from commercial resources without further purification. The Man-CD, Mal-CD and Meli-CD were prepared through a series of chemical procedures. ^{1}H NMR spectrum were recorded on Bruker Ultrafield Avance 300, JEOL Excalibur 400 and JEOL ECA 600 spectrometers. 2D NMR spectrum were recorded on JEOL ECA 600 spectrometer.

3.2.2 Job's plot experiments

Job's plot experiments were conducted by 300 MHz ^{1}H NMR spectrum corresponding to chemical shifts' change of the protons of IBUNa's aromatic ring in the presence of CDs. The total concentration of CDs and IBUNa was kept at 4.38 mM in experiments. The ratio of CDs is from 0 to 0.8.

3.2.3 NMR titration

The associate constants (Ks) values were evaluated by curve fitting of the proton chemical shift changes in ^{1}H NMR spectrum. With this method, the concentration of guest IBUNa was kept at 1.75 mM in D_2O and the concentrations of host CDs were varied from 0 mM to 2.63 mM in D_2O.

3.3 Results and discussion

3.3.1 Inclusion ability of Man-CD

Chemical shift of IBUNa was affected by formation of inclusion complex. Total host and guest concentration [H + G] was constant (4.38 mM) and ratio of [H] to [H + G] was ranging from 0 to 0.8. The wide-ranging ^{1}H NMR spectrum recorded the chemical shifts' change of protons of IBUNa with the increasing ratio of β-CD and Man-CD (Figure 2 and Figure 3). In Figure 2, the signal peak of H-4 proton of IBUNa shifted to upper magnetic field obviously with the increasing ratio of β-CD. In Figure 3, the signal peak of H-3 proton of IBUNa shifted to low magnetic field obviously with the increasing ratio of Man-CD. In addition, the peak of methyl proton H-7 of IBUNa had unobvious chemical shift change toward lower magnetic field with increment of β-CD or Man-CD.

Based on the observations in Figure 2 and 3, the H-3 and H-4 protons were selected as the referential protons for the Job's plot experiment and Ks values' calculation.

Figure 4 showed partial ^{1}H NMR spectra of β-CD/IBUNa and Man-CD/IBUNa with different host-guest ratio. With increment of β-CD concentration, the peak of H-4 of aromatic ring of IBUNa significantly shifted upper magnetic field, while the peak of H-3 was slightly shifted (Figure 4 (a)). Peak broadening and splitting observed at H-3 was probably due to use of racemic mixture of IBUNa, which was located in a chiral cavity of β-CD. On the other hand, inclusion with Man-CD resulted in

chemical shift change of H-3. Interestingly, H-3 was shifted toward lower magnetic field (Figure 4 (b)).

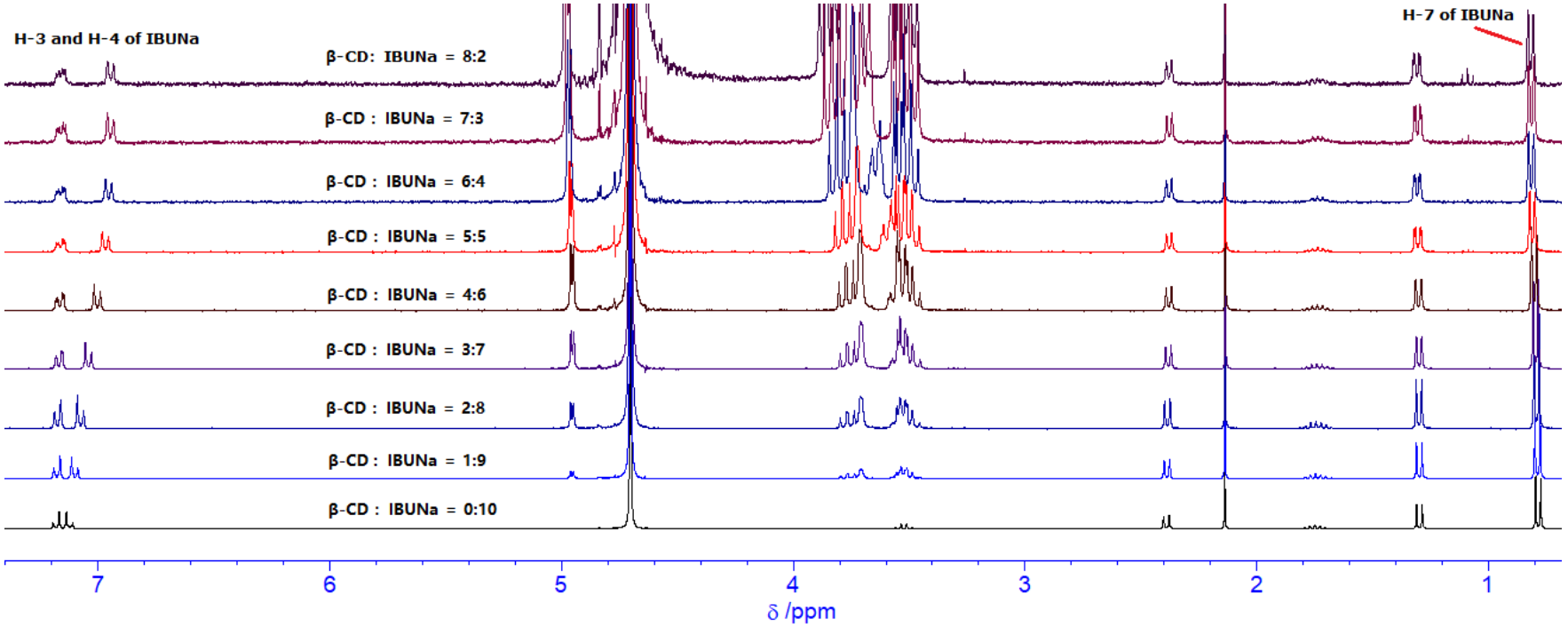

Figure 2. The 300 MHz ^{1}H NMR spectrum of IBUNa with the increasing ration of β-CD in D_2O.

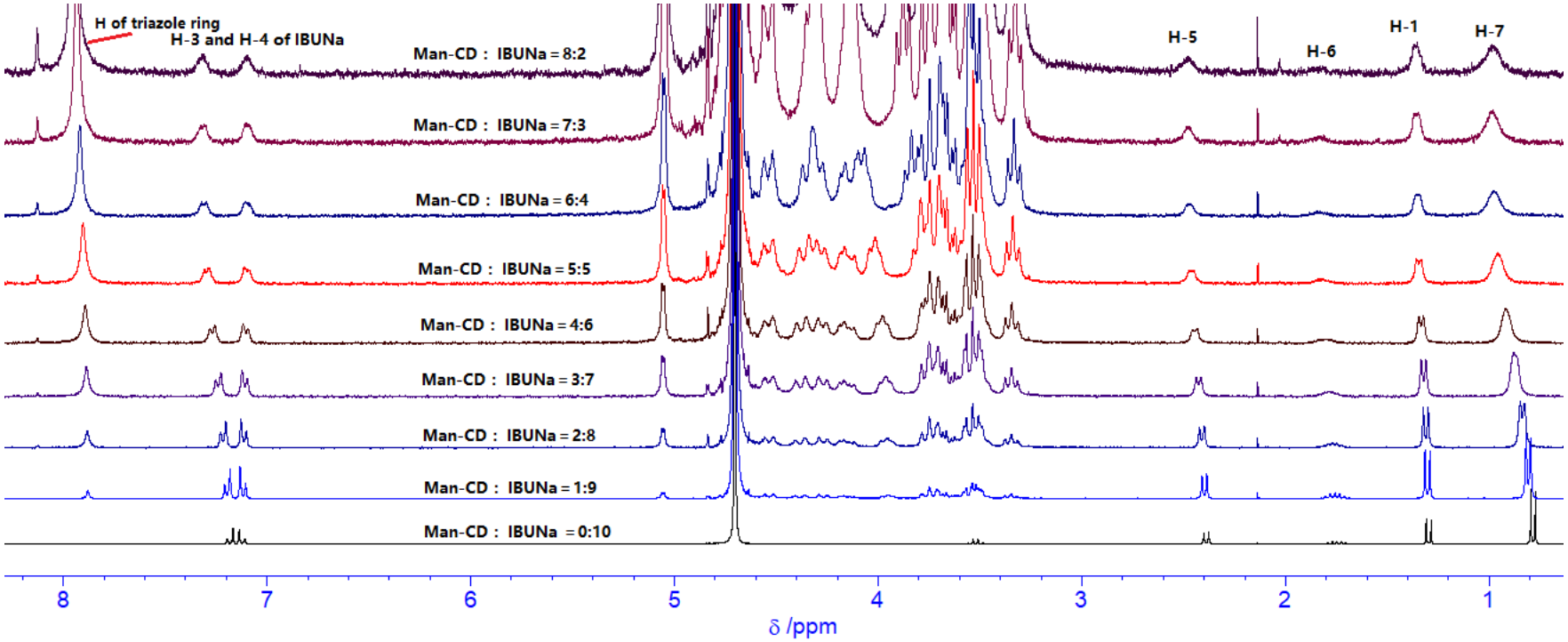

Figure 3. The 300 MHz ^{1}H NMR spectrum of IBUNa with the increasing ration of Man-CD in D_2O.

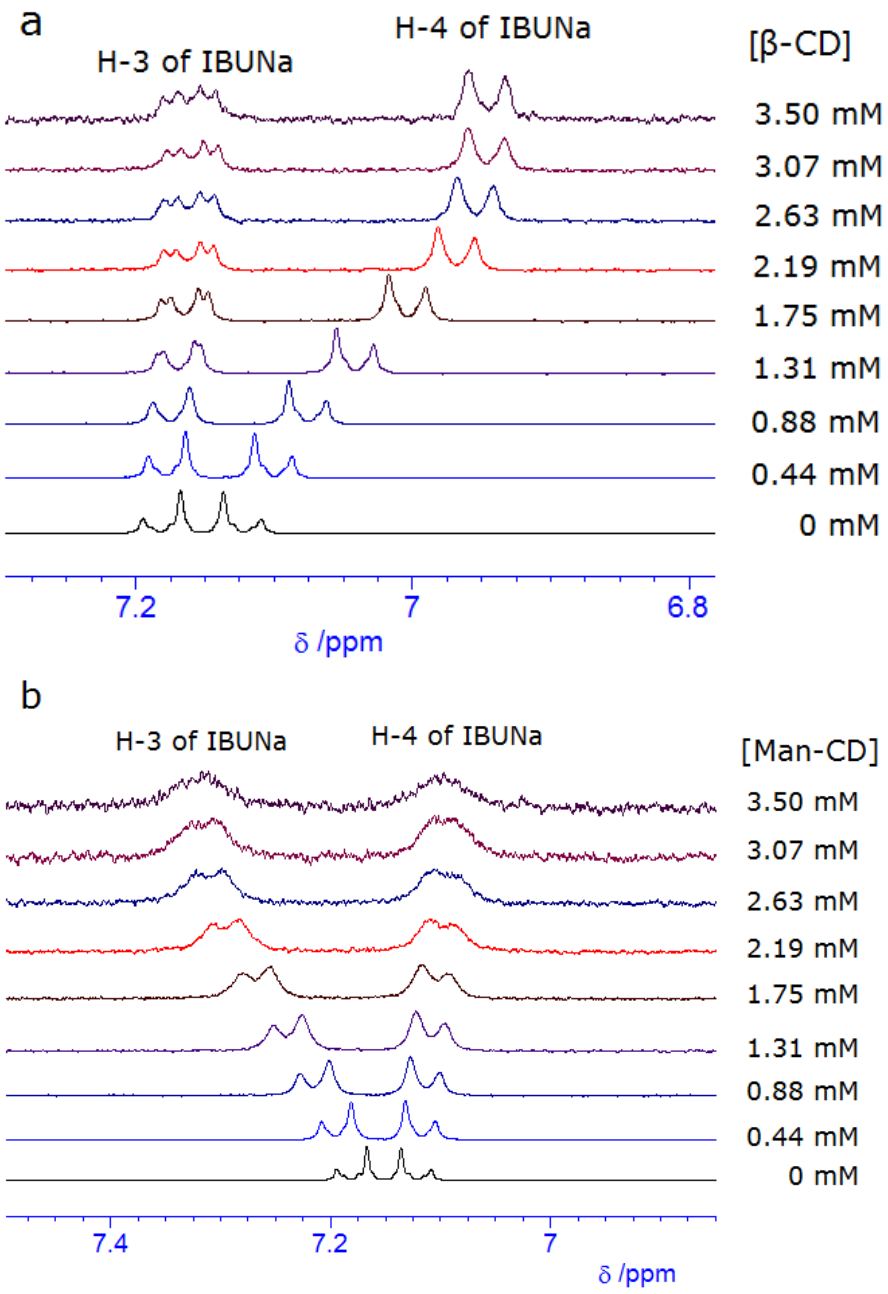

Figure 4. Partial 300 MHz ^{1}H NMR spectrum (aromatic region) of inclusion complex of IBUNa in D_2O. Total concentration of CD and IBUNa was kept at 4.38 mM, CD ratio was ranging from 0 to 0.8. (a) β-CD. (b) Man-CD.

β-CD/IBUNa in D_2O

Ratio of β-CD	Chemical shifts' change of H-4 of IBUNa
0	0
0.1	-0.0226
0.2	-0.0473
0.3	-0.0819
0.4	-0.1198
0.5	-0.1549
0.6	-0.1689
0.7	-0.1763
0.8	-0.1772

Man-CD/IBUNa in D_2O

Ratio of Man-CD	Chemical shifts' change of H-3 of IBUNa
0	0
0.1	+0.0143
0.2	+0.0348
0.3	+0.0595
0.4	+0.087
0.5	+0.1158
0.6	+0.132
0.7	+0.1405
0.8	+0.1501

Table 1. The relative chemical shifts' change for job's plot curves.

Based on these data of chemical shifts' change (Table 1), Job's plot of continuous variation was obtained as shown in Figure 5. Job's plot curves based on the chemical shifts of selected aromatic protons in IBUNa

denoted the 1:1 inclusion mode of β-CD/IBUNa and Man-CD/IBUNa inclusion complex[52].

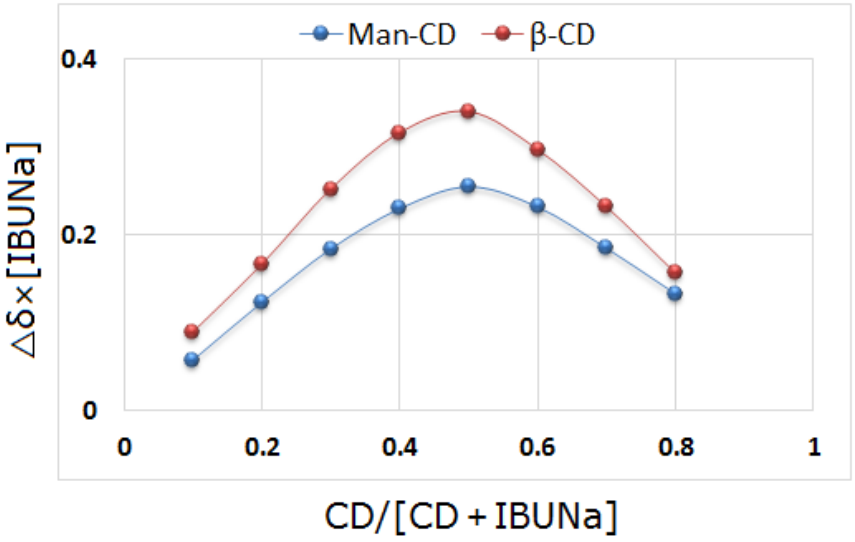

Figure 5. Job's plots corresponding to chemical shifts' change of the protons of IBUNa's aromatic ring in the presence of CDs. The total concentration of CD and IBUNa was kept at 4.38 mM in experiments.

In addition, the associate constants (Ks) values could also be evaluated by curve fitting of the proton chemical shift changes[53]. With this method, the concentration of guest IBUNa was kept at 1.75 mM in D_2O and the concentration of host CDs was varied from 0 mM to 2.63 mM in D_2O. With the increasing concentrations of host CDs, the chemical shift changement of aromatic protons of IBUNa occurred regularly in NMR measurement (Figure 6). Based on the experimental data, the Ks values for β-CD/IBUNa and Man-CD/IBUNa complex were calculated as 0.87×10^4 and 2.9×10^4 M^{-1}, respectively (Figure 7). The Ks values for Man-CD/IBUNa is 3.3-fold higher than β-CD/IBUNa, the potential reason

hypothesized is that the hydrophobic area which formed in the process of “click reaction” to synthesis Man-CD. Seven triazole rings which locate beside the narrow side of Man-CD may generate a hydrophobic area, and the hydrophobic area is equivalent to an effective enlargement of the hydrophobic inner cavity of Man-CD. Consequently, the inclusion ability of Man-CD is preferable to β-CD in this research.

a

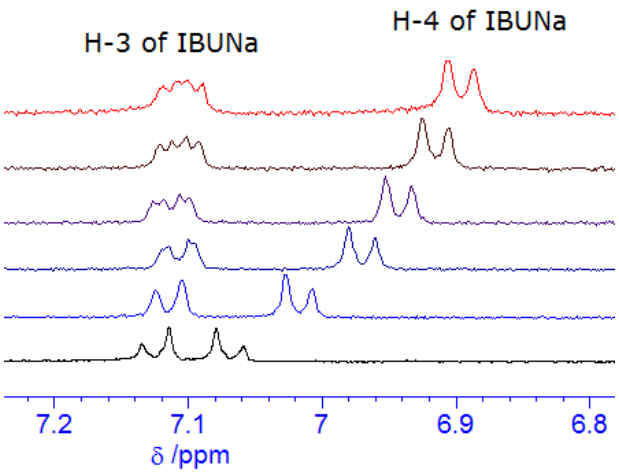

b

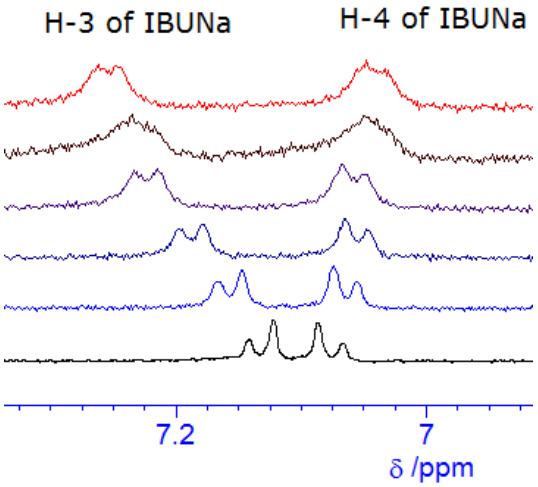

c

CDs' concentrations (mM)	0	0.44	0.88	1.31	1.75	2.63
Chemical shifts' change of H-4 of IBUNa in β-CD	0	– 0.0511	– 0.0987	– 0.1268	– 0.1536	– 0.1744
Chemical shifts' change of H-3 of IBUNa in Man-CD	0	+ 0.0257	+ 0.0563	+ 0.0929	+ 0.1135	+ 0.1258

Figure 6. (a) Partial 400 MHz ^{1}H NMR spectrum of IBUNa in the presence of β-CD in D_2O, the concentration of IBUNa was kept at 1.75 mM with the increasing concentration of β-CD from 0 to 2.63 mM; (b) Partial 400 MHz ^{1}H

NMR spectrum of IBUNa in the presence of Man-CD in D_2O, the concentration of IBUNa was kept at 1.75 mM with the increasing concentration of Man-CD from 0 to 2.63 mM; (c) The chemical shifts' change of H-4 in the presence of β-CD and the chemical shifts' change of H-3 in the presence of Man-CD.

a

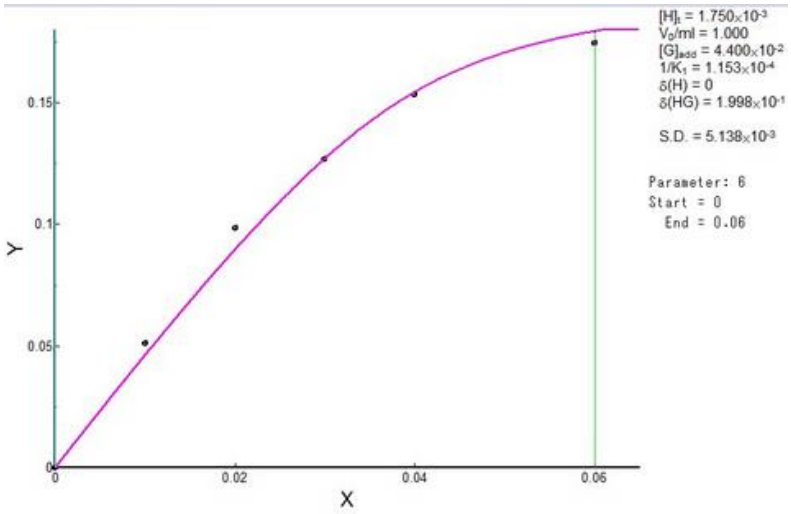

b

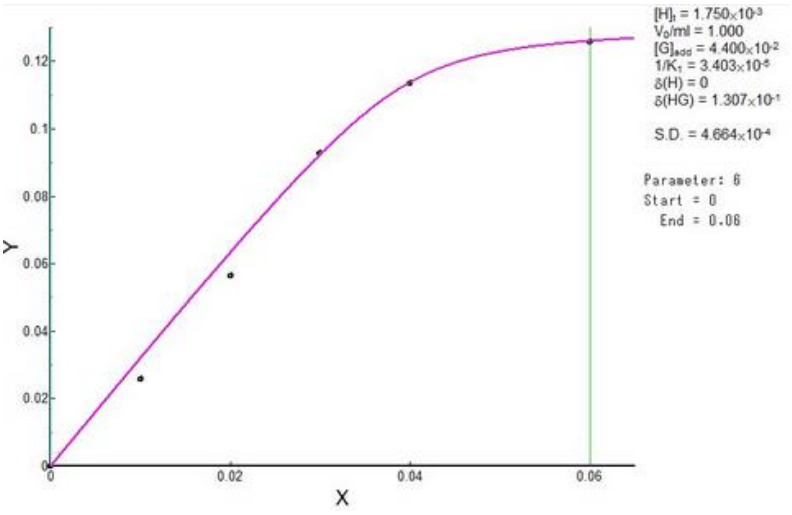

Figure 7. (a) Titration curve of β-CD/IBUNa in D_2O; (b) Titration curve of Man-CD/IBUNa. X represent the volume of CDs (ml), and Y represent the relative chemical shifts' change of aromatic protons of IBUNa.

3.3.2 Inclusion ability of Mal-CD and Meli-CD

Similarly, total CDs and IBUNa concentration [Mal-CD + IBUNa] or [Meli-CD + IBUNa] was constant (4.38 mM) and ratio of [Mal-CD] or [Meli-CD] was ranging from 0 to 0.8. The wide-ranging ^{1}H NMR spectrum also recorded the chemical shifts' change of IBUNa protons with the increasing ratio of Mal-CD and Meli-CD (Figure 8 and Figure 9). In Figure 8, the signal peak of H-3 proton of IBUNa shifted to lower magnetic field obviously with the increasing ratio of Mal-CD. In Figure 9, the signal peak of H-3 proton of IBUNa also shifted to lower magnetic field obviously with the increasing ratio of Meli-CD. Based on the observations in Figure 8 and Figure 9, the H-3 proton was selected as referential proton for the Job's plot experiment and Ks values' calculation. In addition, the signal peak of methyl proton H-7 of IBUNa also had unobvious chemical shifts' change toward lower magnetic field with the increment of Mal-CD or Meli-CD.

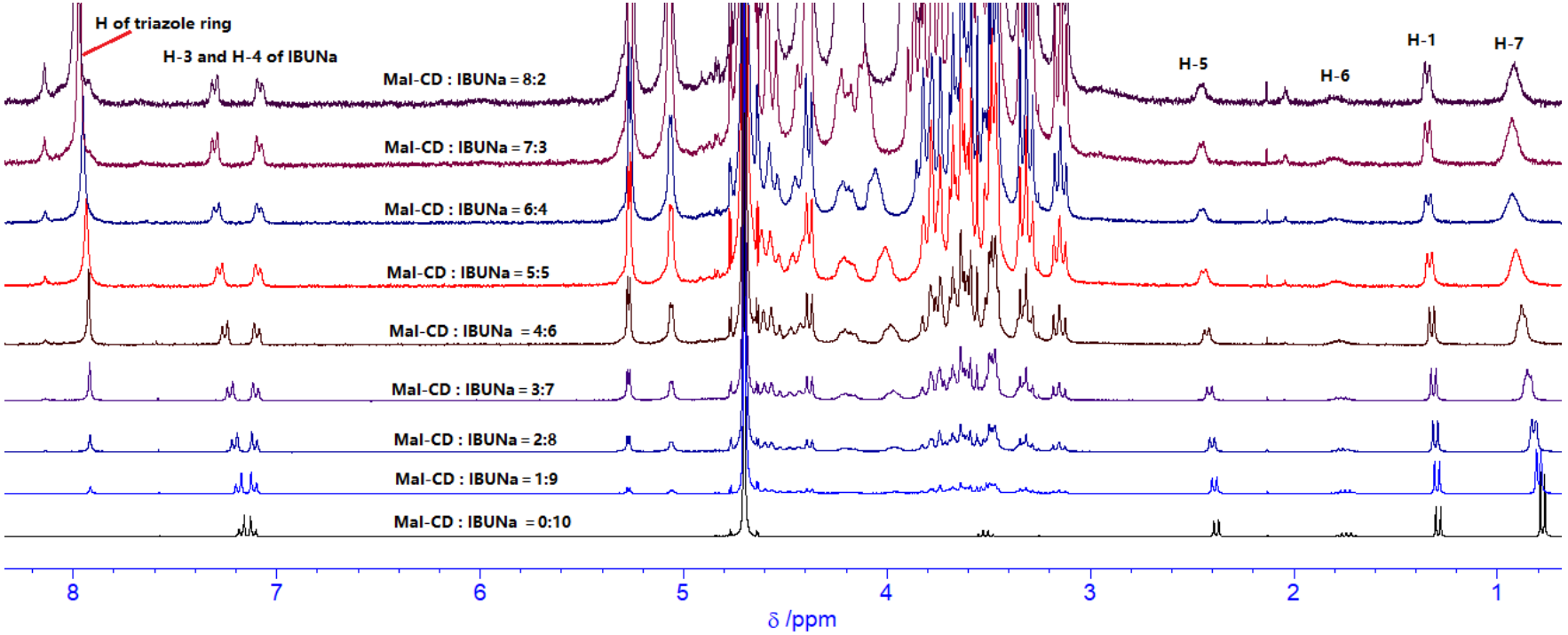

Figure 8. The 300 MHz ^{1}H NMR spectrum of IBUNa with the increasing ration of Mal-CD in D_2O.

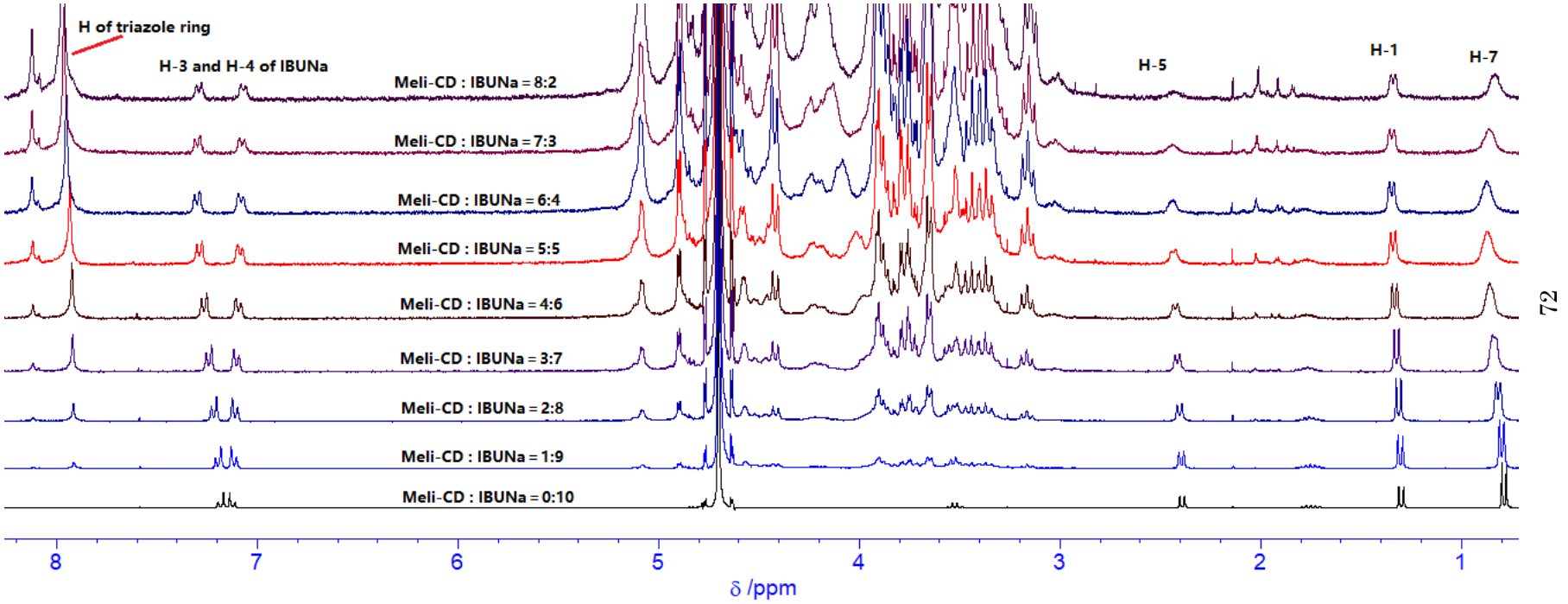

Figure 9. The 300 MHz ^{1}H NMR spectrum of IBUNa with the increasing ration of Meli-CD in D_2O.

Figure 10a and Figure 10b showed partial ^{1}H NMR spectrum of Mal-CD/IBUNa and Meli-CD/IBUNa with different host-guest ratio. With increment of concentration of Mal-CD or Meli-CD, the signal peak of H-3 proton of IBUNa's aromatic ring significantly shifted low magnetic field, and the H-4 proton of IBUNa's aromatic ring shifted to upper magnetic field oppositely. On the other hand, the signal peak of both H of triazole ring and H-7 of IBUNa were also shifted to low magnetic field slightly in the wide-ranging spectrum. The chemical shifts' values were calculated as Table 2. Based on the experimental data of chemical shifts' change, Job's plot curve of continuous variation was obtained as shown in Figure 11. Curves based on the chemical shifts' change of selected H-3 proton in IBUNa indicated the 1:1 inclusion mode of Mal-CD/IBUNa and Meli-CD/IBUNa inclusion complexes.

a

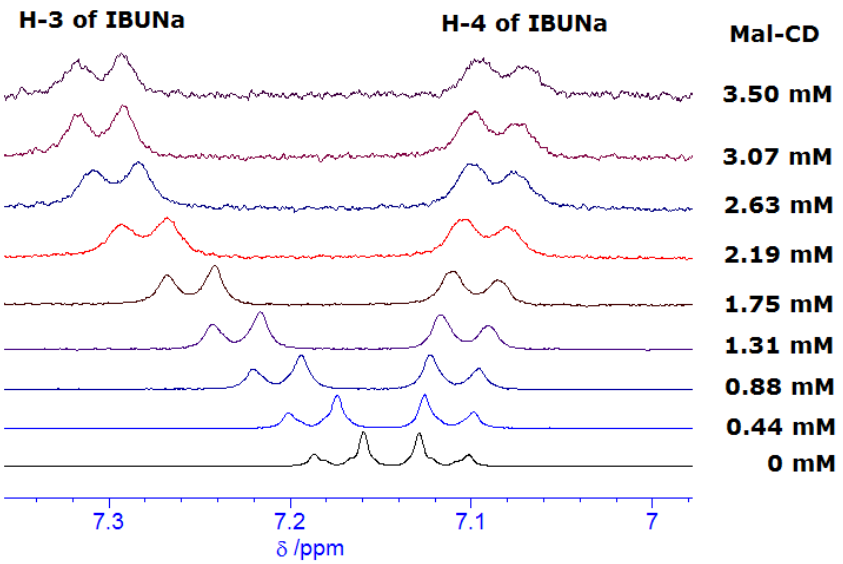

b

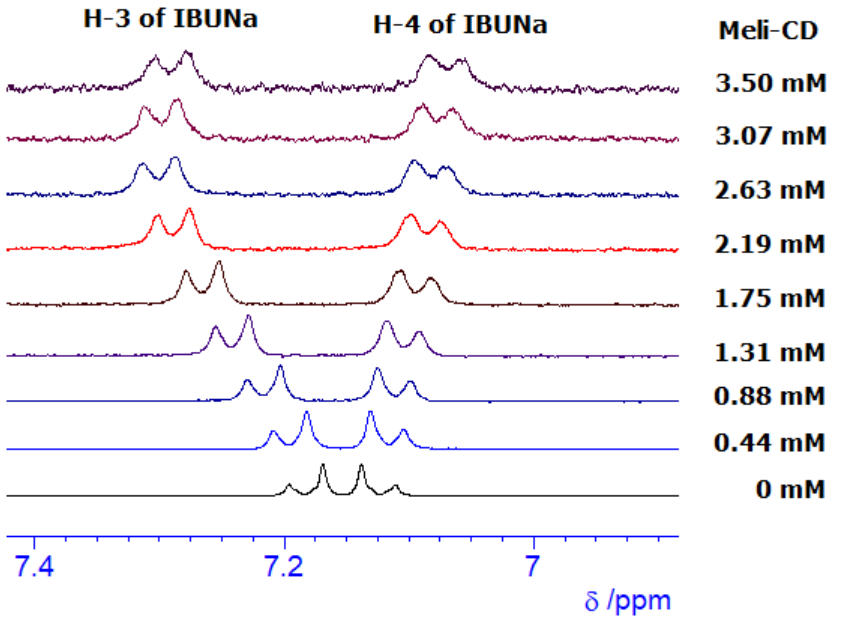

Figure 10. (a) Partial 300 MHz ^{1}H NMR spectrum (aromatic region) of inclusion complex of IBUNa in D_2O with the increasing concentration of Mal-CD; (b) Partial 300 MHz ^{1}H NMR spectrum (aromatic region) of inclusion complex of

IBUNa in D_2O with the increasing concentration of Meli-CD. Total concentration of CDs and IBUNa was kept at 4.38 mM and CDs' ratio was ranging from 0 to 0.8.

(a)

Ratio of Mal-CD	Chemical shifts' change of H-3 of IBUNa
0	0
0.1	+0.0144
0.2	+0.0343
0.3	+0.0572
0.4	+0.0819
0.5	+0.1082
0.6	+0.1244
0.7	+0.1332
0.8	+0.1336

(b)

Ratio of Meli-CD	Chemical shifts' change of H-3 of IBUNa
0	0
0.1	+0.0128
0.2	+0.0339
0.3	+0.0596
0.4	+0.0831
0.5	+0.1076
0.6	+0.1182
0.7	+0.1158
0.8	+0.1103

Table 2. (a) The chemical shifts' change of H-3 in the presence of Mal-CD with different ratios. (b) The chemical shifts' change of H-3 in the presence of Meli-CD with different ratios.

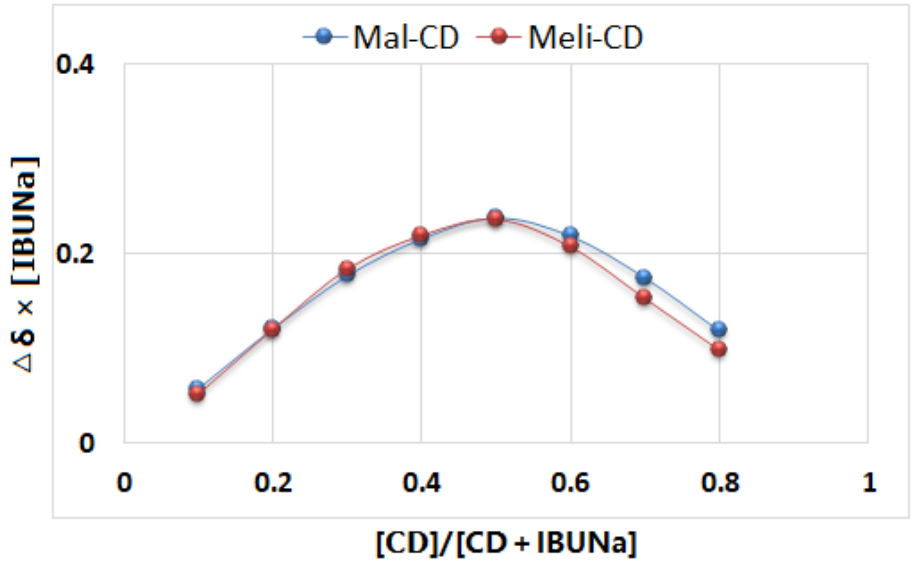

Figure 11. Job's plots corresponding to chemical shifts' change of the H-3 proton of IBUNa's aromatic ring in the presence of CDs. The total concentration of CD and IBUNa was kept at 4.38 mM in experiments.

The associate constants (Ks) values of Mal-CD/IBUNa and Meli-CD/IBUNa were also evaluated by curve fitting of the proton chemical shift changes as it was stated before. The concentration of guest IBUNa was kept at 1.75 mM in D_2O and the concentrations of host Mal-CD and Meli-CD were varied from 0 mM to 2.63 mM in D_2O. With the increasing concentrations of host CDs, the chemical shifts' change of IBUNa aromatic protons occurred regularly in the NMR measurement (Figure 12). According to the experimental data (Table 3), the Ks values for Mal-CD/IBUNa and Meli-CD/IBUNa complex were calculated as 0.64 $\times 10^4$ and 1.9 $\times 10^4$ M^{-1}, respectively (Figure 13).

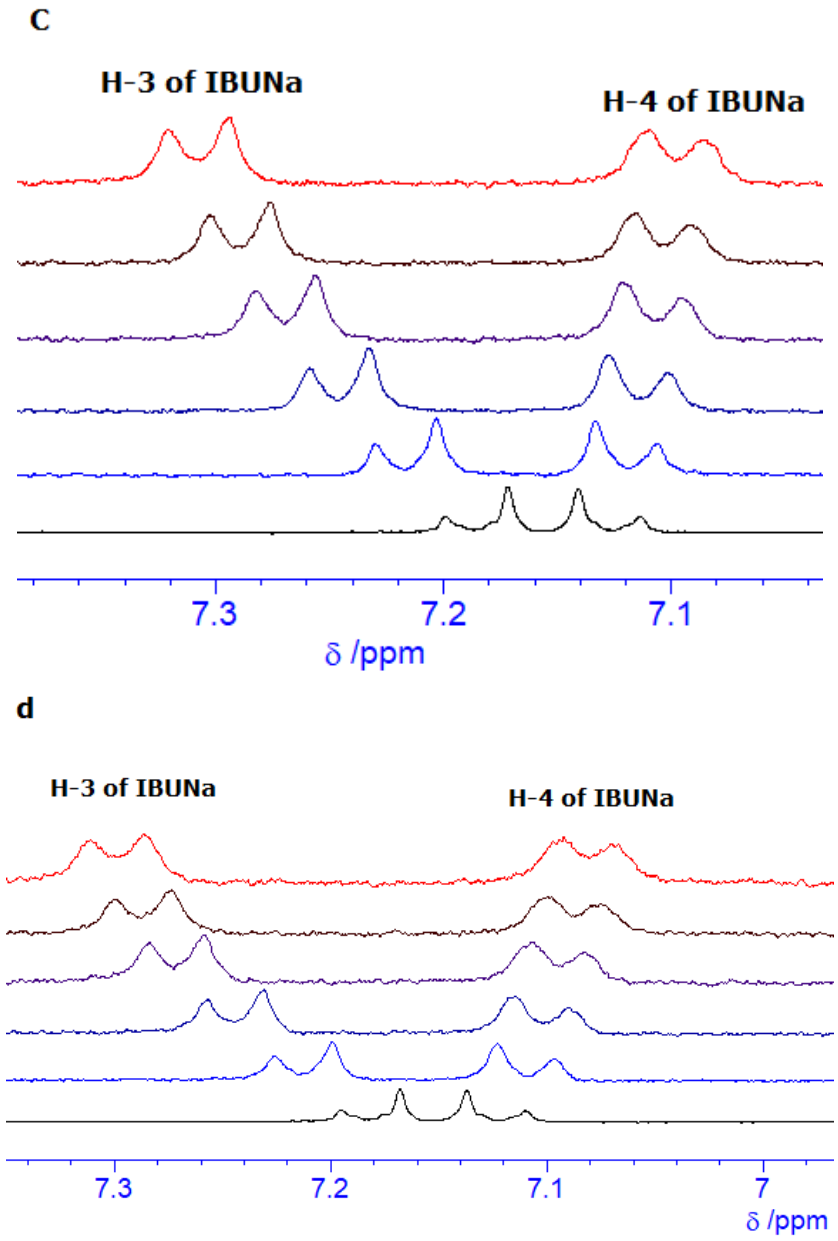

Figure 12. Partial 300 MHz ^{1}H NMR spectrum of IBUNa in the presence of Mal-CD (c) and Meli-CD (d) in D_2O, the concentration of IBUNa was kept at 1.75 mM with the increasing concentration of CDs from 0 to 2.63 mM.

[Mal-CD] mM	0	0.44	0.88	1.31	1.75	2.63
Chemical shifts' change of H-3	0	+0.0313	+0.0613	+0.0848	+0.104	+0.1218
[Meli-CD] mM	0	0.44	0.88	1.31	1.75	2.63
Chemical shifts' change of H-3	0	+0.031	+0.0631	+0.0903	+0.1056	+0.1187

Table 3. The chemical shifts' change of IBUNa's H-3 in the presence of Mal-CD and Meli-CD from 0 to 2.63 mM.

a

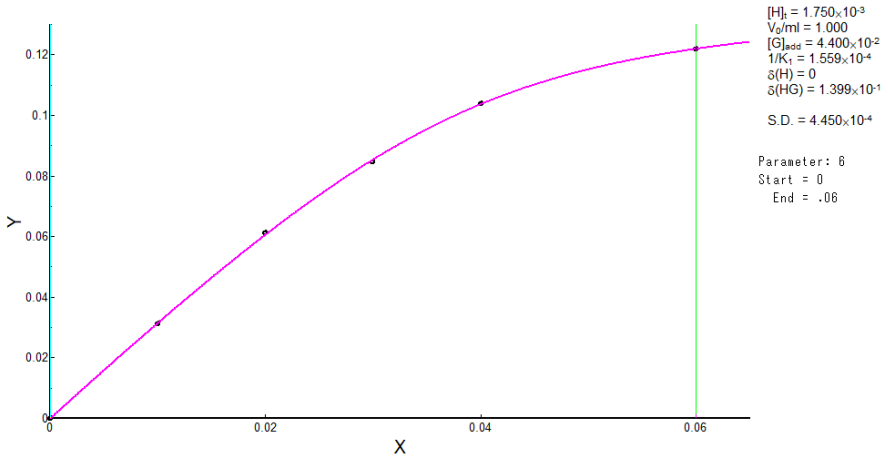

b

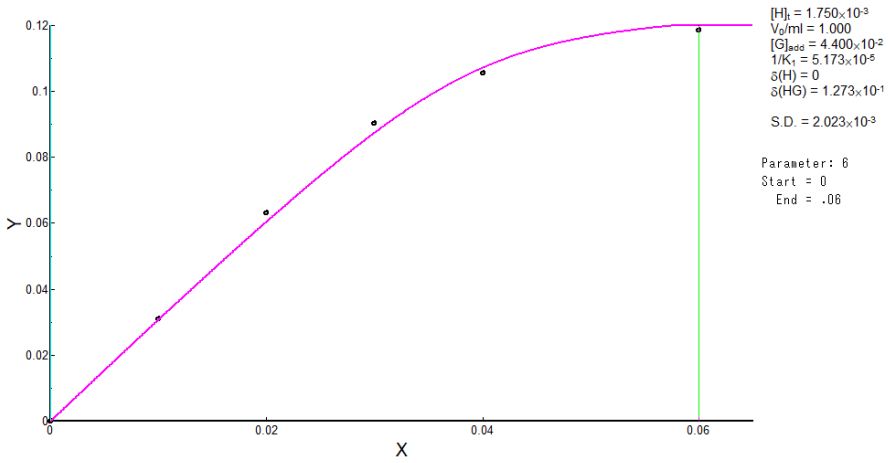

Figure 13. (a) Titration curve of Mal-CD/IBUNa in D_2O; (b) Titration curve of Meli-CD/IBUNa. X represent the volume of CDs (ml), and Y represent the relative chemical shifts' change of aromatic proton H-3 of IBUNa.

3.4 Conclusion

The inclusion behavior between CD-based glyco-clusters and IBUNa was studied by using NMR spectroscopic method, and the experimental results showed the inclusion abilities of CD-based glycol-clusters, which are useful to the recognition on host-guest interaction between CD-based glyco-clusters and guest molecule.

The inclusion properties of CD-based glyco-clusters were studied by using NMR spectrum to calculate the stoichiometry and associate constants (Ks) values for CDs/IBUNa inclusion complexes. Experimental results showed that β-CD/IBUNa, Man-CD/IBUNa, Mal-CD/IBUNa and Meli-CD/IBUNa inclusion complexes are all 1:1 inclusion stoichiometry. The Ks values were evaluated by curve fitting of chemical shifts' change of IBUNa in the presence of CDs, showed the $0.87\times10^4\ M^{-1}$ (β-CD/IBUNa), $2.9\times10^4\ M^{-1}$ (Man-CD/IBUNa), $0.64\times10^4\ M^{-1}$ (Mal-CD/IBUNa) and $1.9\times10^4\ M^{-1}$ (Meli-CD/IBUNa), respectively (Table 4).

	β-CD/G	Man-CD/G	Mal-CD/G	Meli-CD/G
Ks values	$0.87\times10^4\ M^{-1}$	$2.9\times10^4\ M^{-1}$	$0.64\times10^4\ M^{-1}$	$1.9\times10^4\ M^{-1}$

Table 4. The Ks values of CDs/G complexes. G represent IBUNa.

Compared to β-CD/IBUNa inclusion complex, the Man-CD/IBUNa and Meli-CD/IBUNa inclusion complexes demonstrated the relative higher Ks values, but the Mal-CD/IBUNa inclusion complex showed a lower Ks

value. Theoretically, the substituted groups of CD-based glyco-clusters may have an influence on the inclusion behavior. The substituted groups without linkage by α-1,4 glycosidic bonds may have a better flexibility than the cavity of CD moiety. The inclusion conformations of β-CD/IBUNa, Man-CD/IBUNa, Mal-CD/IBUNa and Meli-CD/IBUNa were studied by 2D NMR NOESY or ROESY spectrum in next chapter.

Chapter 4

NMR spectroscopic investigation of the inclusion conformation of CDs/IBUNa inclusion complexes

4.1 Introduction

Some important features of inclusion complex of CD derivatives can be obtained by analyzing nuclear Overhauser effect (NOE) of ^{1}H NMR spectroscopy. With the 1:1 inclusion complexation conformation, 2D ROESY or NOESY spectrum for β-CD/IBUNa, Man-CD/IBUNa, Mal-CD/IBUNa and Meli-CD/IBUNa inclusion complexes were measured to know the protonic correlation between host and guest molecules. It is well known that two protons which located closely in space could produce an NOE cross-correlation between the relevant protons in ROESY or NOESY spectrum. The presence of NOE cross-peaks between protons of two species could indicate spatial contacts within 0.4 nm[54]. Then according to the NOE cross correlations observed in the 2D ROESY or NOESY spectrum, the potential space structure and inclusion conformations of inclusion complexes could be deduced.

As mentioned in Chapter 2, almost all signals of ^{1}H NMR spectra of Man-CD and newly synthesized Mal-CD and Meli-CD were characterized by 2D COSY and TOCSY spectrum. The author's next interest will focused on orientation of the guest molecule in the host compounds, because that the glyco-clusters have different types of monosaccharide or disaccharide constituents. With the 1:1 inclusion complexation conformation, 2D ROESY or NOESY spectrum for β-CD/IBUNa, Man-CD/IBUNa, Mal-CD/IBUNa and Meli-CD/IBUNa inclusion complexes were measured to know the protonic correlation between host and guest molecules.

4.2 Experiment

^{1}H, 2D NOESY and 2D ROESY NMR experiments for the D_2O solutions of 1:1 β-CD/IBUNa, 1:1 Man-CD/IBUNa, 1:1 Mal-CD/IBUNa and 1:1 Meli-CD/IBUNa inclusion complexes were performed on a JEOL ECA 600 spectrometer at High resolution NMR center of Graduate School of Science. The samples were prepared under ultrasonic circumstance by using IBUNa with equimolar CDs.

4.3 Results and discussion

As the 1:1 stoichiometry for the inclusion complexation of IBUNa with CDs was determined, the CDs/IBUNa inclusion complexes for 2D spectrum were prepared by using CDs with equimolar IBUNa.

As the 2D COSY and TOCSY spectrum of Man-CD was measured in advance, the protons of CD moiety and Mannose moiety were named as G and M respectively. For example, G1 means the H1 of CD moiety, and the M1 means the H1 of D-Mannose moiety. Firstly, the wide-ranging ^{1}H NMR spectrum of 1:1 Man-CD/IBUNa and 1:1 β-CD/IBUNa inclusion complexes were measured (Figure 1, from next page).

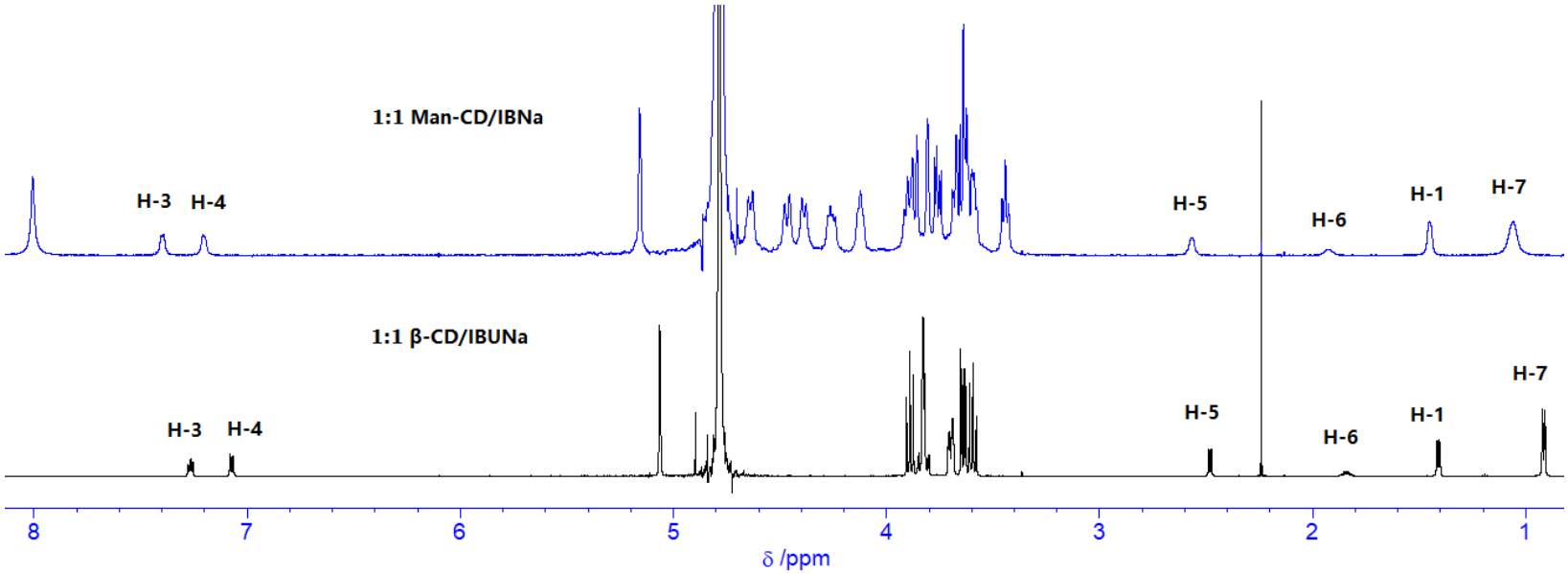

Figure 1. The wide-ranging 600 MHz ^{1}H NMR spectrum of 1:1 β-CD/IBUNa and Man-CD/IBUNa

In Figure 1, it could be observed that the appearance of signal peaks of H-7, H-1, H-6 and H-5 protons of IBUNa from 1.06 to 2.57 ppm; H-4 and H-3 protons of IBUNa from 7.21 to 7.39 ppm in the spectrum of 1:1 Man-CD/IBUNa. Meanwhile, it could be observed that the appearance of signal peaks of H-7, H-1, H-6 and H-5 protons of IBUNa from 0.91 to 2.49 ppm; H-4 and H-3 protons of IBUNa from 7.07 to 7.28 ppm in the spectrum of 1:1 β-CD/IBUNa. The NMR samples was prepared by using 1:1 ratio of IBUNa with β-CD or Man-CD in ultrasonic circumstance.

In addition, the 1:1 Mal-CD/IBUNa and 1:1 Meli-CD/IBUNa inclusion complexes were prepared by using CDs with equimolar IBUNa. As it is stated in Chapter 2, the detailed peaks assignment of Mal-CD and Meli-CD were deduced by 2D NMR COSY and TOCSY spectrum. For Mal-CD, the protons of CD moiety and Maltose moiety were named as G, H and H', respectively. For example, G1 means the H1 of CD moiety, the H1 means the H1 of middle glucosyl moiety, and the H'1 means the H1 of terminal glucosyl moiety. In a similar way, the protons of Meli-CD were also named as G, H and H', respectively. The G1 means the H1 of CD moiety, the H1 means the H1 of middle glucosyl moiety, and the H'1 means the terminal galactosyl moiety. The wide-ranging ^{1}H NMR spectrum of 1:1 Mal-CD/IBUNa and 1:1 Meli-CD/IBUNa inclusion complexes were measured (Figure 2, from next page).

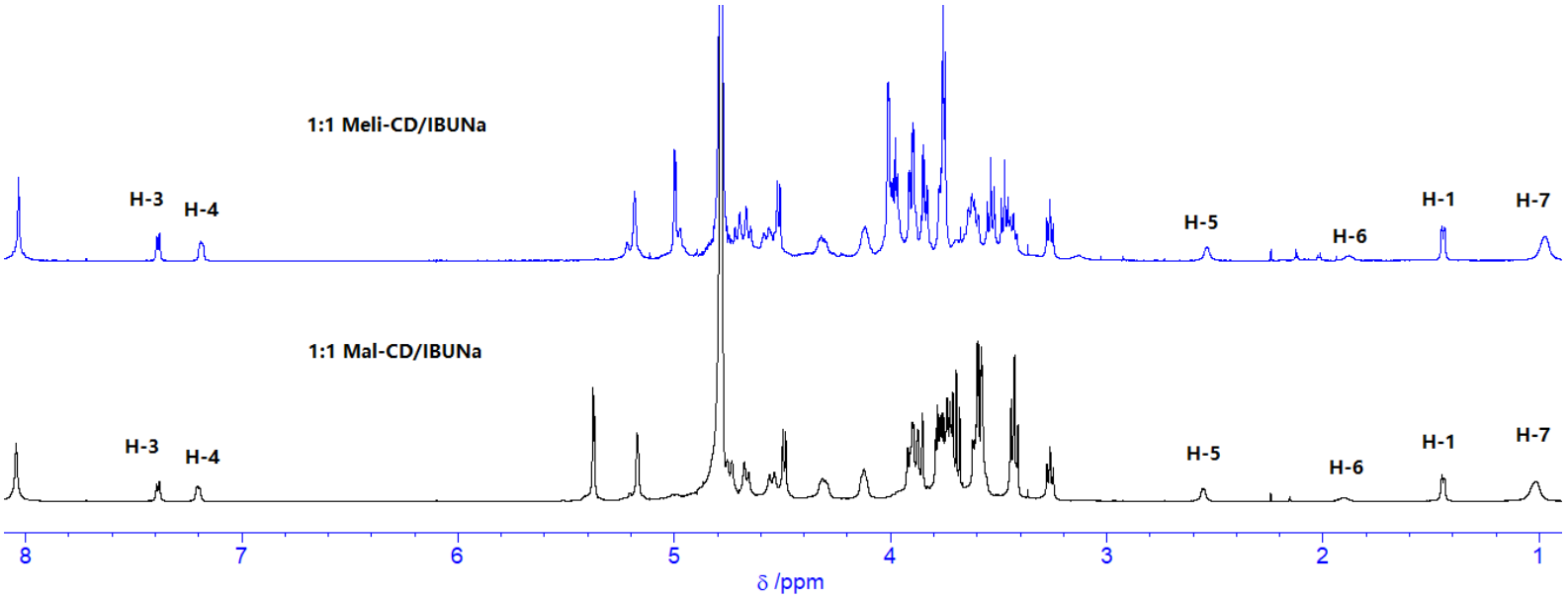

Figure 2. The wide-ranging 600 MHz ^{1}H NMR spectrum of 1:1 Meli-CD/IBUNa and Mal-CD/IBUNa

In Figure 2, it could be observed that the appearance of signal peaks of H-7, H-1, H-6 and H-5 protons of IBUNa from 1.02 to 2.56 ppm; H-4 and H-3 protons of IBUNa from 7.20 to 7.39 ppm in the spectrum of 1:1 Mal-CD/IBUNa. Meanwhile, it could be observed that the appearance of signal peaks of H-7, H-1, H-6 and H-5 protons of IBUNa from 0.97 to 2.53 ppm; H-4 and H-3 protons of IBUNa from 7.18 to 7.39 ppm in the spectrum of 1:1 Meli-CD/IBUNa. The NMR sample was prepared by using 1:1 ratio of IBUNa with Mal-CD or Meli-CD in ultrasonic circumstance.

The NOESY spectrum of Man-CD/IBUNa complex (Figure 3a and Figure 3b, from next page) showed appreciable correlation of H-5 proton of IBUNa (methylene group) with G3, G5 protons of CD moiety, indicated that H-5 proton of IBUNa located into the inner cavity of Man-CD; the correlation of H-7 proton of IBUNa (terminal methyl group) with G5 proton of CD moiety, indicated that H-7 proton of IBUNa located near the narrow side of Man-CD. Furthermore, the correlation of H-3 proton of IBUNa with G3 proton (aromatic proton) of CD moiety, indicated that H-3 proton of IBUNa located near the wider side of Man-CD. On the other hand, the correlation of another aromatic proton, H-4 proton of IBUNa with G3, G5 protons of CD moiety, indicated that H-4 proton of IBUNa also located into the inner cavity of Man-CD. In addition, the molecular size of IBUNa and β-CD moiety should be taken into consideration when analyze 2D spectrum. Taken the above-mentioned observations and 1:1 stoichiometry for the inclusion complex into consideration, the possible inclusion conformation of IBUNa with Man-CD was deduced as a structure shown in Figure 4, where the most hydrophilic carboxylate group of IBUNa located outside of the wider rim of CD cavity.

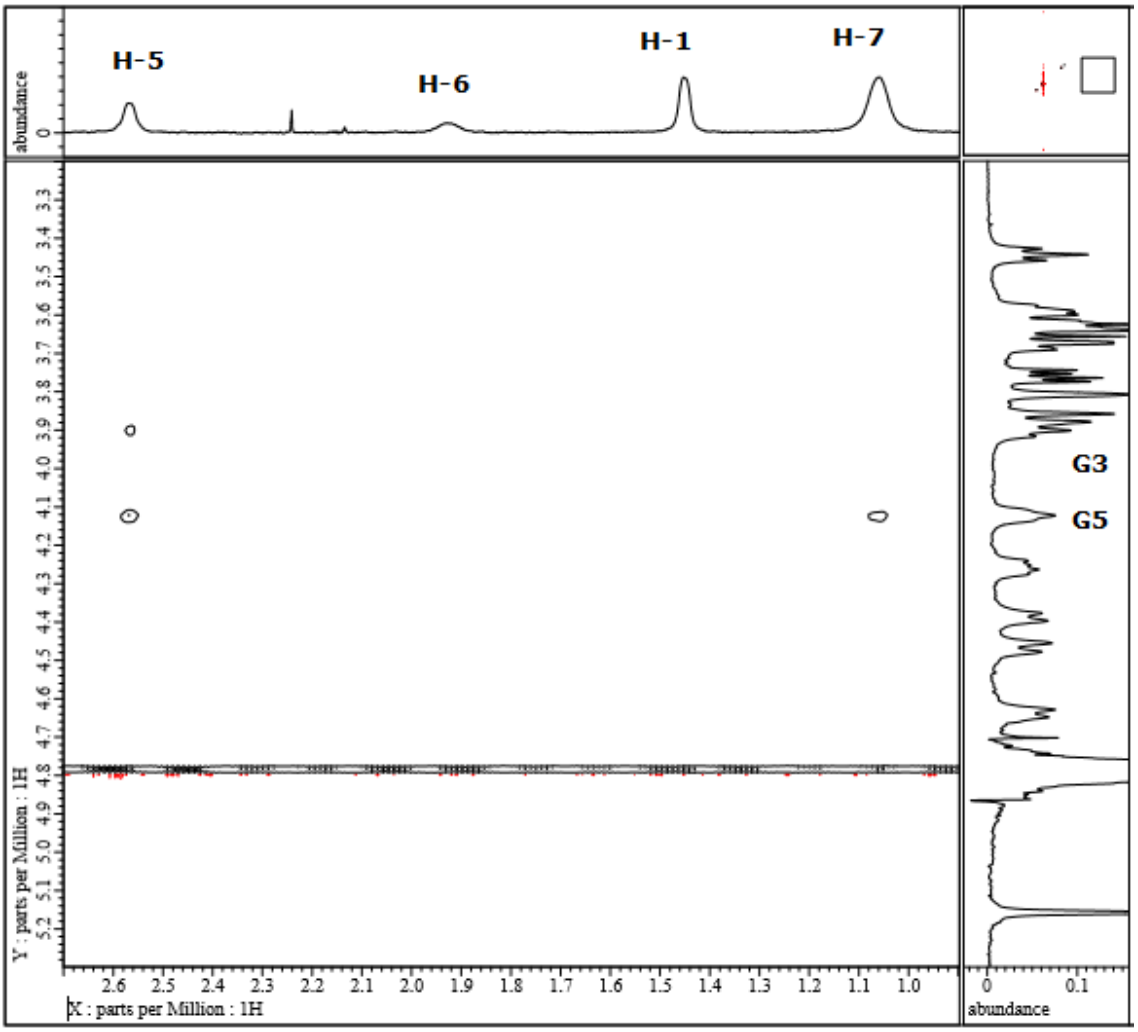

Figure 3a. The 600 MHz NOESY spectrum of 1:1 Man-CD/IBUNa complex in D_2O, showed the correlation between Man-CD and IBUNa protons (H-5 and H-7).

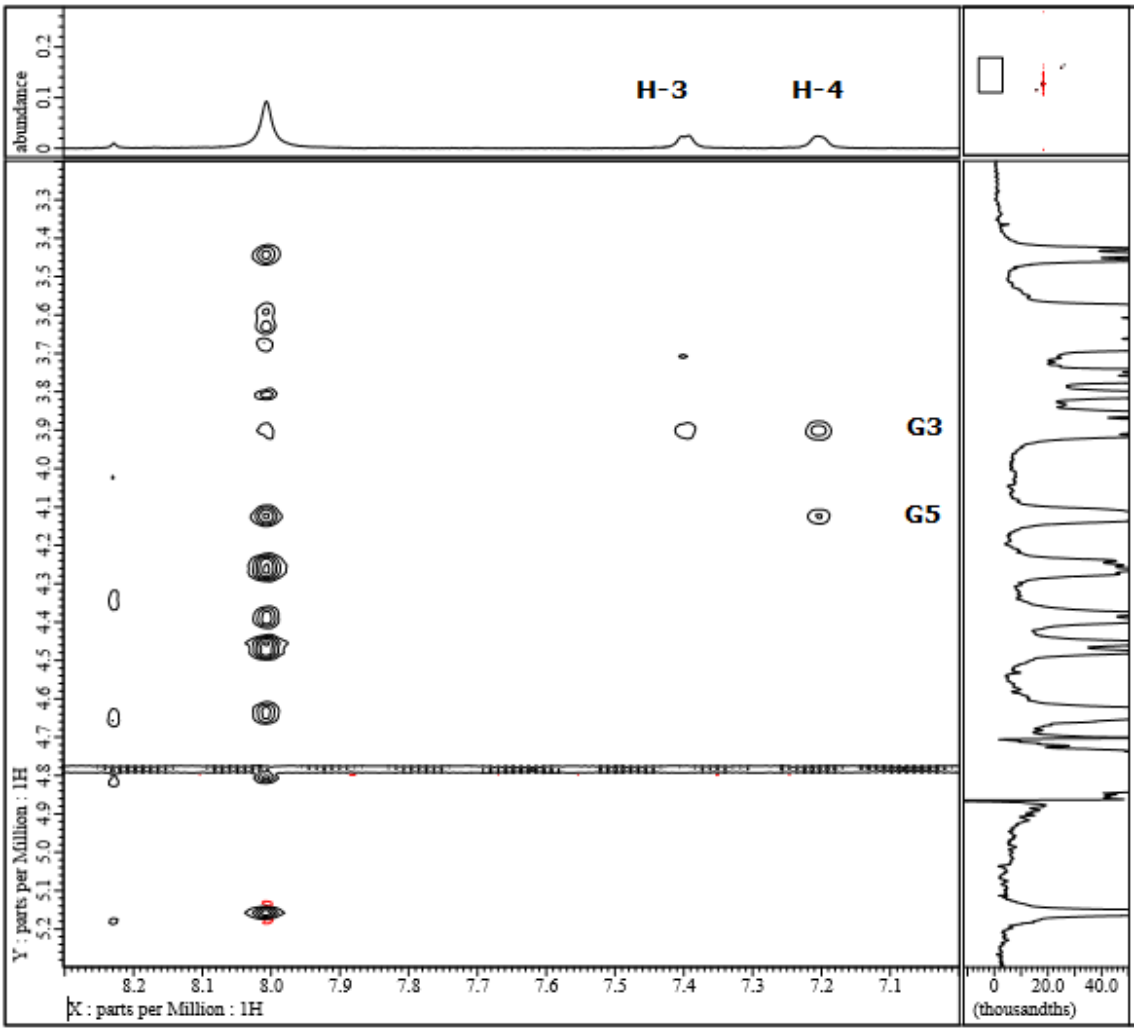

Figure 3b. The 600 MHz NOESY spectrum of 1:1 Man-CD/IBUNa complex in D_2O, showed the correlation between Man-CD and IBUNa protons (H-3 and H-4).

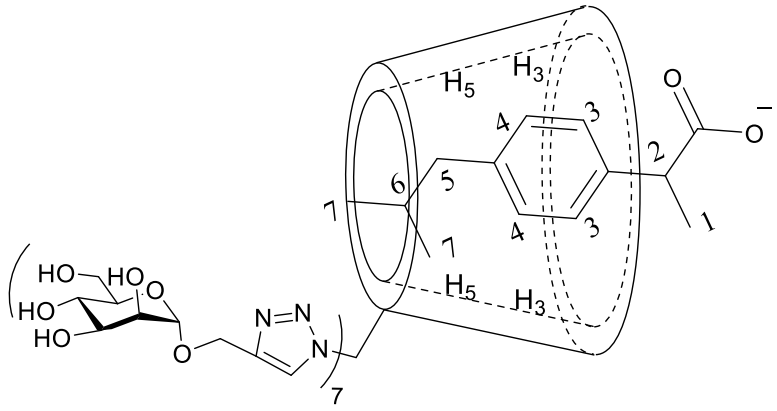

Figure 4. The possible inclusion conformation of 1:1 Man-CD/IBUNa complex deduced on the basis of 600 MHz NOESY spectrum.

In order to compare the inclusion mode of Man-CD and original β-CD, some protonic correlation between β-CD and IBUNa were also observed in the ROESY spectrum of β-CD/IBUNa complex (Figure 5a and Figure 5b, from next page). Surprisingly, the ROESY spectrum was extremely complicated. Analyzing the information in ROESY spectrum, the author could hypothesize that the β-CD/IBUNa complex has two different inclusion conformations: mode A and mode B.

The ROESY spectrum showed appreciable correlation of H-4 proton of IBUNa with G3, G5 protons of β-CD; the correlation of H-5 proton of IBUNa with G3, G5, G6 protons of β-CD. Moreover, the correlation of H-7 proton of IBUNa with G3, G5, G6 protons of β-CD; the correlation of H-1 proton of IBUNa with G2, G4 protons of β-CD; the correlation of H-3 proton of IBUNa with G2 proton of β-CD.

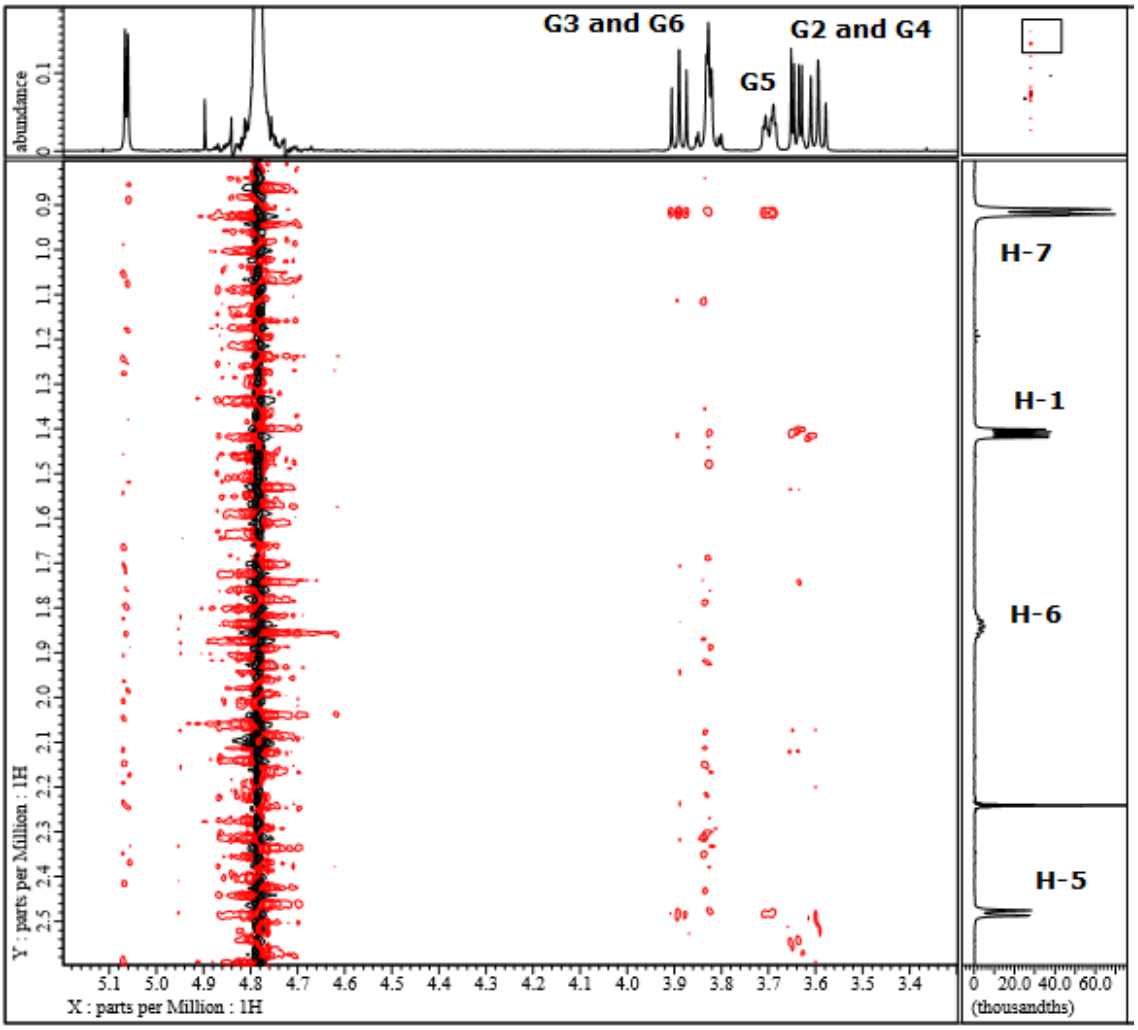

Figure 5a. The 600 MHz ROESY spectrum of 1:1 β-CD/IBUNa complex in D_2O, showed the correlation between β-CD and IBUNa protons (H-7, H-1 and H-5).

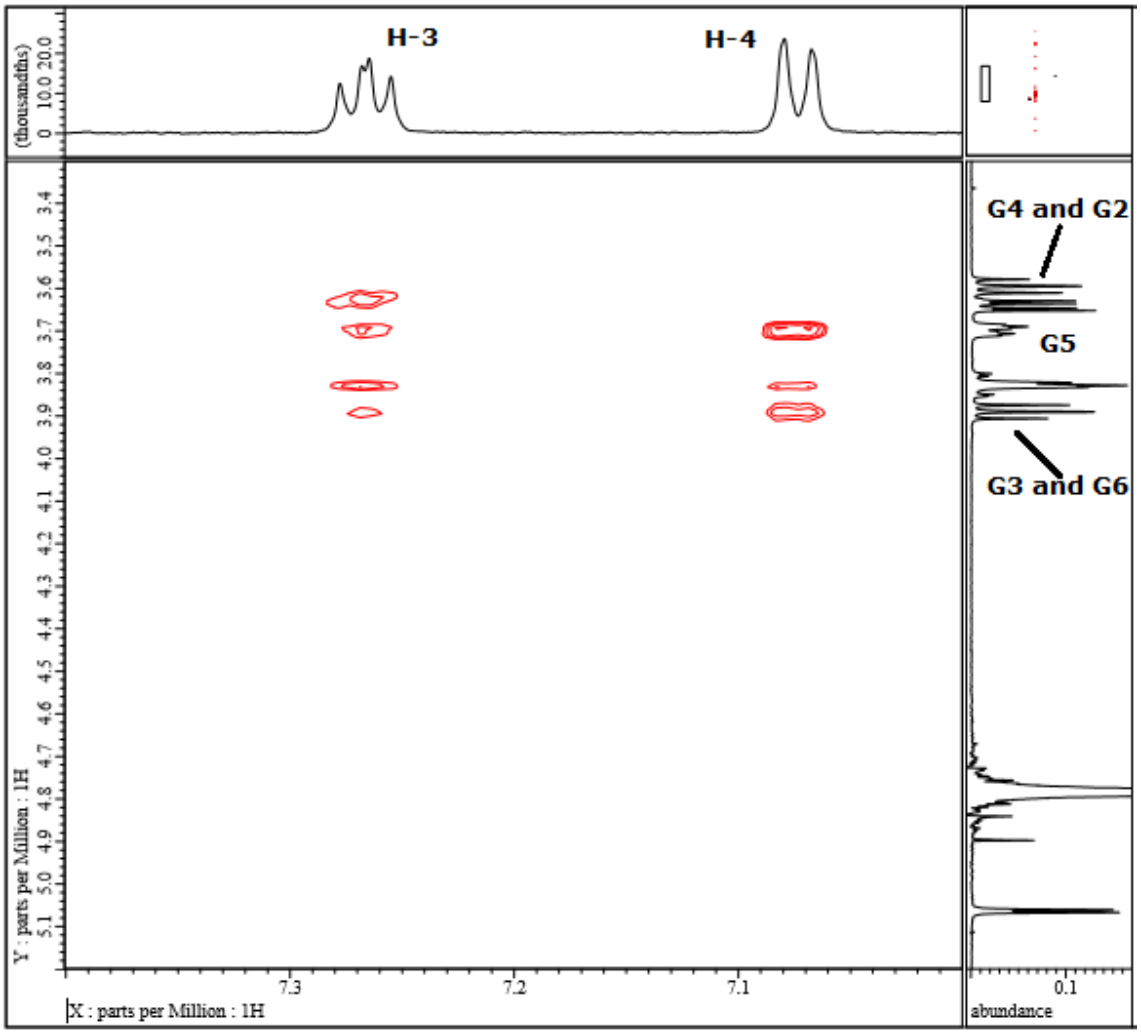

Figure 5b. The 600 MHz ROESY spectrum of 1:1 β-CD/IBUNa complex in D_2O, showed the correlation between β-CD and IBUNa protons (H-3 and H-4).

Taken the above-mentioned observations and 1:1 stoichiometry for the inclusion complex into consideration, the possible inclusion mode A of IBUNa with β-CD was deduced (Figure 6 (a)), where the protons are close to the carboxylate group of IBUNa (H-3 and H-1) located outside of wider

rim of β-CD's inner cavity and could had correlations with the external G2, G4 protons of other β-CD molecules possibly.

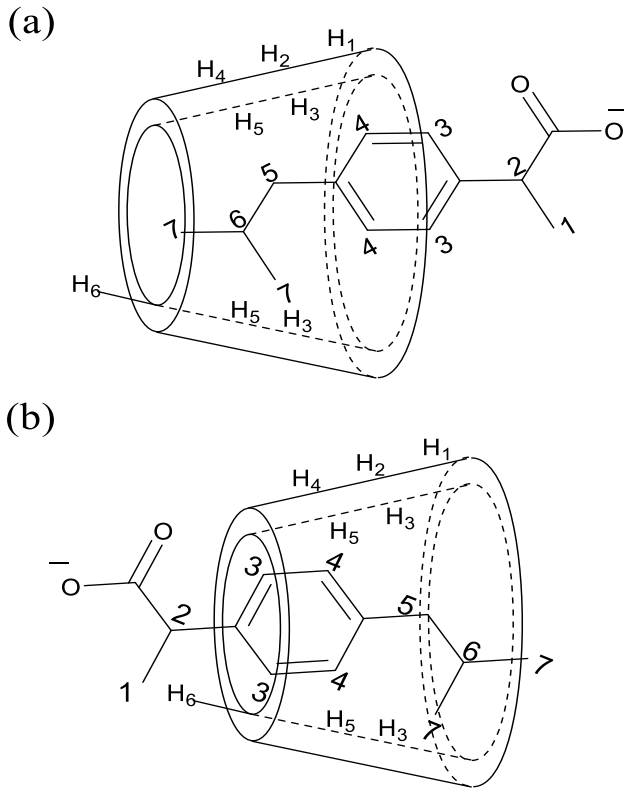

Figure 6. A and B mode of possible inclusion conformations of β-CD/IBUNa complex deduced on the basis of 600 MHz ROESY spectrum. The carboxylate group of IBUNa is located at secondary rim of β-CD (a) and at primary rim (b).

On the other hand, the ROESY spectrum of β-CD/IBUNa complex also showed appreciable correlation of H-1 proton of IBUNa with G6 proton of β-CD; the correlation of H-3 proton of IBUNa with G3, G5, G6 protons of β-CD; together with the correlation of H-4 proton of IBUNa with G3, G5, G6 protons of β-CD; the correlation of H-5 proton of IBUNa with G3, G5 protons of β-CD; and the correlation of H-7 proton of IBUNa

with G3, G5 protons of β-CD. Taken the above-mentioned observations and 1:1 stoichiometry for the inclusion complex into consideration, the possible inclusion mode B of IBUNa with β-CD was deduced (Figure 6 (b)), where the protons are close to the carboxylate group of IBUNa (H-3 and H-1) located outside of the narrow rim of β-CD. The evidence that two possible orientations of the guest molecule were presented in IBUNa/β-CD complex was not thought to be inconsistent with the evidence that only one set of 1D ^{1}H NMR was observed. The formation of the inclusion complex may occur under fast exchange conditions relative to the NMR time scale.

In a similar way, the inclusion conformations of the CD-based glyco-clusters with disaccharide substituents groups (Mal-CD and Meli-CD) were examined by using ROESY spectroscopy. For the Mal-CD/IBUNa and Meli-CD/IBUNa complexes, the 2D ROESY spectrum showed the NOE correlations which differ from β-CD/IBUNa and Man-CD/IBUNa complexes. As it was stated before, the protons of Mal-CD were named as G, H and H', respectively. In the ROESY spectrum of 1:1 Mal-CD/IBUNa complex (Figure 7a and Figure 7b, from next page), intramolecular NOE correlation was observed between the proton of triazole ring and G5 of CD moiety. This was suggested that partial substituted maltose groups were included into the cavity of CD moiety. Furthermore, weak correlation between H-4 proton of IBUNa and G3 proton and almost no correlation between H-3 proton of IBUNa and G3 proton were observed, suggested that partial IBUNa was not located into the CD cavity. In contrast to these evidences, correlations between the IBUNa protons and protons of maltose

substituents were observed: the correlation of H-3 proton of IBUNa with H5 and H’3 protons of Mal-CD; the correlation of H-4 proton of IBUNa with H5 proton of Mal-CD; the correlation of H-1 proton of IBUNa with H’3 proton of Mal-CD.

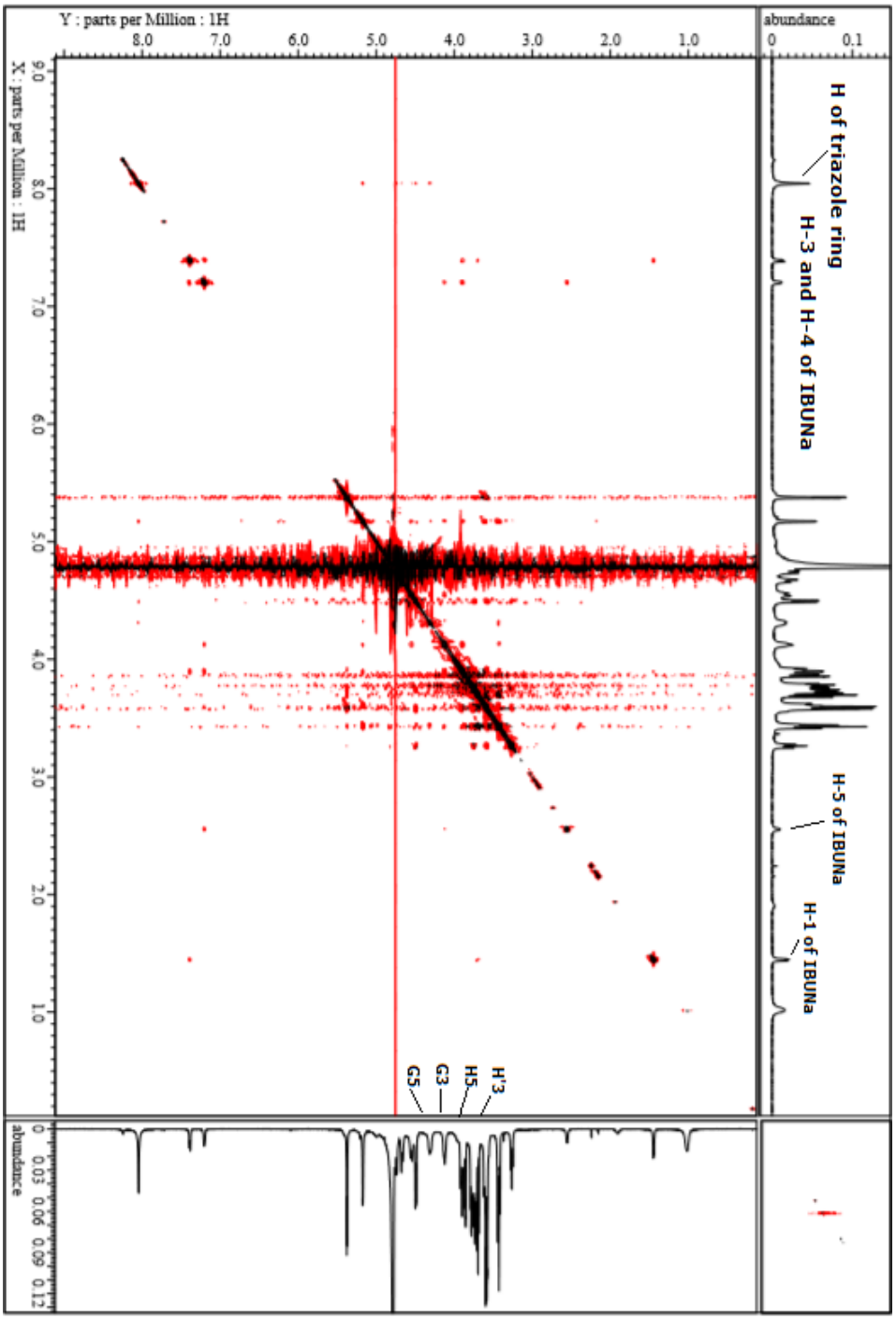

Figure 7a. The wide-ranging 600 MHz ROESY spectrum of 1:1 Mal-CD/IBUNa complex in D_2O.

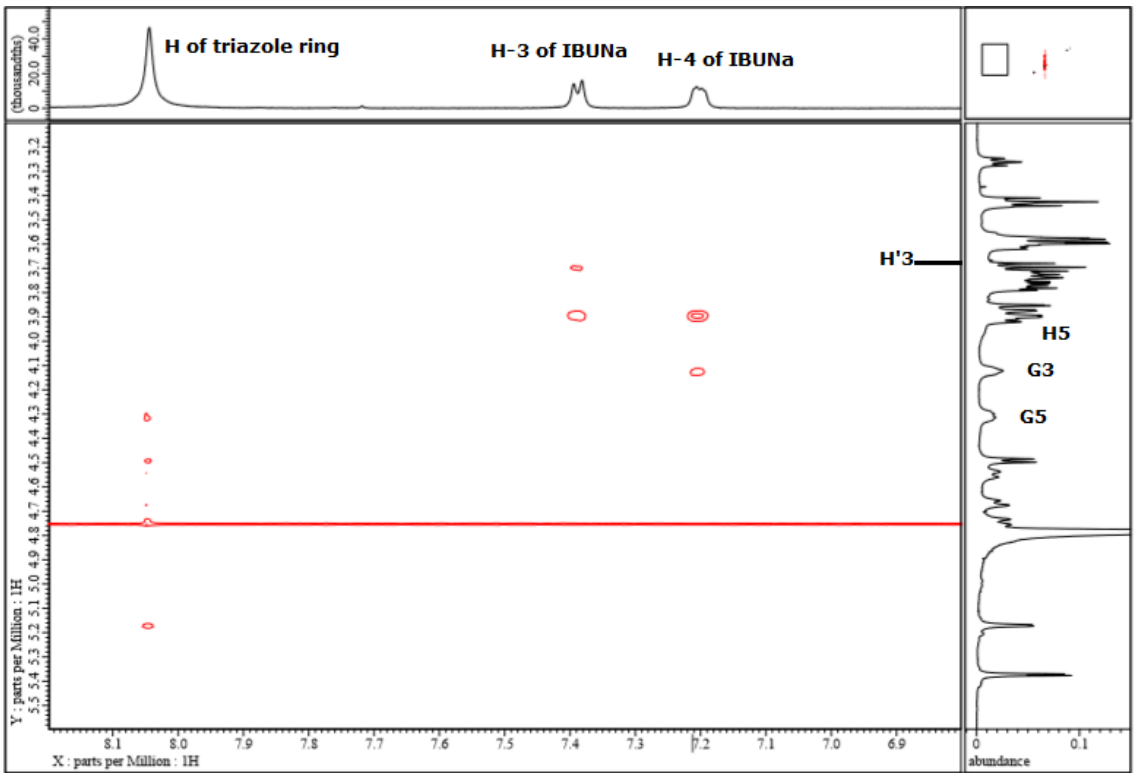

Figure 7b. The partial 600 MHz ROESY spectrum of 1:1 Mal-CD/IBUNa complex in D_2O, showed the correlation of H-3 and H-4 protons of IBUNa with protons of Mal-CD.

Taken the observations in 2D NMR ROESY spectrum and the 1:1 stoichiometry into consideration, the two potential inclusion modes of 1:1 Mal-CD/IBUNa complex were deduced (Figure 8a and Figure 8b).

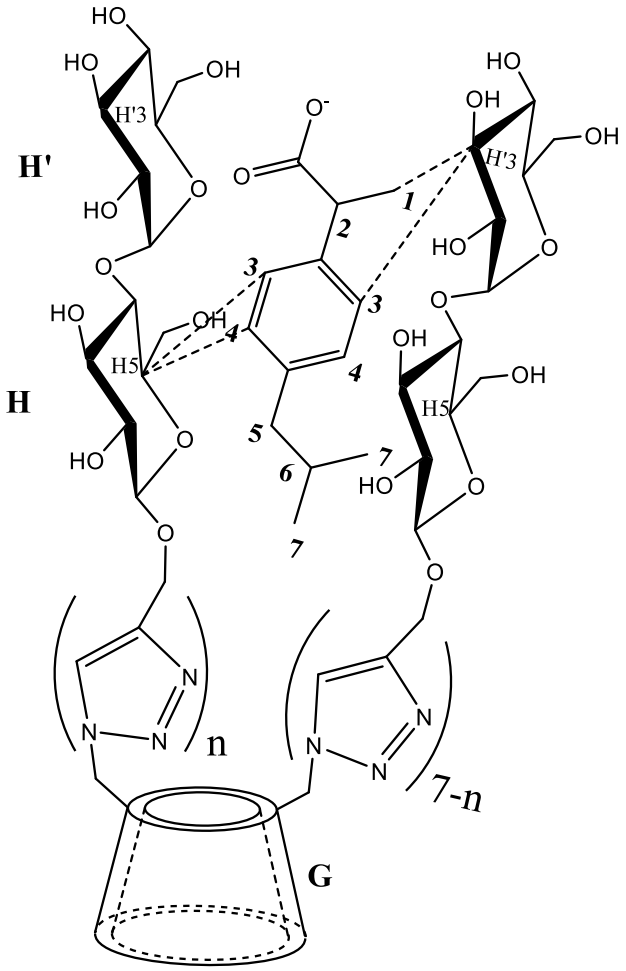

Figure 8a. Possible inclusion mode A of Mal-CD/IBUNa complex deduced on the basis of 600 MHz ROESY spectrum (Inclusion mode A was supposed as the unstable mode in the entire 1:1 inclusion system, because that the flexibility of substituted groups).

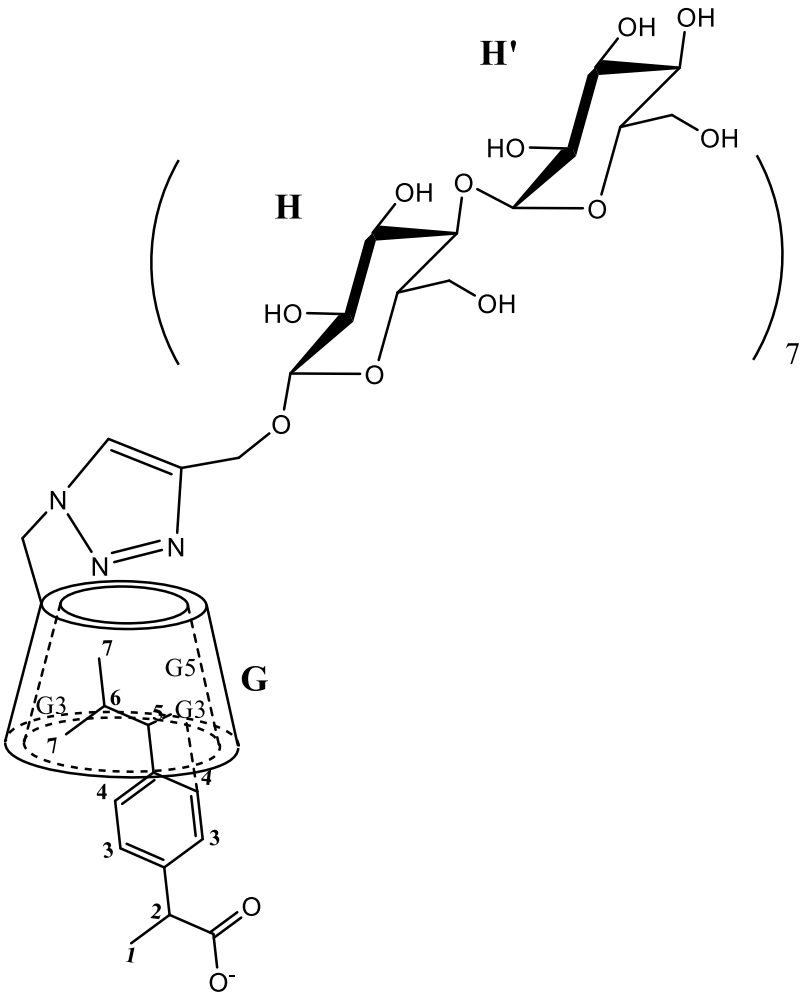

Figure 8b. Possible inclusion mode B of Mal-CD/IBUNa complex deduced on the basis of 600 MHz ROESY spectrum (Inclusion mode B was supposed as the primary mode in the entire 1:1 inclusion system).

Mode A showed the correlation of H-3 proton of IBUNa with H5, H’3 protons of Mal-CD; the correlation of H-4 proton of IBUNa with H5 proton of Mal-CD; the correlation of H-1 proton of IBUNa with H’3 proton of Mal-CD. Mode B showed the correlation of H-4 and H-5 protons of IBUNa with G3 proton of Mal-CD. Based on the correlation of triazole ring

proton with G5 proton of Mal-CD, it could be supposed that some substituted groups may entered into the cavity of CD moiety.

Similarly, because of its complicated structure, the protons of Meli-CD were also named as G, H and H', respectively. In the 2D NMR ROESY spectrum of 1:1 Meli-CD/IBUNa, some correlations were observed (Figure 9a and Figure 9b).

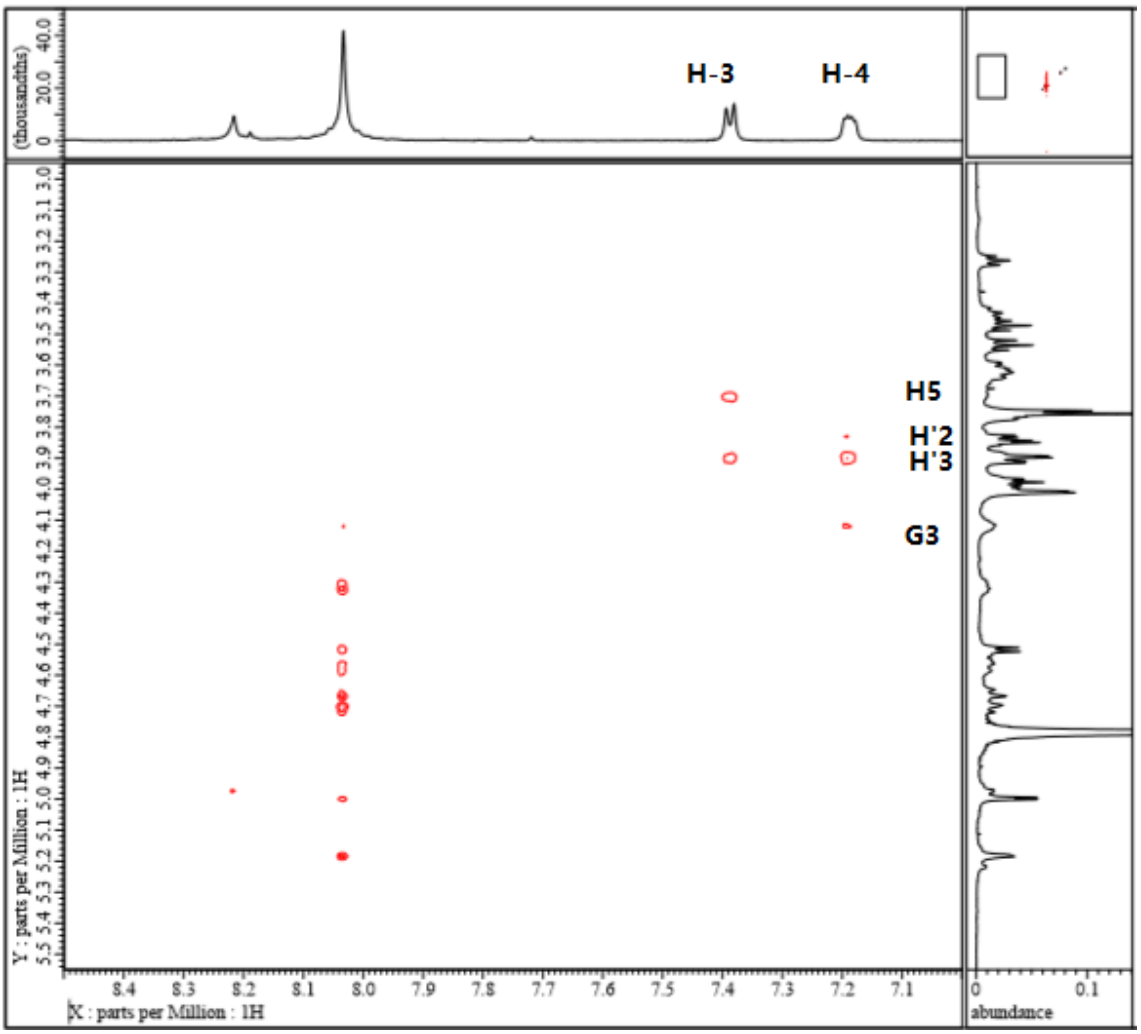

Figure 9a. The partial 600 MHz ROESY spectrum of 1:1 Meli-CD/IBUNa complex in D_2O, showed the correlation of H-3 and H-4 protons of IBUNa with protons of Meli-CD.

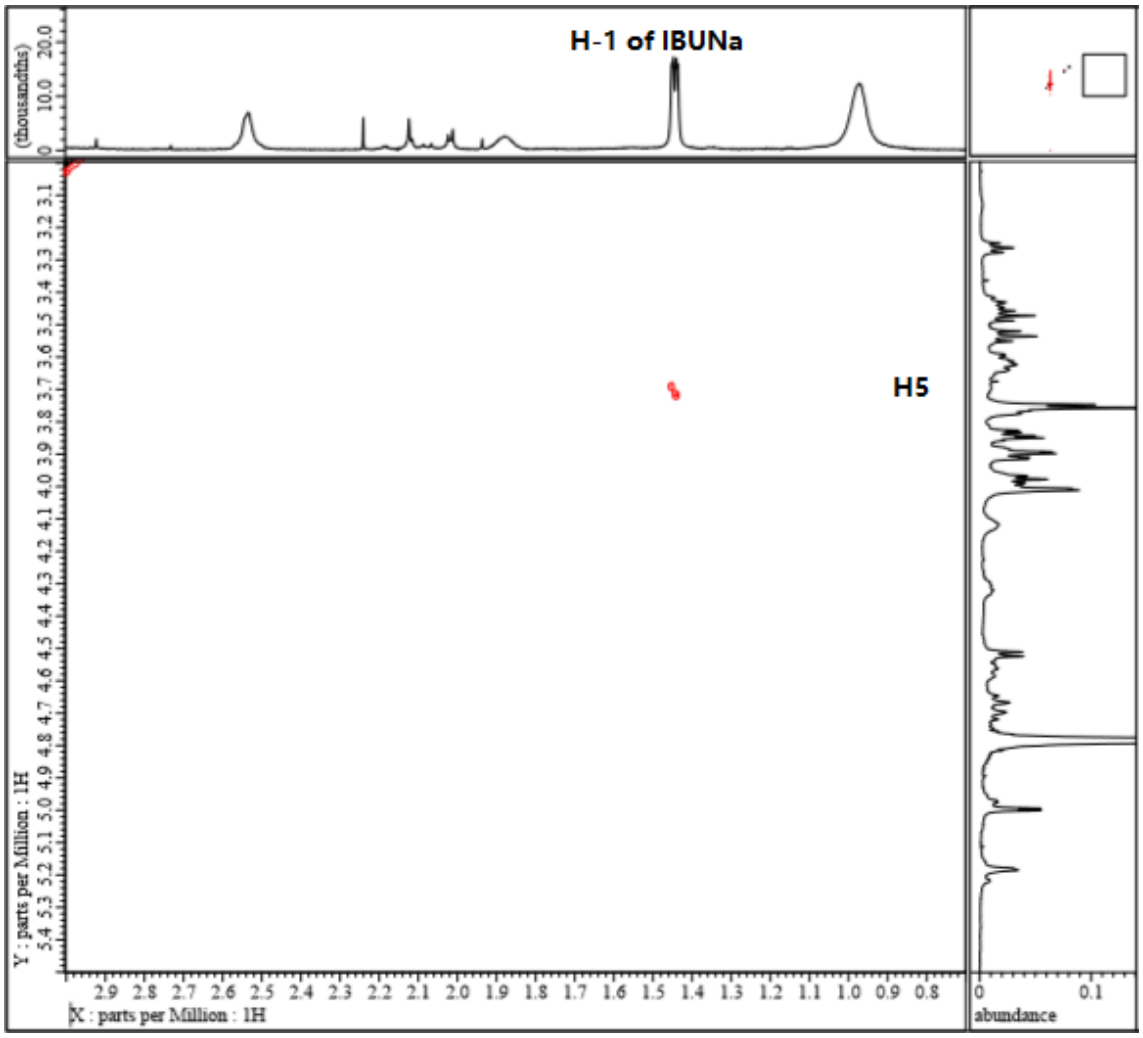

Figure 9b. The partial 600 MHz ROESY spectrum of 1:1 Meli-CD/IBUNa complex in D_2O, showed the correlation of H-1 proton of IBUNa with H5 proton of Meli-CD.

Some correlations were observed in the ROESY spectrum of 1:1 Meli-CD/IBUNa: the correlation of H-3, H-4 protons of IBUNa with H'3 proton of Meli-CD; the correlation of H-3, H-1 protons of IBUNa with H5 proton of Meli-CD; the correlation of H-4 proton of IBUNa with H'2 and G3 protons of Meli-CD.

Taken the observations in ROESY spectrum and 1:1 stoichiometry into consideration, two potential inclusion modes of 1:1 Meli-CD/IBUNa complex (Figure 10a and Figure 10b) were also deduced as well as the 1:1 Mal-CD/IBUNa complex.

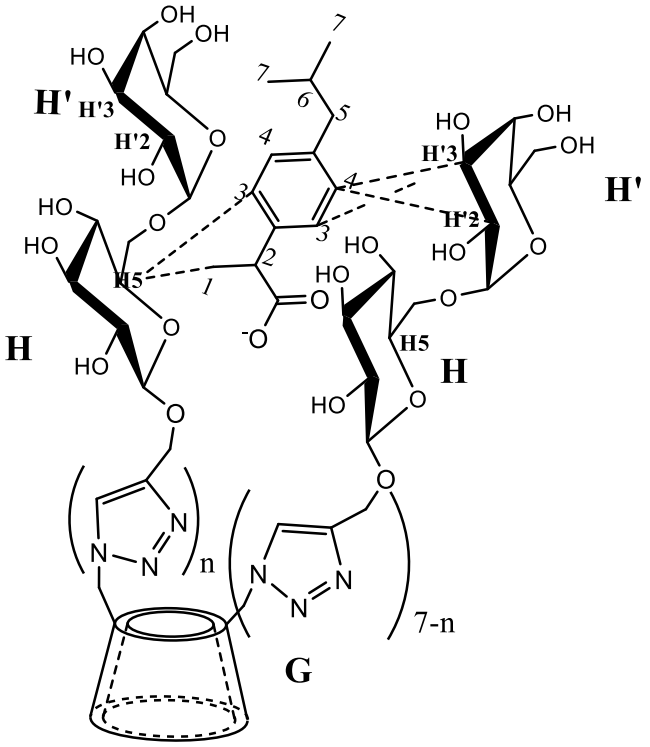

Figure 10a. Possible inclusion mode A of Meli-CD/IBUNa complex deduced on the basis of 600 MHz ROESY spectrum (Inclusion mode A was supposed as the unstable mode in the entire 1:1 inclusion system, because that the flexibility of substituted groups).

Mode A reflected the correlation of H-3 proton of IBUNa with H5, H'3 protons of Mal-CD; the correlation of H-4 proton of IBUNa with H'3, H'2 protons of Mal-CD; and the correlation of H-1 proton of IBUNa with H5 proton of Mal-CD. Mode B reflected the correlation of H-4 proton of IBUNa with G3 proton of Meli-CD.

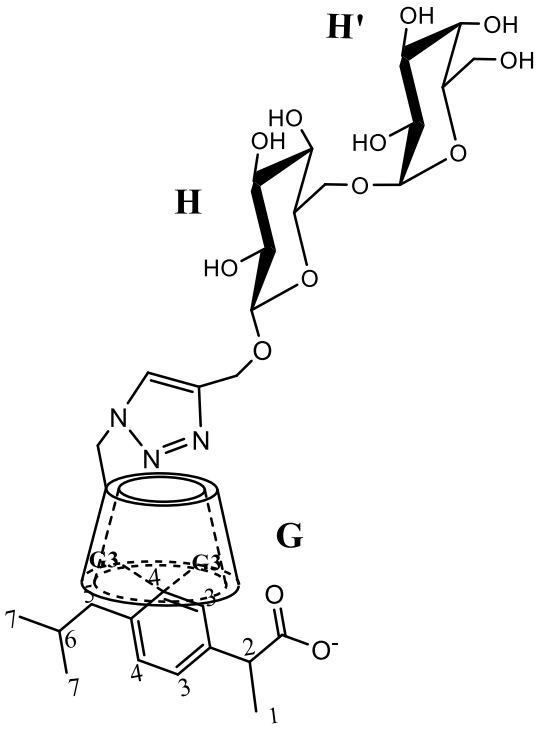

Figure 10b. Possible inclusion mode B of Meli-CD/IBUNa complex deduced on the basis of 600 MHz ROESY spectrum (Inclusion mode B was supposed as the primary mode in the entire 1:1 inclusion system).

The possible inclusion conformations of 1:1 Mal-CD/IBUNa and 1:1 Meli-CD/IBUNa inclusion system indicated one possibility that IBUNa guest molecule was not only included into the cavity of CD moiety, but also included into the core area formed by flexible substituted groups.

Based on the extremely observations in ROESY spectrum, some understandable suppositions were deduced.

Besides the 1:1 inclusion modes A, B of Mal-CD/IBUNa and Meli-CD/IBUNa inclusion complexes, there may have a possibility that another inclusion mode of Mal-CD/IBUNa and Meli-CD/IBUNa also existed in the entire 1:1 inclusion system. The Job's plot curve of both Mal-CD/IBUNa and Meli-CD/IBUNa showed the 1:1 inclusion mode at the same time, the author supposed that the 1:1 stoichiometry of Mal-CD/IBUNa and Meli-CD/IBUNa complexes could be regarded as an average situation for the entire 1:1 inclusion system. In the entire 1:1 inclusion system of Mal-CD/IBUNa complex, the inclusion system has self-included Mal-CD, Mal-CD/IBUNa complex of 1:1 inclusion mode A, Mal-CD/IBUNa complex of 1:1 inclusion mode B, and the 1:2 Mal-CD/IBUNa inclusion complex. For the 1:2 Mal-CD/IBUNa inclusion complex, the IBUNa guest molecules were included into the CD cavity and substituted groups from two directions.

In the first supposition, the 1:1 Mal-CD/IBUNa inclusion system has four kinds of molecules, but they formed an entire 1:1 inclusion system. In the second supposition, the 1:1 Mal-CD/IBUNa inclusion system has two kinds of molecules, the 1:1 Mal-CD/IBUNa complexes of A mode and B mode. The second supposition explained the possibility that one dynamic process existed between 1:1 Mal-CD/IBUNa complexes of inclusion mode A and inclusion B, the two kinds of inclusion modes could be converted to

each other in the entire 1:1 inclusion system. The CD moieties and substituted sugar groups constituted a deeper cavity space than CD cavity.

Similarly, the 1:1 Meli-CD/IBUNa inclusion system was also supposed to have two different situations. In the first situation, the 1:1 Meli-CD/IBUNa inclusion system has four kinds of molecules: self-included Meli-CD, Meli-CD/IBUNa complex of 1:1 inclusion mode A, Meli-CD/IBUNa complex of 1:1 inclusion mode B, and the 1:2 Meli-CD/IBUNa inclusion complex. For the 1:2 Meli-CD/IBUNa inclusion complex, the IBUNa guest molecules were included into the CD cavity and substituted groups from two directions. In the second situation, there has a possibility that the existence of dynamic process between 1:1 Meli-CD/IBUNa complex of inclusion mode A and 1:1 Meli-CD/IBUNa complex of inclusion mode B.

With the consideration of very complicated inclusion conformations of Mal-CD/IBUNa and Meli-CD/IBUNa complexes, the measurement of lectin recognition abilities should be improved. Some IBUNa molecules were included into the flexible substituted sugar groups, so that the inclusion mode A of Mal-CD/IBUNa and Meli-CD/IBUNa inclusion complexes was supposed as unstable. The lectin recognition experimental results of Meli-CD/IBUNa (Figure 11) could be used as a reference for the supposed inclusion situation.

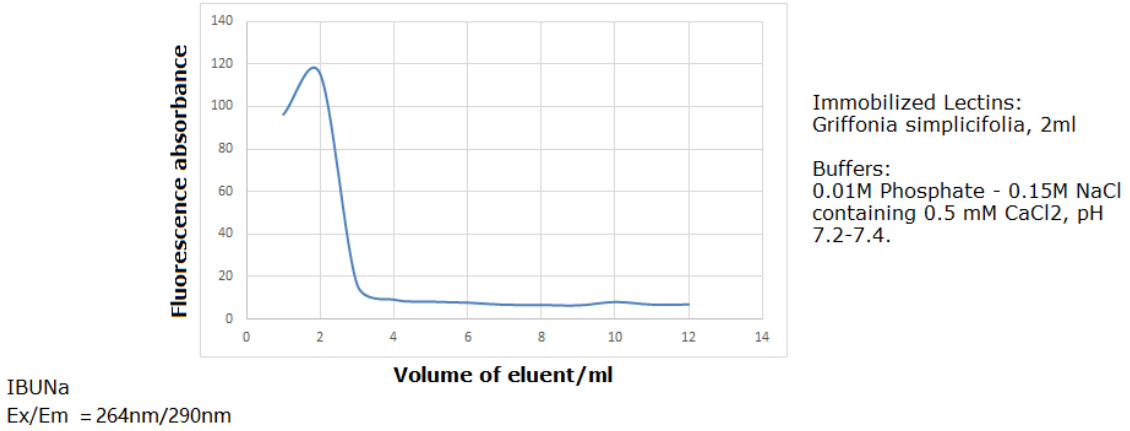

Figure 11. The lectin recognition experimental results of the 1:1 Meli-CD/IBUNa inclusion system.

The initial obvious fluorescence signals of IBUNa were observed, indicated that the IBUNa molecule came out from immobilized lectins directly. If the Meli-CD/IBUNa inclusion system was stable, the fluorescence signals of IBUNa should not be observed with the consideration of specific recognition abilities of Melibiose to Griffonia simplicifolia.

4.4 Conclusion

With the consideration of 1:1 stoichiometry for β-CD/IBUNa Man-CD/IBUNa, Mal-CD/IBUNa and Meli-CD/IBUNa inclusion complexes. The inclusion conformations of β-CD/IBUNa, Man-CD/IBUNa, Mal-CD/IBUNa and Meli-CD/IBUNa complexes were deduced through the 2D ROESY and NOESY spectrum. Interestingly, the β-CD/IBUNa, Mal-CD/IBUNa and Meli-CD/IBUNa complexes has different potential inclusion modes but the Man-CD/IBUNa has only one potential inclusion mode, indicating that the substituted sugar groups may have an influence on the inclusion behavior, which should be studied deeply. In addition, there existing two supposed inclusion situations for 1:1 Mal-CD/IBUNa and Meli-CD/IBUNa inclusion complexes. The first situation has four kinds of molecules in the entire 1:1 inclusion system; the second situation has one supposed dynamic process between inclusion mode A and inclusion mode B.

Based on the complicated observations in ROESY spectrum, the potential inclusion modes of 1:1 Mal-CD/IBUNa and 1:1 Meli-CD/IBUNa complex were supposed as much as possible. The supposition showed that the substituted groups could influence and play a role in the process of inclusion behavior. The substituted groups may have the better flexibility than the CD moiety, but it may bring new questions. As it is stated, the terminal α-galactosyl and α-glucosyl is the key factor for the lectin recognition abilities, so that the appropriate experimental methods to

measure the lectin recognition abilities of such CD-based glyco-clusters are necessary.

Chapter 5

Conclusion and Prospects

The Man-CD was successfully obtained by slightly modified Cu-mediated “click reaction” and characterized by ^{1}H and 2D NMR spectrum. Meanwhile, the Mal-CD and Meli-CD were also prepared by using Cu-mediated “click reaction” and characterized by ^{1}H NMR, 2D NMR and Mass spectrum. Experimental results showed that the CD-based glyco-clusters of high purities were obtained. As it was stated, the study on inclusion behavior of Man-CD, Mal-CD and Meli-CD is necessary with the consideration of multi-substituted groups and complicated space distribution, so that the detailed peaks assignment of Man-CD, Mal-CD and Meli-CD were analyzed by 2D COSY and TOCSY spectrum.

The host-guest inclusion behavior between IBUNa and CD-based glyco-clusters prepared by "click chemistry" was investigated by using NMR methods, and the parent β-CD was also applied to have a contrast to examine the influence from the substituent groups. It could be concluded that the CDs/IBUNa complexes were successfully obtained with 1:1 stoichiometry with different associate constants (Ks) values. Furthermore, presence of single conformation of the Man-CD/IBUNa inclusion complex was inferred from the results of NOESY experiments, but the inclusion conformation of Mal-CD/IBUNa and Meli-CD/IBUNa complexes based on ROESY experiments are very complicated. Based on the observations in 2D ROESY spectrum, the potential inclusion conformations of Mal-CD/IBUNa and Meli-CD/IBUNa inclusion complexes were deduced

as much as possible. Experimental results showed that the substituted groups of Mal-CD and Meli-CD may influence the inclusion behaviors deeply. As the specific recognition ability of α-mannopyranosyl, α-glucosyl and α-galactosyl residues to lectins, inclusion complexes could be ideal model molecule in the research of lectin recognition ability. With the consideration of the influence from substituted groups and the complicated inclusion conformations of Mal-CD/IBUNa and Meli-CD/IBUNa complexes, the research on lectin recognition abilities and extremely accurate molecular modelling should be continued to conduct.

References

1. Bertozzi, C. R.; Kiessling, L. L. *Science*. 2001, *291*, 2357–2364.

2. Lis, H.; Sharon, N. *Chem. Rev*. 1998, *98*, 77–674.

3. Varki, A.; Cummings, R.; Esko, J. D.; Freeze, H.; Hart, G.; Marth, J. *Essentials in Glycobiology*. Plainview, NY: Cold Spring Harbor Laboratory Press; 2002.

4. Roseman, S. *J. Biol. Chem*. 2001, *276*, 41527–41542.

5. (a) Seeberger, P. H.; Werz, D. B. *Nat. Rev. Drug Discovery*. 2005, *4*, 751–763. (b) Werz, D. B.; Seeberger, P. H. *Chem. Euro. J*. 2005, *11*, 3194–3206. (c) Seeberger, P. H.; Werz, D. B. *Nature*. 2007, *446*, 1046–1051.

6. (a) Stevens, J.; Blixt, O.; Paulson, J. C.; Wilson, I. A. *Nat. Rev. Microbiol*. 2006, *4*, 857–864. (b) Rosati, F.; Capone, A.; Della, G. C.; Brettoni, C.; Focarelli, R. *Int. J. Dev. Biol*. 2000,*44*, 609–618.

7. Focarelli, R.; La, S. G. B.; Balasini, M.; Rosati, F. *Cells Tissues Organs*. 2001, *168*, 76–81.

8. Crocker, P. R.; Feizi, T. *Curr. Opin. Struct. Biol*. 1996, *6*, 679–691.

9. Ziska, S. E.; Henderson, E. J. *Proc. Natl. Acad. Sci. U.S.A.* 1988, *85*, 817–821.

10. Geijtenbeek, T. B. H.; Kwon, D. S.; Torensma, R.; Van, V. S. J.; Van, D. G. C. F.; Middel, J.; Cornelissen, I. L. M. H. A.; Nottet, H. S. L. M.; Kewalramani, V. N.; Littman, D. R.; Figdor, C. G.; Van, K. Y. *Cell*. 2000, *100*, 587–597.

11. Geijtenbeek, T. B. H.; Torensma, R.; Van, V. S. J.; Van, D. G. C. F.; Adema, G. J.; Van, K. Y.; Figdor, C. G. *Cell*. 2000, *100*, 575–585.

12. Irwin, J. G.; Colleen, E. H. *Advances in Carbohydrate Chemistry and Biochemistry.* 1978, *35*, 127-340.

13. Anthony, P. D.; Richard, S. W. *Angew. Chem. Int. Ed*. 1999, *38*, 2978-2996.

14. Sharona, E.; Boaz, S. *Trends in Biochemical Sciences*. 1997, *22*, 462-467.

15. Malcolm, N. J. *Advanced Drug Delivery Reviews*. 1994, *13*, 215-250.

16. Yoshiki, O.; Hironari, Y.; Machiko, M.; Kenjiro, H.; Takashi, Y. *Bioorg.*

Med. Chem. 2008, *16*, 8830–8840.

17. Zhang, Q.; Cai Y.; Wang, X. J.; Xu, J. L.; Ye, Z.; Wang, S.; Seeberger, P. H.; Yin, J. *ACS Appl. Mater. Interfaces*. 2016, *8*, 33405-33411.

18. Challa, R.; Ahuja, A.; Ali, J.; Khar1, R. K. *AAPS PharmSciTech*. 2005, *6*, 329-357.

19. Uekama, K.; Hirayama, F.; Irie, T. *Chem. Rev*. 1998, *98*, 2045-2076.

20. Okimoto, K.; Miyake, M.; Ohnishi, N.; Rajewski, R. A.; Stella, V. J.; Irie, T.; Uekama, K. *Pharmaceutical Research*. 1998, *15*, 1562-1568.

21. Martin, D. V. E. M. *Progress Biochemistry*. 2004, *39*, 1033-1046.

22. Yao, Y.; Xie, Y.; Hong, C.; Li, G.; Shen, H.; Ji, G. *Carbohydrate Polymers*. 2014, *110*, 329-337.

23. Venuti, V.; Cannava, C.; Cristiano, M. C.; Fresta, M.; Majolino, D.; Paolino, D.; Stancanelli, R.; Tommasini, S.; Ventura, C. A. *Colloids and Surfaces B: Biointerfaces*. 2014, *115*, 22-28.

24. Hirayama, F.; Minami, K.; Uekema, K. *J. Pharm. Pharmacol*. 1996, *48*, 27-31.

25. Udo, K.; Hokonohara, K.; Motoyama, K.; Arima, H.; Hirayama, F.; Uekama, K. *International Journal of Pharmaceutics*. 2010, *388*, 95-100.

26. Liu, Y.; Sun, J.; Cao, W.; Yang, J.; Lian, H.; Li, X.; Sun, Y.; Wang, Y.; Wang, S.; He, Z. *International Journal of Pharmaceutics*. 2011, *421*, 160-169.

27. Tao, J.; Xu, J.; Chen, F.; Xu, B.; Gao, J.; Hu, Y. *European journal of Pharmaceutical Sciences*. 2018, *111*, 540-548.

28. Yao, H.; Ng, S. S.; Tucker, W. O.; Tsang, Y.; Man, K.; Wang, X.; Chow, B. K. C.; Kung, H. F.; Tang, G. P.; Lin, M. C. *Biomaterials*. 2009, *30*, 5793-5803.

29. Ooya, T.; Utsunomiya, H.; Eguchi, M.; Yui, N. *Bioconjugate Chem*. 2005, *16*, 62-69.

30. Tiwari, V. K.; Mishra, B. B.; Mishra, K. B.; Mishra, N.; Singh, A. S.; Chen, X. *Chem. Rev*. 2016, *116*, 3086-3240.

31. Kolb, H. C.; Finn, M. G.; Sharpless, K. B. *Angew. Chem. Int. Ed*. 2001, *40*, 2004-2021.

32. Moses, J. E.; Moorhouse, A. D. *Chem. Soc. Rev*. 2007, *36*, 1249-1262.

33. Sathya, S.; Katye, M. F.; Theresa, M. R. *J. Am. Chem. Soc*. 2008, *130*, 4618-4627.

34. Zhang, Y.; Guo, Z.; Ye, J.; Xu, Q.; Liang, X.; Lei, A. *J. Chromatogr. A*. 2008, *1191*, 188-192.

35. Gadelle, A.; Defaye, J. *Angew. Chem. Int. Ed. Engl*. 1991, *30*, 78-80.

36. Xu, J.; Liu, S. *J. Polym. Sci. Pol. Chem*. 2008, DOI: 10.1002/pola.23157.

37. Li, M.; Neoh, K. G.; Xu, L.; Yuan, L.; Leong, D. T.; Kang, E. T.; Chua, K, L.; Hsu, L. Y. *Pharm. Res*. 2016, *33*, 1161-1174.

38. Zhang, Q.; Su, L.; Collins, J.; Chen, G.; Wallis, R.; Mitchell, D. A.; Haddleton, D. M.; Becer, C. R. *J. Am. Chem. Soc*. 2014, *136*, 4325-4332.

39. Percec, V.; Leowanawat, P.; Sun, H. J.; Kulikov, O.; Nusbaum, C. D.; Tran, T. M.; Bertin, A.; Wilson, D. A.; Peterca, M.; Zhang, S.; Kamat, N. P.; Vargo, K.; Moock, D.; Johnson, E. D.; Hammer, D. A.; Pochan, D. J.;

Chen, Y.; Chabre, Y. M.; Shiao, T. C.; Bergeron, B. M.; Andre, S.; Roy, R.; Gabius, H. J.; Heiney, P. A. *J. Am. Chem. Soc.* 2013, *135*, 9055-9077.

40. Shun-ichiroh, O.; Takahashi, M.; Akira, K. *J. Biol. Chem.* 1975, *78*, 687-696.

41. Ohyama Y; Kasai K; Nomoto H; Inoue Y. *J. Biol. Chem*. 1985, *260*, 6882-6887.

42. Laitinen, L. *Histochem. J*. 1987, *19*, 225-234.

43. Kiekeby, S.; Winter, H. C.; Goldstein, I. J. *Xenotransplantation*, 2004, DOI: 10.1111/j.1399-3089.2004.00108.x.

44. Davies, N. M. *Clin. Pharmacokinet*. 1998, *34*, 101-154.

45. Hergert, L. A.; Escandar, G. M. *Talanta*. 2003, *60*, 235-246.

46. Chow, D. D.; Karara, A. H. *Int. J. Pharmaceut*. 1986, *28*, 95-101.

47. Oh, I.; Lee, M. Y.; Lee, Y. B.; Shin, S. C.; Park, I. *Int. J. Pharmaceut*. 1998, *175*, 215-223.

48. Geisslinger, G.; Stock, K. P.; Bach, G. L.; Loew, D.; Brune, K. *Agents. Actions*. 1989, *27*, 455-457.

49. Lien, A. N.; Hua, H.; Chuong, P. H. *Int. J. Biomed. Sci*. 2006, *2*, 85-100.

50. Mohammed, A. R.; Weston, N.; Coombes, A. G. A.; Fitzgerald, M.; Perrie, Y. *Int. J. Pharmaceut*. 2004, *285*, 23-34.

51. (a) Wan, M. M.; Sun, X. D.; Liu, S.; Ma, J.; Zhu, J. H. *Micropor. Mesopor. Mat*. 2014, *199*, 40-49. (b) Fan, B.; Wei, G.; Zhang, Z.; Qiao, N. *Corros. Sci*. 2014, *83*, 75-85.

52. Floare, C. G.; Pirnau, A.; Bogdan, M. *J. Mol. Struct*. 2013, *1044*, 72-78.

53. Tan, Z. J.; Zhu, X. X.; Brown, G. R. *Langmuir*. 1994, *10*, 1034-1039.

54. Saha, S.; Roy, A.; Roy, K.; Roy, M. N. *Sci. rep*. 2016, *6*, DOI: 10.1038/srep35674.

Acknowledgement

I would like to express my gratitude to all those who helped and encouraged me during the doctoral time in the past 4 years. I would like to express my deepest gratitude to my supervisor, Professor Nobuo Sakairi, appreciate his great support, detailed introduction and constant kindness in the doctoral time. Thanks for detailed introduction from Prof. Katsuaki Konishi and Prof. Fuyuhiko Matsuda, thanks for the careful reading and intelligent suggestion. Thanks for high-resolution ^{1}H NMR spectroscopic measurement from Dr. Yasuhiro Kumaki in Faculty of Science, Hokkaido University.

I also want to say “thank you” to the laboratory members, for your constant support and sincere communication. Thanks for Miss. Sayaka Fujita, Mr. Koki Ishizaki, Mr. Yuuki Takeda, Mr. Kento Takahashi, Mr. Kichi Tajima, Mr. Takahiro Kawano, Mr. Ryosuke Sato and other friends in laboratory. Thanks for Mr. Li Guanglei and Mr. Li Long for constant help and support. We had a good time together, the past 4 years will be always in my memory.

Finally, I want to express my gratitude to my family: my father and my mother. Thanks for your love and care. Thank you very much.